



# labex RESSOURCES 21

Strategic metals of the XXI<sup>st</sup> century

## Annual report 2022

Special focus on Metals for Electric Mobility

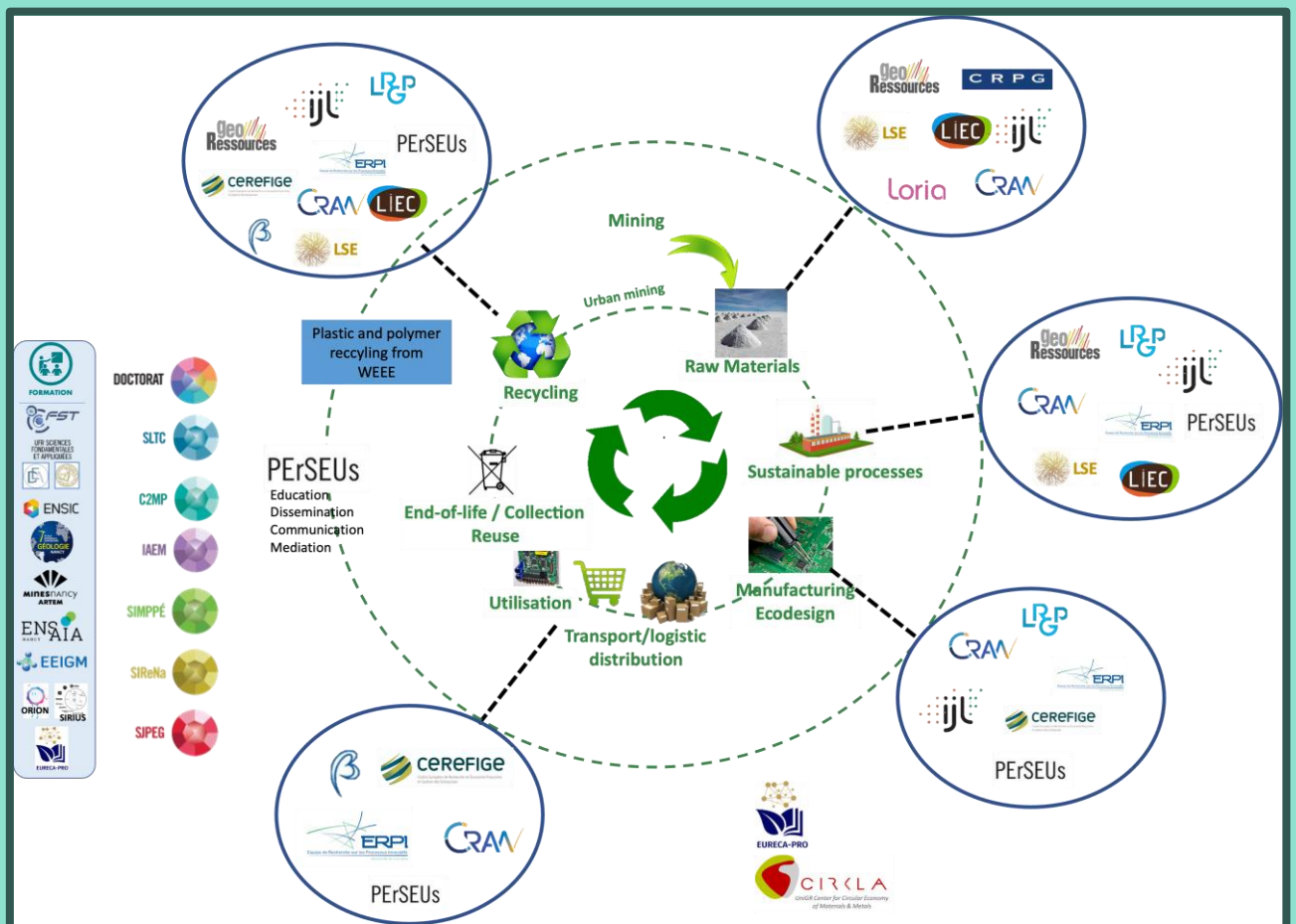


# Contents

Foreword	3
Quick facts	5
<b>Research Highlights</b>	<b>6</b>
Integrated project on Nickel	7
Integrated project on Rare Earth Elements	13
Integrated project on Lithium	19
Imerys Beauvoir programme	41
Integrated project on Gold in French Guiana	53
And more	59
<b>Education and Dissemination</b>	<b>66</b>
Postdoctoral fellows and researchers in 2022	71
PhD theses defended in 2022	72
Ongoing PhD theses in 2022	74
MSc theses funded in 2022	77
<b>Publications</b>	<b>79</b>
Publications in 2022	80
Publications in 2021	83

# foreword

After 11 years of activity of the LabEx RESSOURCES21, we started a reflection on the research program which would be likely to continue under the impetus of Lorraine University of Excellence after the end of the LabEx in 2024. The reflections resulting from the discussions with the members of the LabEx and with other laboratories from Université de Lorraine have led to a research program entitled Sustainable supply of critical metals for energy and digital transitions: 'One step ahead for the future resources'. This unifying program (whose actors are identified in the Figure below) aims to address the entire metal value chain of energy and digital transitions by focusing on the role of primary resources and secondary resources in the circular economy. This proposal will be refined during the year 2023, and we will know whether this research program will be selected by Lorraine Université d'Excellence during the year 2023 for a start in 2025.



# foreword

In 2022, the LabEx funded Education and research actions, as it does every year. The LabEx notably contributed with Lorraine Université d'Excellence and the EIT RawMaterials to the development of an e-learning program on the circular economy focusing more particularly on the value chain of metals (SPICE-MP). This e-learning program in French and English was made possible thanks to the involvement of 14 researchers. During 2023, this program will be enriched with visits of industries, interviews and a book. This year, the e-learning program was 'tested' by MSc students from the engineering school of Geology (ENSG), by students from the DENSYS Master's program and by 13 PhD students from the Doctoral School SIRENA from the Université de Lorraine. Positive feedbacks encourage us to continue to enrich the content. This program will be extended in 2024 to the Greater Region as part of the University of the Greater Region.

The call for projects 2022 of the LabEx was dedicated to all the main targets supported during the last four calls, i.e. nickel, rare earths, lithium and associated rare metals, gold in Guyana. The call covered all the approaches that made it possible to complete the state of knowledge on the geochemical cycle of these metals and the methods of processing primary and secondary resources containing these metals, the environmental, societal and economic impacts of mining and extractive metallurgy as well as the development of tools for acquiring, extracting and consolidating data in order to feed databases and models. This led to the financing of 43 research projects for a total of 3 121 731 euros, making it possible to fund 18 doctoral students and 17 years of postdocs in addition to 46 MSc internships.

This activity report for the year 2022 will not only allow you to learn more about the progress of our research teams but also about the various actions of the LabEx.

# Quick facts

## Research



**136** Research projects

**4** Major programmes

## Education



**40** PhD graduates

**39** Post-graduates

**184** Masters

## Production



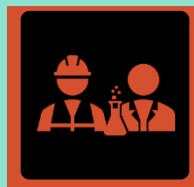
**329** Publications with LabEx RESSOURCES21 signature

## International networking



**3** Privileged countries for international collaborations: Australia, China and Canada

## People



**74** Academic staff members

**1** Scientific chair

**4** Senior researchers

## Collaborations



**15** International visitors

**3** Long research stays abroad

**8** co-supervised PhDs

## Conferences and workshops



**5** Workshops

**8** Major annual conferences

**2** Thematic school

## Funding



**13 M** Euros for 14 years

## Shanghai ranking ARWU (mining) in 2022



**17** Université de Lorraine – the first European University in Mining and Mineral Engineering since 2020



# Research Highlights

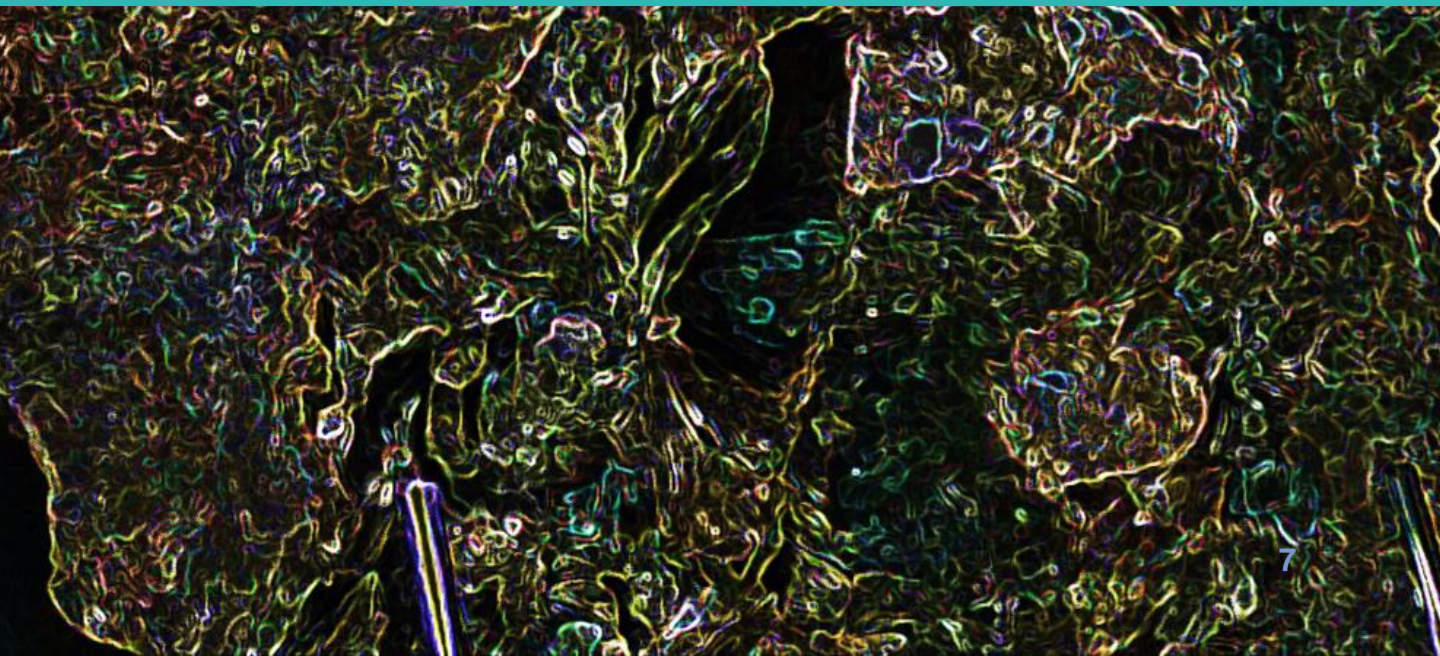


28 58.693

**Ni**

Nickel

# Integrated project on Nickel



Sylvain FAVIER<sup>1</sup>, Yoram TEITLER<sup>1</sup>, Fabrice GOLFIER<sup>1</sup>, Michel CATHELINÉAU<sup>1</sup>

<sup>1</sup>: Université de Lorraine, CNRS-CREGU, UMR 7359 GeoRessources, 54506 Vandoeuvre-lès-Nancy, France

Scientific topic:

## Context

Weathering processes are involved with many of the current challenges of the geoscience community such as climate regulation, the critical zone formation and the supergene deposits formation of highly demanded metals (Co, Ni, Sc, PGE, U,...). Yet, understanding the different processes controlling the weathering remains a major challenge. The impact of physical and chemical heterogeneities on the weathering front progression is still not totally understood.

In New Caledonia, **Ni-laterite supergene deposits** result from the **weathering** of the **peridotite** by the **downward** progression of **rainwater**. The dissolution-precipitation process leads to the progressive **enrichment** in **Ni** in the **saprolite** and to a lesser extent, in the **oxide horizon**. Therefore Ni distribution can be used as a **proxy** of the **weathering front progression**.

However, the progression of the weathering front is not uniform because of the existence of **hydro-chemical heterogeneities**, with notably a thick **fracture network** controlling it. These hydro-chemical heterogeneities hence result in an **heterogeneous Ni distribution** with **Ni rich fractures** and **Ni zonation** in the **matrix**.

The study of the Ni heterogeneous distribution in New Caledonia is therefore an excellent case study to **shed light on the impact of fractures on the formation of weathering heterogeneities**.

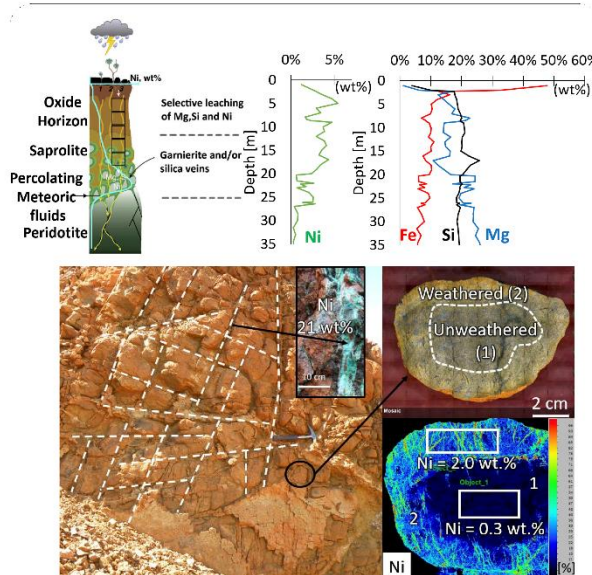


Fig 1. Typical geochemical profile of a laterite soil, and typical outcrop organization

## Methods

A discrete fracture matrix model (**DFM Model**) is built to study the impact of the **fracture connectivity** on the weathering.

The fractures correspond to the rock mass under advection. They are characterized by a hydraulic aperture and a penetration length. The matrix corresponds to the rock mass under diffusion.

The **two different geochemical fractures** and matrix **sub-domains** are **coupled** with an **exchange term**, which controls the **diffusive exchange** of the solutes.

Different fracture permeability configurations are studied to recreate field observations.

## Results

Integrating **explicitly** the geometry of the fracture network allows to successfully recreate Ni heterogeneities (and thus **weathering heterogeneities**) observed on the field. **Ni preferentially** migrates in the **fractures** before **diffusing** in the **matrix** creating **boulders with concentration zonation**.

The **local modification** of the **fracture permeability**, **controls** the **weathering progression front**. Flow barriers prevent its migration allowing to **recreate weathering configurations** observed in the field.

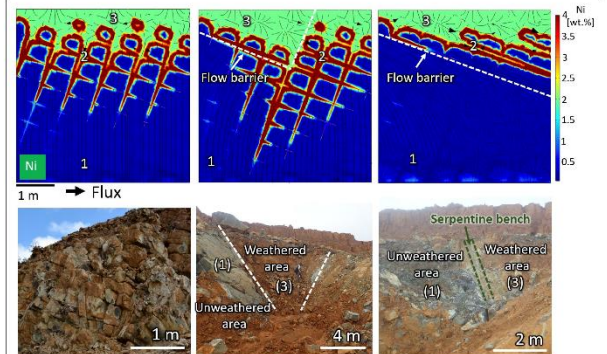


Fig 2. Ni distribution for different outcrop configurations and comparison with the field organization

## Conclusions

The **DFN modelling** allows to go deeper in the understanding of the impact of a **complex fracture network** on the weathering front progression. Depending on its **geometry** and **permeability**, the fracture network controls the fluid flow, hence favouring the formation of **topological weathering heterogeneities**.



## NICKEL ENRICHMENT FACTORS IN SAPROLITE ORES IN NEW CALEDONIA

CATHELINÉAU Michel – GOLFIER Fabrice  
FAVIER Sylvain – TEITLER Yoram

### General framework

Laterite nickel-ore deposits are of primary interest for Ni supply as they represent about 60% of the world resources in 2020. Laterite nickel-ore formation in New Caledonia is classically assumed to be governed by downward migration of waters with Ni, Si, Mg release from upper parts of the weathering profile and Ni-enrichment at the saprolite-bedrock interface.

### Objectives

Although the classical *per descensum* downward migration model broadly succeeds in explaining metal redistribution in laterite profiles, lateral heterogeneities in Ni ore distribution are commonly observed and cannot be solely explained by current 1D models. These heterogeneities seem to have been favored by secondary processes controlled by the combined effects of inherited tectonics, geomorphological evolution and hydrologic systems since the main laterite formation. Fluid flow and mass transfer processes are not purely downward at low temperature conditions, but can be also related to lateral fluid circulations, and local drainage along damaged zones in the vicinity of faults. Based on previous multi scale observations, this study investigates through reactive transport modelling the impact of the fracture connectivity on the Ni distribution.

### Methods

The modelling consists of dissolving a fractured olivine where fractures are the main channels of the fluid-flow. The fractures correspond to the rock mass under advection and diffusion. They are characterized by a hydraulic aperture governing their permeability, and a penetration length, which represent the quantity of olivine under advection. On the other hand, the matrix consists of the rock mass under diffusion. The two different geochemical sub-domains are coupled with an exchange term which controls the diffusive exchange of the solutes. Different fracture permeability configurations are studied to recreate field observations and in particular, their behaviour as both drain and permeability wall.

### Results

The classical outcrop organization in the saprolite horizon in New Caledonia, is characterized by an intensively fractured rock mass, where the fractures drive the weathering front progression (Fig1). Fractures are, therefore, particularly rich in Ni (up to 21wt%). The sub-orthogonal organization of the fracture network results in the formation of boulders in the matrix, which display a spheroidal weathering. While the most outer part of the boulder is weathered, hence displaying a Ni enrichment of ca. 2wt%, the inner part remains mostly unweathered (Fig1).

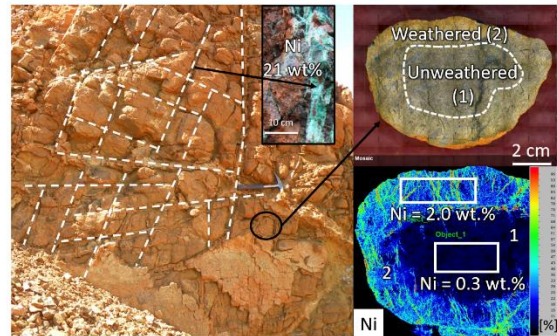


Figure 1. Typical outcrop organization on the saprolite horizon, with its Ni distribution in the fractures and in the boulders

The modelling of an olivine block characterized by a sub-orthogonal fracture network, successfully recreates the outcrop organization (Fig2.a). Indeed, the model can be divided into 3 different areas. The first one (1) at the bottom of the model consists of the unweathered part of the block which has not yet been reached by the weathering front. The second area (2) corresponds to a transition area, where the weathering front progression is driven by the fracture network. Ni is mainly located in the fractures and begins to diffuse in the matrix, resulting in the formation of boulders. The last area (3) corresponds to the weathered part of the model, where the diffusive weathering front has dissolved all the silicates into a 2%wt-Ni-rich goethite.

The addition of permeability walls materialized by (i) a dihedral (Fig2.b) and (ii) a sub-horizontal layer (Fig2.c), highlights the impact of permeability

FAVIER Sylvain, TEITLER Yoram

LABORATORY: GeoRessources

PROJECT LEADERS: CATHELINÉAU Michel, GOLFIER Fabrice

heterogeneities on the flux distribution and therefore on the weathering processes. Indeed, by concentrating the flux at its lowest point, the dihedron favours a more intense weathering of the matrix in the vicinity of the fractures situated below (zone (a)), and conversely favours the formation of poorly weathered areas (zone (b)). The field organisation of the regolith in presence of a dihedron tends to agree with this result, even though only the upper part of the dihedron is visible. Indeed,

a weathered area (zone 3) is clearly visible between two unweathered planes delimiting a poorly weathered area (zone 1) (Fig2.b). Likewise, the flow barrier drives a lateral weathering by inhibiting the role of the sub-vertical fractures. The weathering only occurs at the hanging wall of the flow barrier (zone 3), while the foot wall remains mostly unweathered (zone 1), which is consistent with the field observations (Fig.2c).

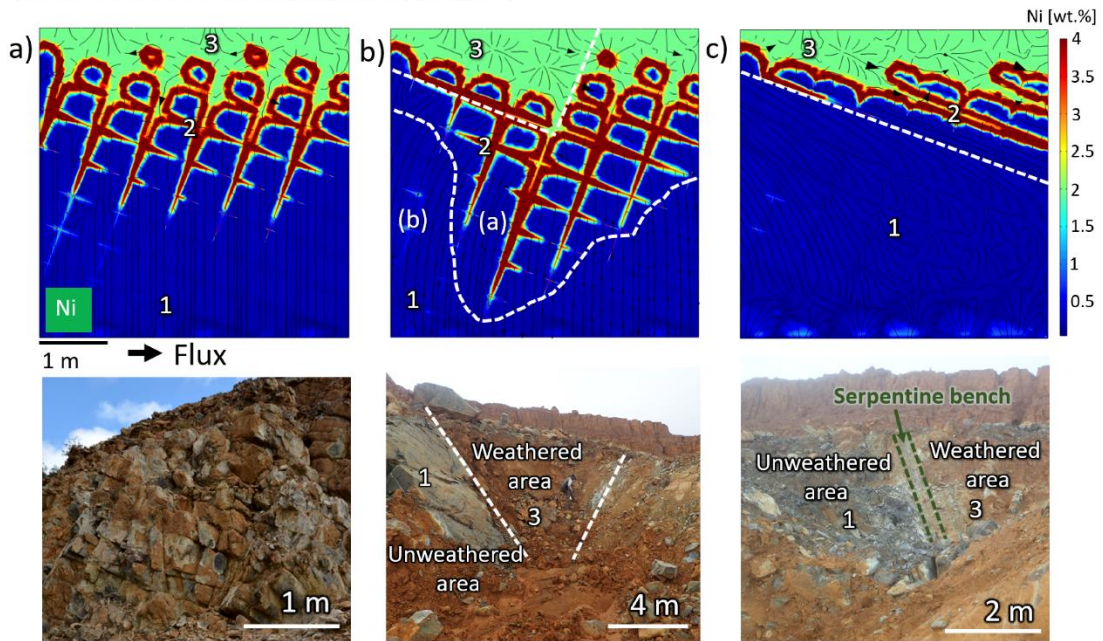


Figure 2. a) Ni distribution and outcrop organization in New Caledonia similar to DFM models for a) a typical outcrop configuration, b) a dihedron configuration, c) a flow barrier

### Perspectives

The Discrete Fracture Matrix (DFM) modelling allows to go deeper in the understanding of the impact of a complex fracture network in the Ni heterogeneous distribution in the saprolite horizon. Depending on its geometry and permeability, the fracture network controls the fluid flow, hence favouring the formation weathering heterogeneities. However, fractures are not the only permeability heterogeneities encountered in the field. Indeed, each part of the laterite profile, ie. bedrock, saprolite horizon, and oxide level, are characterized by a different permeability which can then impact the weathering front progression and thus, the Ni distribution. Hence, next steps, would be to dynamically take into account the impact of mineralogical changes on the permeability distribution in the matrix.

### Acknowledgements

This work is part of S. Favier PhD Thesis (MESR fellowships) cofunded by the CNRT project "TRANSNUM", and LabEx RESSOURCES21.

## BREEDING THE ULTIMATE EUROPEAN NICKEL PHYTOMINING CROP: A BIOMOLECULAR AND ECO-PHYSIOLOGICAL STUDY

Serigne N. LY, Antony van der ENT, Mark G. M. AARTS, Stéphanie OUVRARD, Guillaume ECHEVARRIA

### General framework

Nickel is an important metal used in a wide variety of industrial processes such as in the manufacture of superalloys, stainless steel, and rechargeable batteries. Due to the latter one, its demand increases proportionally. However, the mining sites are being exhausted due to many factors (expanding economics, burgeoning populations, and disarrayed industrialization) (Sheoran et al., 2009). Agromining is a variant of phytoextraction which use hyperaccumulators species to extract nickel from contaminated or naturally rich soils (low grade for mining) followed by many operations for bio-ore recovery. To be efficient, nickel agromining requires selected HA ('metal crops') with some exceptional traits (van der Ent et al., 2015) such as high biomass and Ni accumulation (Li et al., 2003).

### Objectives

During the last decade, intense research has been carried out to improve the agromining ability of certain promising hyperaccumulators plants (Bani et al., 2015; Kidd et al., 2018; Nkrumah et al., 2019). However, no study has focused on breeding these wilds species with exception of the works carried out by Li et al., 2003 and Sterckeman et al., 2019 on

*Odontarrhena chalcidica* and *Noccea caerulescens* respectively. Most of the research was concentrated on discovering new hyperaccumulating plants, understanding their ecophysiology, and showing their genetic difference in metal uptake and biomass production, rather than breeding them for domestication (Bhargava et al., 2012). This work aimed to provide more information on the phenotypic variability of *Bornmuellera emarginata* and hence to analyze the accessions in the purpose of plant breeding.

### Methods

The accessions used during this study were collected at late July 2021 from different regions in Greece. We did a phenotypic characterization which was based on visually traits. The biomass components (plant height, number of ramifications, leaf length and width) was recorded. The accumulated nickel was measured by grinding leaves and stems, then 0.5 g were digested using 5 mL HNO<sub>3</sub> and 2.5 mL H<sub>2</sub>O<sub>2</sub>. After cold digestion during 16h, samples were placed in a DigiPREP system for 180 min and filtered before ICP analysis.

### Results

The nickel accumulation recorded among the accessions differed significantly (Fig.1a). We have observed that most of the accession had the threshold of 1000 mg kg<sup>-1</sup> Ni in their shoot (Fig.1b) which confirms their hyperaccumulator status. The highest concentration was found in the group from Metsovo (MV1 genotypes 6,246.97 mg kg<sup>-1</sup>) (Fig.1b).

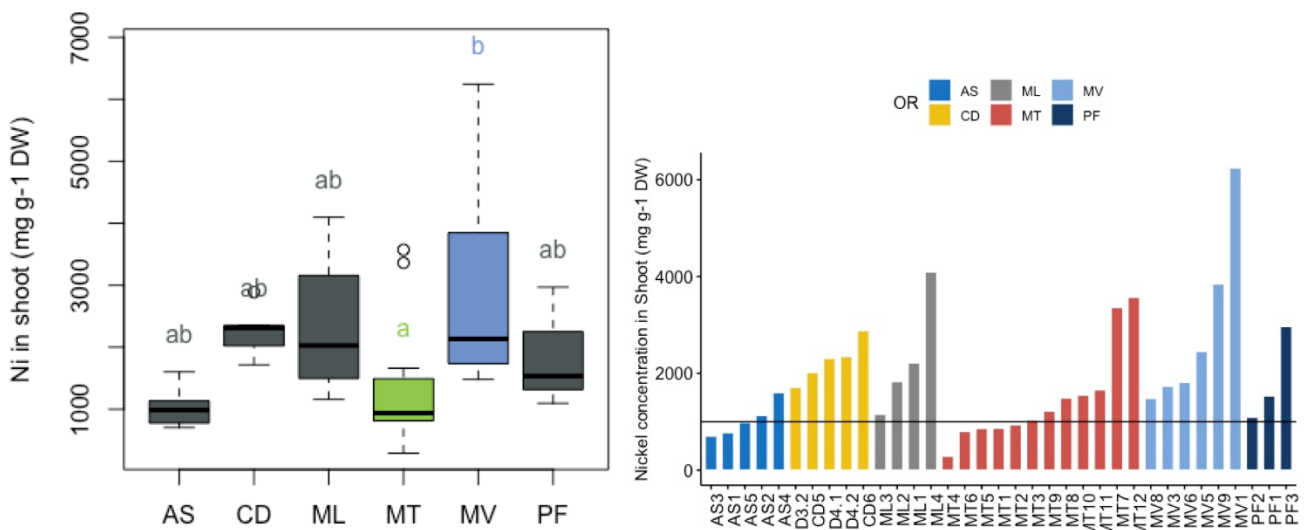


Fig 1. a) Mean of Ni shoot concentration in 6 populations. The vertical bar represents the SD and the letter above are significant level of difference. b) Nickel concentration for each genotype. The black line represents the threshold (1000 mg. g<sup>-1</sup>) of Ni accumulation

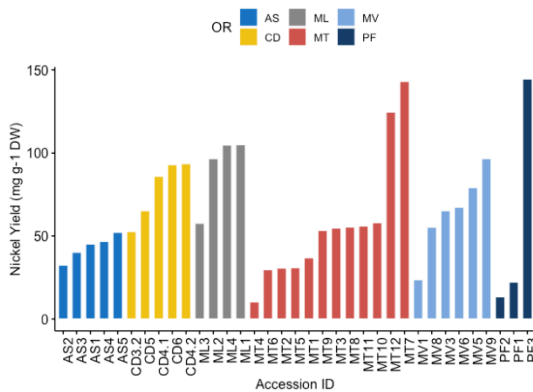
SERIGNE LY

LABORATORY : LABORATOIRE SOL ET ENVIRONNEMENT

PROJECT LEADER: GUILLAUME ECHEVARRIA

However, AS1, AS3, AS5 did not reach the threshold and had a concentration of 775.34, 705.1 and 985.51 mg kg<sup>-1</sup> of Ni respectively (Fig.1b). This trend has been observed in some genotypes of the Mantoudi population. The genotypes MT1, MT2, MT4, MT5 and MT6 also did not reach 1000 mg kg<sup>-1</sup> Ni concentration.

The nickel yields (Fig.2a), which are biomass times Ni shoot concentration, showed a huge variation among Mantoudi (MT) and Pefki (PF) genotypes.



However, a low variation was recorded within AS and CD genotypes. The genotypes PF3, MT7, MT12, ML1 and ML4 produce the highest Ni yields (Fig.2a). These genotypes could be interesting for Ni agromining.

The mean value of the 8-phenotypic traits was used to generate a cluster to see how close all the accessions were. We observed four clusters with AS and CD grouped in one cluster are less close to the others population.

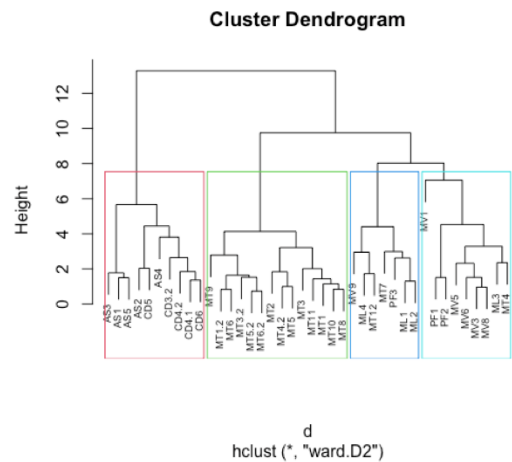


Fig 2. a) Nickel Yields of all the genotypes from different population. b) Euclidian distance and clustering dendrogram based on the phenotypic traits

Although they are grouped in different clusters, the populations from MT, ML, MV, PF and MV share some similarities.

### Perspectives

We are making the transcriptomic study to unravel the genes involved in Ni uptake, translocation, and storage in *B. emarginata*. The impact of pH and Ni variation will be evaluated on the Ni physiology.

We will go further and produce three more generations for the fixation of the best traits. We plan to test the most promising genotypes in the field to decipher their capacity for Ni agromining.



REEs

# Integrated project on Rare Earth Elements

# High-energy interference-free K-lines synchrotron X-ray fluorescence microscopy of rare earth elements in hyperaccumulator plants

Antony van der Ent<sup>1</sup>, Dennis Brueckner<sup>2</sup>, Clément Layet<sup>1,3</sup>, Marie Le Jean<sup>3</sup>, Damien Blaudez<sup>3</sup>

<sup>1</sup>Université de Lorraine, INRAE, LSE, F-54000 Nancy, France.

<sup>2</sup>Deutsches Elektronen-Synchrotron DESY, D-22607 Hamburg, Germany.

<sup>3</sup>Université de Lorraine, CNRS, LIEC, F-54000 Nancy, France.

## General framework

The use of X-ray fluorescence methods is non-destructive and able to quantify a wide range of covering most of the Periodic Table. Synchrotron-based micro-X-ray fluorescence analysis ( $\mu$ XRF) is a non-destructive and highly sensitive technique, but not able to differentiate between rare earth elements (REEs) due to their overlapping L-shell X-ray emission lines in the presence of high concentrations of common transition elements. We aimed to test high-energy interference-free excitation of the REE K-lines in hyperaccumulator plant tissues.

## State of the art

Hyperaccumulator plants can accumulate and tolerate high concentrations of toxic elements in their living shoots. Thus far, ~700 plant species have been reported globally to hyperaccumulate a large variety of metals and metalloids, less than 25 plant species are known as REE hyperaccumulators. The uptake and transport mechanisms of REEs are yet to be fully understood, which limits the development of phytotechnologies by using these REE hyperaccumulator plants. The distribution of REEs is most frequently analysed with LA-ICP-MS but the destructive nature of this technique is a major disadvantage. In contrast, synchrotron-based micro-X-ray fluorescence analysis ( $\mu$ XRF) is a non-destructive and highly sensitive technique that has been used to investigate numerous plants. Most synchrotron  $\mu$ XRF beamlines are limited to <21 keV incident energy for the end station due to the use of Kirkpatrick-Baez (K/B) mirror optics, which cannot be used at higher energies as the rhodium coating of the K/B mirror results in a high-energy cut-off of 23 keV, well below that required to excite the K-lines of the REEs (38.92 keV absorption edge for La). SDD detectors with an energy-resolution of 125 eV are typically not able to differentiate between the various REEs due to their overlapping L-shell X-ray emission lines that are separated only by tens of eVs in the presence of transition elements (such as Ti, Fe, Mn, Cr).

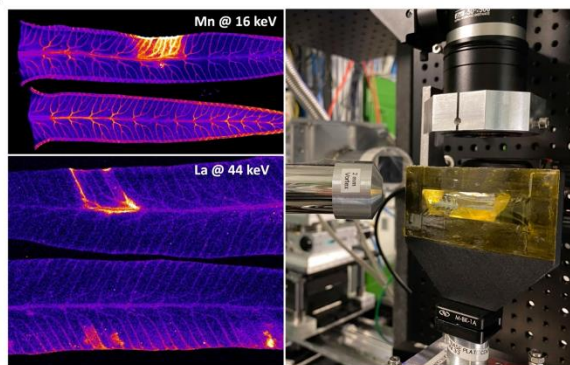


Fig 1. Synchrotron  $\mu$ XRF maps of Mn and La in freeze-dried *Dicranopteris linearis* pinnules at 16 and 44 keV incidence energy.

## Methodology

The X-ray fluorescence microscopy experiment was undertaken at PETRA III (Deutsches Elektronen-Synchrotron DESY), a 6 GeV synchrotron radiation source, specifically at the hard X-ray microprobe undulator beamline P06. This study used a combination of CRL optics to obtain a focused incident beam with an energy of 44 keV and an extra-thick silicon drift detector (SDD) optimized for high-energy X-ray detection to detect the K-lines of yttrium (Y), lanthanum (La), cerium (Ce), praseodymium (Pr) and neodymium (Nd) without any interferences due to line overlaps, as with their respective L-lines.

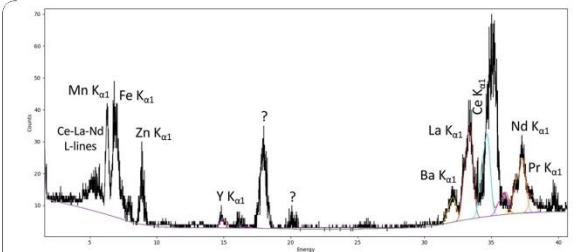


Fig 2. Representative XRF spectra of the REE hyperaccumulator *Dicranopteris linearis* acquired at 44 keV.

## Results

High-energy excitation of La and Ce in the hyperaccumulator organs was successful, but highly inefficient and therefore slow (approx. 10-fold slower than similar maps at lower incident energy) and only useful for high concentration REE samples. This limits application to frozen-hydrated or freeze-dried specimens with high prevailing REE concentrations. In this experiment we used a 2 mm thick SDD which has substantially greater efficiency (approx. 10%) compared to the standard 0.45 mm thick chips (<1%). Still, detection efficiency is rather low for the La K-line. Detectors with greater stopping power, such as germanium detectors, could be used, but these are typically not suitable for imaging due to their slow speed. The high energy fluorescent X-rays (as well as scatter) excite the internal structure of the SDD detector, resulting in a massive noise floor at <10 keV, and distinct tin (Sn) peak (from the solder inside the electronics board).

## Perspectives

The use of high-energy K-line excitation of REEs under the experimental conditions described here is relatively slow (per pixel dwell in the order of 100–500 ms) and is only suitable for highly concentrated samples (>1000 mg kg<sup>-1</sup> tREE bulk concentration). If interfering elements (Cr–Ni) are not abundant, or at least 10–100-fold lower than the REEs in the sample in question, then L-line excitation of REEs using lower energy (11–16 keV) is much more efficient (close to 100% efficiency on standard SDD detectors) permitting 5–20 ms dwell times per pixel.

## HIGH-ENERGY X-RAY FLUORESCENCE MICROSCOPY OF RARE EARTH ELEMENTS IN HYPERACCUMULATORS

Antony van der Ent, Damien Blaudez,  
Clément Layet, Marie Le Jean

### General framework

Hyperaccumulator plants can accumulate and tolerate high concentrations of toxic elements in their living shoots. Thus far, ~700 plant species have been reported globally to hyperaccumulate a large variety of metals and metalloids, less than 25 plant species are known as REE hyperaccumulators. The uptake and transport mechanisms of REEs are yet to be fully understood, which limits the development of phytotechnologies by using these REE hyperaccumulator plants. The distribution of REEs is most frequently analysed with LA-ICP-MS but the destructive nature of this technique is a major disadvantage. In contrast, synchrotron-based micro-X-ray fluorescence analysis ( $\mu$ XRF) is a non-destructive and highly sensitive technique that has been used to investigate numerous plants. However, it is not able to differentiate between rare earth elements (REEs) due to their overlapping L-shell X-ray emission lines in the presence of high concentrations of common transition elements.

### Objectives

This study uses a combination of CRL optics to obtain a focused incident beam with an energy of 44 keV

and an extra-thick silicon drift detector (SDD) optimized for high-energy X-ray detection to detect the K-lines of yttrium (Y), lanthanum (La), cerium (Ce), praseodymium (Pr) and neodymium (Nd) without any interferences due to line overlaps.

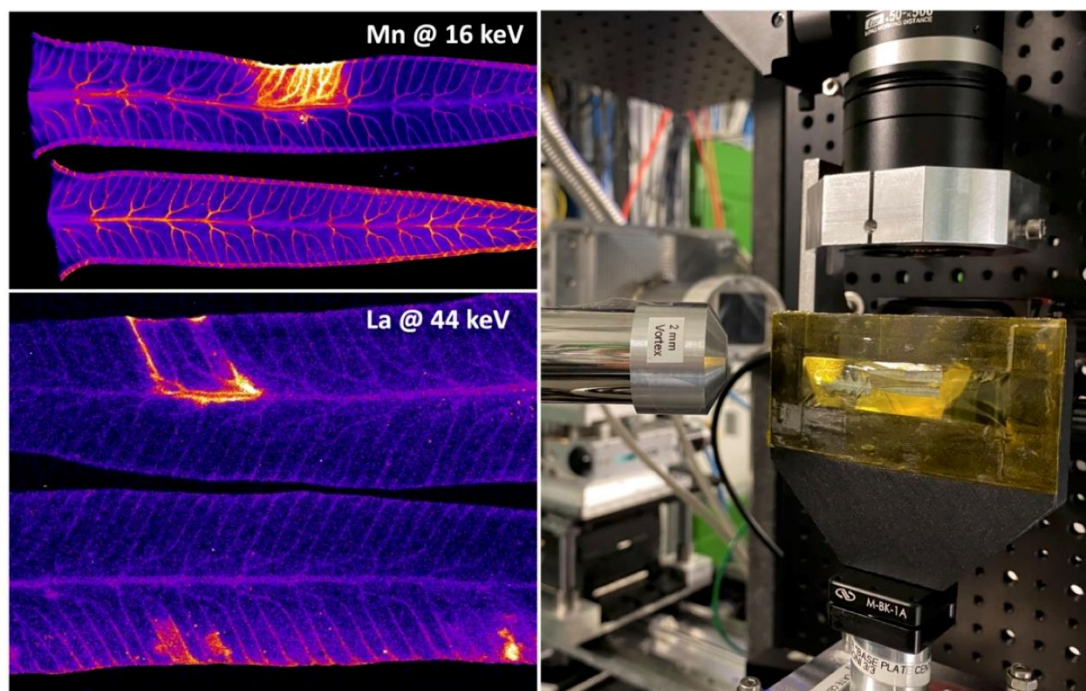
### Methods

The X-ray fluorescence microscopy experiment was undertaken at PETRA III (Deutsches Elektronen-Synchrotron DESY), a 6 GeV synchrotron radiation source, specifically at the hard X-ray microprobe undulator beamline P06. We aim to test high-energy interference-free excitation of the REE K-lines on hyperaccumulator plant tissues.

### Results

High-energy excitation of La and Ce in the hyperaccumulator organs was successful, but highly inefficient and therefore slow (approx. 10-fold slower than similar maps at lower incident energy) and only useful for high concentration REE samples. This limits application to frozen-hydrated or freeze-dried specimens with high prevailing REE concentrations. Most synchrotron  $\mu$ XRF beamlines are limited to < 21 keV incident energy for the end station due to the use of Kirkpatrick-Baez (K/B) mirror optics, which cannot be used at higher energies as the rhodium coating of the K/B mirror

Figure 1. Synchrotron  $\mu$ XRF maps of Mn and La in freeze-dried *Dicranopteris linearis* pinnules at 16 and 44 keV incidence energy.



results in a high-energy cut-off of 23 keV, well below that required to excite the K-lines of the REEs (38.92 keV absorption edge for La). There are few X-ray optics that are useable for higher energies, and only CLR lenses can be used. We were limited to 44 keV (just reaching the absorption edge of Nd at 43.57 keV) due to the limitation of digital pulse processors which have their upper limit at 42 keV, although this can be overcome by recalibration of the digital pulse-processor. The high energy of the fluorescent X-rays makes detection using conventional detectors very inefficient. In this experiment we used a 2 mm thick SDD which has substantially greater efficiency (approx. 10%) compared to the standard 0.45 mm thick chips (<1%). Still, detection efficiency is rather low for the La K-line. Detectors with greater stopping power, such as germanium detectors, could be used, but these are typically not suitable for imaging due to their slow speed. The high energy fluorescent X-rays (as well as scatter) excite the internal structure of the SDD detector, resulting in a massive noise floor at <10 keV, and distinct tin (Sn) peak (from the solder inside the electronics board).

In earlier studies La and Ce were detected in the conducting tissues, epidermis and in necroses in *D. linearis* and here we confirmed the distribution of La (Figure 1), Ce, Pr and Nd (data not shown) in conducting tissues and necrosis. However, the detection efficiency with 44 keV XRF scans was worse when compared to that with 16 keV scans. We have also undertaken a study using proton-induced X-ray emission (PIXE) analysis which is capable of exciting all of the REEs at their K-lines. However, it also suffers from low detection efficiency at high-energy due to the use of the Maia detector system (with a 0.5 mm chip thickness).

### Perspectives

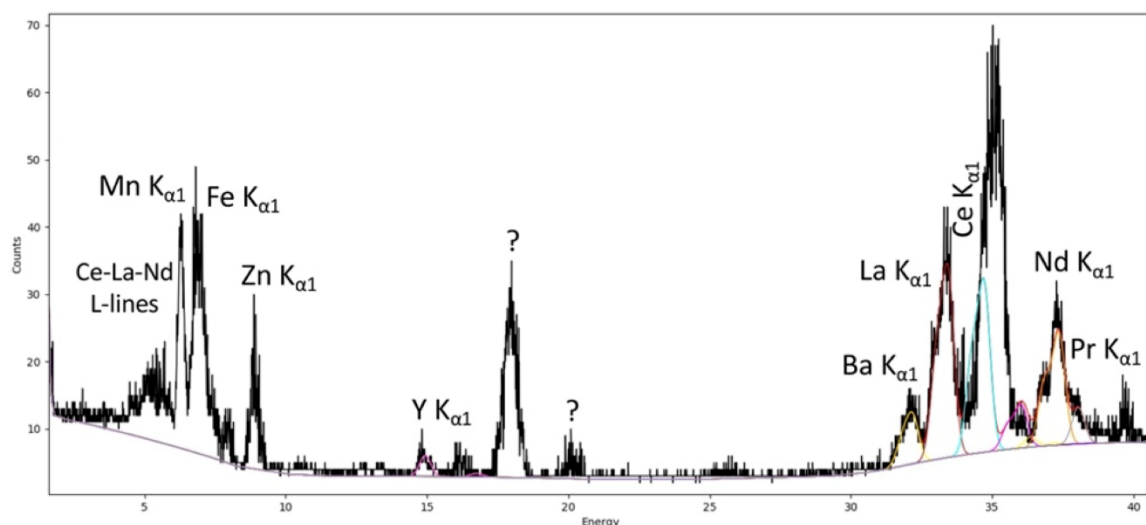
K-line excitation of REEs has scope for application in samples that are particularly prone to REE interfering elements, such as soil samples with high concomitant Ti, Cr, Fe, Mn, Ni concentrations. The use of high-energy K-line excitation of REEs under the experimental conditions described here is relatively slow (per pixel dwell in the order of 100–500 ms) and is only suitable for highly concentrated samples (>1000 mg kg<sup>-1</sup> tREE bulk concentration). If interfering elements (Cr–Ni) are not abundant, or at least 10–100-fold lower than the REEs in the sample in question, then L-line excitation of REEs using lower energy (11–16 keV) is much more efficient (close to 100% efficiency on standard SDD detectors) permitting 5–20 ms dwell times per pixel. However, this may be problematic in many plant samples as co-localization of La-Ce-Sm-Gd occurs, as has been shown previously in the REE (hyper)accumulator *D. erythrosora* (Le Jean et al. 2022).

### References

van der Ent A, Brueckner D, Spiers KM, Gerald Falkenberg G, Layet C, Liu W-S, Zheng H-X, Le Jean M, Blaudez D (2023) High-energy interference-free K-lines synchrotron X-ray fluorescence microscopy of rare earth elements in hyperaccumulator plants. *Metallomics*. Manuscript in Preparation.

Le Jean M, Montarges-Pelletier E, Rivard C, Grosjean N, Chalot M, Vantelon D, Spiers K, Blaudez D (2022) Locked up inside the vessels: Rare earth elements are transferred and stored in the conductive tissues of the accumulating fern *Dryopteris erythrosora*. *Environmental Science & Technology*. Manuscript under revision.

Figure 2. Representative XRF spectrum of a sample of the REE hyperaccumulator plant *Dicranopteris linearis* acquired at 44 keV.





Clément Layet

LABORATORY: LSE, LIEC

PROJECT LEADERS: Catherine Sirguez, Damien Blaudez, Patrick Billard, Marie Le Jean, Jean-Louis Morel

---

## COUPLING BIOLEACHING AND PHYTO-EXTRACTION OF RARE EARTHS FROM SOILS (PHYTOLIXTER)

### General framework

Rare earth elements (REEs) have currently a strategical interest for the development of new technologies, especially in the field of renewable energies. China is the main producer of these elements, from bastnasite, xenotime extractions, or clay adsorbed ions. However, REEs are also present at lower concentrations in some European deposits or soils. The main issue with REE extraction is that conventional methods involve a high risk of environmental degradation. The challenge is thus to develop innovative tools and processes to better control and exploit metal present in soils.

### Objectives

Among the metal extraction methods, agromining represents a promising way of exploiting low concentration deposits and recovering metal-rich wastes such as mine tailings. It is hypothesized that by increasing the bioavailability of REEs through carefully selected amendments and microorganisms, an increased quantity would be transferred to the accumulating species, thus improving site remediation and the development of the REE agromining. We aim to 1) identify microorganisms that bioleach REEs, 2) and locate new areas with REEs concentrations of interest for agromining.

### Methods

#### *Soil sampling and analysis*

The first search for soils of interest in Lorraine was carried out on the basis of outcropping geological materials. According to the literature, the Aalenian geological stage could lead to a higher concentration of REEs in soils developed on these materials. This geological layer has been exploited for iron

ore mining in northern Lorraine. We decided to extend our research to soils from former iron blast furnace slag areas. Several works highlighted that REEs can be transferred to slag after iron ore use in blast furnace. Thus, several sampling sites were selected on the basis of the presence of slags on aerial pictures of Lorraine during the beginning of 20<sup>th</sup> century. On each site, samples were collected, sieved at 2 mm and dried at 40 °C for three days before storage at 20°C. REE content in samples was measured by ICP-MS after total digestion by hydrofluoric acid.

#### *Selection of REE bioleaching bacteria*

A new screening method based on a whole cell biosensor that emits light in a dose-dependent manner when exposed to REE was used for selecting bacteria with REE leaching ability.

The bacterial strains were inoculated in a soil from a metallurgy slag area for 24h. Soil-water extracts were then prepared filtered at 0.22 µm and assayed for bioavailable REE content with the biosensor (figure 2a) to evaluate the solubilization of REEs by the different strains. The bioassays were performed in 96-well microtiter plates, and luminescence was measured using a FLX-Xenius (SAFAS, Monaco) plate reader. A standard curve was generated with known concentrations of NdCl<sub>3</sub> and used to calculate the REE equivalent concentrations of the samples.

### Results

#### *Concentrations of REEs in soil from iron blast furnace areas*

The total REE concentrations in soils from mine tailings and blast furnace slags are presented in figure 1. These results highlight that soils from blast furnace slag areas have a higher REE concentration than those of the iron ore developed soils (figure 1a). Furthermore, these REE concentrations can be compared to other REE concentrations from

Clément Layet

LABORATORY: LSE, LIEC

PROJECT LEADERS: Catherine Sirguez, Damien Blaudez, Patrick Billard, Marie Le Jean, Jean-Louis Morel

Chinese mine tailings and red mud in figure 1b. Equivalent concentrations between the iron blast furnace slag heaps and certain sampling areas in China and red mud can be

found. Furthermore, total REEs concentrations are higher than concentrations found in French soils with an average concentration of  $160\text{mg}\cdot\text{kg}^{-1}$  (figure 1b).

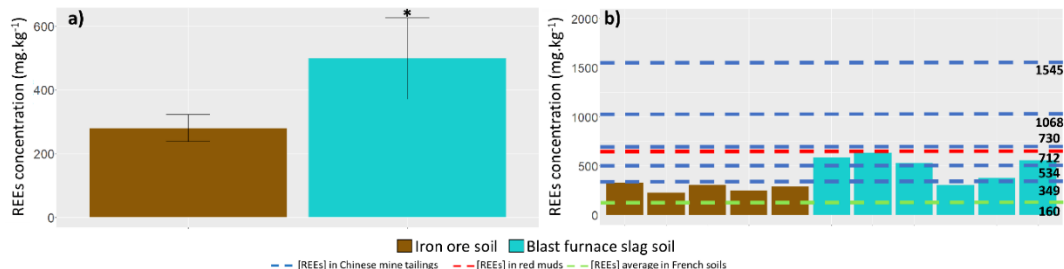


Figure 1: REE concentration in iron ore soils and blast furnace slag soils, with a Kruskal Wallis comparison (\* denotes a significant difference) based on soil type (a), and the different total REE distribution for each sampled soils (b), with REE concentration of various REE sources from mine tailings, red mud, and average concentration in French soil represented by dashed lines.

### Example of REE bioleaching potential of two bacterial strains

The ability of two bacterial isolates to leach REE from soil is presented in figure 2b. The REE concentration in water-soil extract from the control sample was below the limit of quantification. In contrast, the inocula-

tion of two selected bacteria significantly increased REE availability in soil after 24h of incubation. There was also a significant difference of solubilization between the two strains studied. This first result supports the use of the biosensor-based approach to select new strains more efficient in the REE solubilization process.

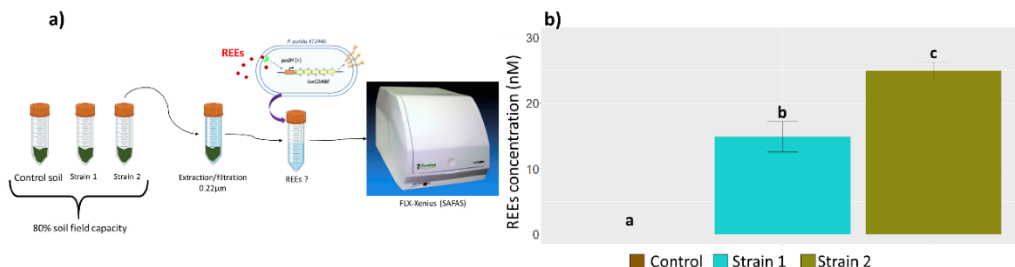
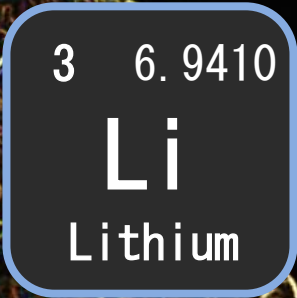


Figure 2: Biosensor based-assay of REE bioavailability in soil inoculated or not with bacterial strain (a), and REE concentrations of soil-water extracts after 24 h incubation (b). The concentration of the control sample was below the limit of quantification. Different letters (b) denote significant differences between modalities (Kruskal-Wallis test).

### Perspectives

The results show that we can increase the panel of areas in Lorraine where it is possible to have REEs concentrations of interest for agromining. Based on a database from the CEREMA agency, we will estimate the total area where it is likely to find higher REEs concentrations. The biosensor protocol allowed us to highlight a significant higher REE concentration in bacterium inoculated soil solutions. This method is now developed for several bacteria strains and

combined to ICP-MS analyses to confirm the solubilization of REEs in soils. We are currently working on the solubilization potential of different classes of REE-rich soils (mine tailing, slags, etc.) by different bacterial strains. In parallel with the biosensors and soil prospections, we have developed a plant cultivation tool inspired by the RHIZOtest. This system will allow us to observe more easily the modifications induced in different soils by plants, or the amendments chosen to improve REE phytoextraction.



# Integrated project on lithium

Vincent BOS

LABORATORY: GéoRessources UMR 7359

PROJET LEADER: Y. Gunzburger ; A. Chagnes, A. Samper.

---

## RECONFIGURATION OF LITHIUM GEO-ECONOMY : A GLOBAL PRODUCTION NETWORKS AND INFRASTRUCTURES APPROACHS IN AUSTRALIA AND LATIN AMERICA

Vincent Bos<sup>1</sup>

### General framework

Lithium-based energy transition provokes a reconfiguration of the global chains of lithium and its geographies whether we consider the stages of extraction or transformation of the resource. The evolution of the global chains of lithium are analyzed through the Global Production Networks (GPN) approach, a heuristic framework that helps to better understand the organization of the chains of interconnected functions, operations and transactions through which a service (electrification of mobility) or good (lithium products and lithium-based devices such as Lithium-Ion Batteries), is produced, distributed and consumed in a globalized yet fragmented economic system (Coe, Dicken, Hess, 2008)<sup>2</sup>. To do so we focus on two core state of the lithium industry in the extractive chains: Australia and Chile. The analyze pays particular attention to the transformations led by the lithium industry through a multi-scalar and pluri-actors perspective analyzing the strategies of companies, States and even indigenous communities involved at each stage. Australia is a blind spot in the social sciences analysis of the lithium economy, yet it produces about 50% of the resource followed by Latin America (about, 33%) (USGS, 2022) and is characterized by a vivid transformation of the chains as the local industrialization of lithium around several clusters in Western Australia demonstrates. Our unique cross-analysis relies on our

expertise of the Latin American chains of lithium (Bos, Forget, 2021)<sup>3</sup>. We demonstrated that the global chain of lithium is characterized by a forward and backward integration process between actors that control the deposits and actors from the manufacturing stage who want to secure their access to the resource (Bos, Forget, 2021; Forget, Bos, 2022). We also demonstrated the central role of States in the reorganization of the practices and, hence the networks territoriality due to their function of inter-scalar mediators, between local deposits and companies and global markets (*idem*). The focus on infrastructures enriches the research conducted in economic geography through the GPN lengths (Coe, 2020)<sup>4</sup>. Being a dynamic way of cooperation between social sciences and geosciences, infrastructures constitute a shared object by our different disciplines. This approach favors the analysis of local transformations in mining territories and industrial clusters and helps understanding how global energy transition (re)shape local territories.

### Objectives

At a global scale, the GPN approach allow **to identify** the main sites of lithium production (extraction + transformation) in Australia and their operators to categorize them based on the sectors and strategies followed, precisng our previous observations (Bos, Forget, 2021; Forget, Bos, 2022<sup>5</sup>). At a local scale, identifying and mapping the connections between mining sites and industrial areas (industries of transformation, ports of export) demonstrate how the global (companies) affect the local and how the local (geology, networks of actors and infrastructures, practices and governance, etc.) (re)shape the global. The two fieldworks realized in both countries in the main and future

---

<sup>1</sup> The post-doctorate contract began in September, 2021 and ended in November, 2022.

<sup>2</sup> Coe N. M., Dicken P., Hess M. "Global Production Network: realizing the potential", *Journal of Economic Geography*, 2008, vol. 8, Issue 3, pp. 271-295. <https://doi.org/10.1093/jeg/lbn002>

<sup>3</sup> Bos V., Forget M.E., 2021. « Global Production Networks and the lithium industry. A Bolivian perspective », *Geoforum*, vol. 125, pp. 168-180. <https://doi.org/10.1016/j.geoforum.2021.06.001>

<sup>4</sup> Coe N.M., "Logistical geographies", *Geography Compass*, 2020, vol. 14, Issue 10. <https://doi.org/10.1111/gec3.12506>

<sup>5</sup> Forget M.E., Bos V. "Harvesting lithium and sun in the Andes. Exploring new materialities and energy justice of energy transition", *Energy Research & Social Science*, 2022, vol. 87, <https://doi.org/10.1016/j.erss.2021.102477>

Vincent BOS

LABORATORY: GéoRessources UMR 7359

PROJET LEADER: Y. Gunzburger ; A. Chagnes, A. Samper.

territories of extraction and transformation gave us **better insights** of the forms, dynamics and strategies of entrepreneurial, state and social strategies towards the transformation of the lithium mining industry and its socio-environmental consequences that could help identify brakes and levers of mining activity in the two States but also elsewhere, especially in France regarding the strategy of local extraction and industrialization (giga-factories). Both objectives contribute **to develop a methodology that can be reproduced** on other territories and commodities such as critical minerals of energy transition (nickel, manganese, rare earths, copper, etc.).

### Methods

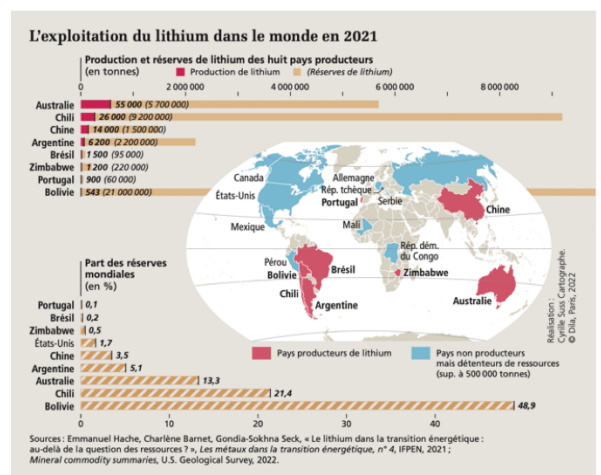
Crossing the GPN and infrastructure approaches is used for precisizing the role played by logistics in the reconfiguration of the GPN of lithium and how infrastructures affect territories and actors.

### Results

We have created the first satellite maps produced in social sciences of the lithium mine of Greenbushes (Australia) and SQM in Chile (see report 2021). Crossing the satellite imagery of lithium mines in the two countries with key interviews and *in situ* observations of mining and industrial area allowed us to produce the first visual analysis of the lithium industry through the choremes, *id est* the elementary structures of the geographical space. This constitutes a unique achievement of the lithium-based energy transition in geography. We demonstrate how the lithium-based energy transition transform local territories following a pattern of “remote extraction

sites / industrial transformation sites around cluster / maritime interfaces”. This enriches the results of extractive industries in Latin America published at the end of 2021<sup>6</sup>. **4 papers are to be published** in 2023 based on this post-doctorate. One in the French press on the dynamics of the lithium industry in Chile and Australia<sup>(see, Fig. 1; Bos, Forget, 2023)<sup>7</sup></sup>. One on the ecosystems of the lithium-based energy transition in both countries mobilizing a landscape perspective combining the GPN and infrastructures approaches<sup>(Bos, Forget, Gunzburger, 2023)<sup>8</sup></sup>. An introductory paper to a Special Issue on the lithium dynamics that I coordinate with three colleagues from France, Chile and Australia<sup>(Forget, Bos, Prieto, Carballo, 2023)<sup>9</sup></sup>. A paper in legal-geography on the strategies of access and tactics of resistance in Maricunga, the new coveted territory of lithium extraction in Chile<sup>(Nicolas-Artero, Forget, Bos, 2023)<sup>10</sup></sup>. **2 were published in 2021 and 2022**. The post-doctorate generated **15 conferences in 3 languages in 4 countries**<sup>(two will take place in 2023)</sup>.

Figure 1. Global lithium production and resources in 2021.



<sup>6</sup> Forget M.E., Carrizo S.C. Bos V., 2021. « Ressources extractives sud-américaines. Mondialisation et territorialisation des marges », *L'information géographique*, vol. 85, pp. 37-60. <https://doi.org/10.3917/lig.854.0037> We are waiting for the peer-reviews of the schemes before publishing them here (see note 7).

<sup>7</sup> Bos V., Forget M.E., 2023. « Géopolitique du lithium. Perspectives latino-américaines et australiennes », *Questions Internationales*.

<sup>8</sup> Bos V., Forget M.E., Gunzburger Y. 2023. « The eco-systems of the lithium-based energy transition, from local to global. Characterizing lithium landscapes materialities in Chile and Australia », *The Extractive Industries and the Society*.

<sup>9</sup> Forget M.E., Bos V., Prieto M., Carballo A.S. 2023. « Lithium Dynamics. Global trends and local spatializations », *The Extractive Industries and Society*.

<sup>10</sup> Nicolas-Artero Ch., Forget M.E., Bos V. 2023. « Overlaps. Strategies of access and tactics of resistance. Lithium Dynamics in Maricunga, Chile. A geogical perspective », *Journal of Latin American geography*.

POSTDOC RESEARCHER: BALLOUARD Christophe

LABORATORY : GeoRessources/CRPG

PROJECT LEADER : MERCADIER Julien, MARROCCHI Yves

## ORIGIN AND EVOLUTION OF LI-PEGMATITE AS SEEN THROUGH A MULTI-ISOPTOPIC STUDY: APPLICATION TO THE ORANGE RIVER PEGMATITE BELT (SOUTH AFRICA)

BALLOUARD Christophe – MERCADIER Julien – MARROCCHI Yves – EGLINGER Aurélien – MILLOT Romain\* – LACH Philippe\* – MELLETON Jérémie\* - PICHAVANT Michel\*\* (\*: BRGM Orléans, \*\*: ISTO, Orléans)

### General framework

Peraluminous rare-metal pegmatites represent the main source of hard-rock lithium and related critical metals (e.g., Nb, Ta). However, the processes involved in their genesis are not fully understood. These include the degree of fractional crystallization needed to generate such highly evolved melts, and the impact of late magmatic-hydrothermal processes for the genesis of economic mineralizations. Those problems related to Li-pegmatite genesis in general pertain to the Mesoproterozoic Orange River pegmatite belt in Southern Africa (Ballouard et al., 2020, [doi.org/10.1016/j.oregeorev.2019.103252](https://doi.org/10.1016/j.oregeorev.2019.103252)). In this region, about 30000 pegmatite dykes were emplaced at ca. 1000 Ma including barren as well as Li-mineralized pegmatites hosting spodumene and lepidolite. The trace element compositions of early magmatic muscovite suggest that the parental melts of barren intrusions were depleted in rare-metals compared to that of Li-mineralized pegmatites but the processes controlling the fertility of those melts are uncertain. Moreover, a significant part of the Li-mineralization hosted by the pegmatites, such as lepidolite, occurs as replacements or overgrowths on early magmatic mineral phases, and the nature and origin of the media from which these Li-rich micas have crystallized remain unclear.

### Objectives

Our main objective is to understand why some pegmatites from the Orange River belt are Li-fertile or Li-barren by tracing the differentiation processes that may have impacted Li enrichment from source to emplacement crustal levels. The large mass differences between the two isotopes of lithium ( $^7\text{Li}$  and  $^6\text{Li}$ ) can lead to significant fractionation in relatively low temperature felsic magmatic systems such as pegmatites. Therefore, the Li isotope systematic has a good potential as a tracer for the processes controlling Li enrichment in pegmatites, such as fractional crystallization, liquid-liquid immiscibility, degassing or metasomatism. However, previous Li isotope studies of pegmatites were

focused on bulk analyses that do not allow to identify micrometer-scale kinetic or equilibrium fractionation processes that can occur in such magmatic-hydrothermal systems. *In situ* analyses of Li isotope in mica by ion microprobe (SIMS) was developed in order to tackle this issue.

### Methods

Mica reference materials for *in situ*  $\delta^7\text{Li}$  analyses were developed based on homogeneity test using SIMS (CRPG) before bulk analyses via solution MC-ICP-MS (BRGM). We now have eight mica reference materials, including two (Fe)-muscovites, two biotites, two lepidolites and two zinnwaldites. Our results indicated that SIMS measurements of  $\delta^7\text{Li}$  are highly affected by matrix effects. Such instrumental mass fractionation (IMF) involves the use of strictly matrix-matched standards for the correction of the isotope composition of Fe-Mg-rich micas (biotite-zinnwaldite series). However, muscovite-lepidolite series mica compositions can be corrected based on the anticorrelation between IMF and differences between the proportion of trioctahedral Si and sum of bivalent cations in the octahedral mica sites (Fe, Mg, Mn). Such correction was applied to muscovite-lepidolite micas of the Orange River belt pegmatites. SIMS analyses of muscovite and coexisting rhyolite glass, using NIST 610 as reference material, were performed on the Macusani Tuff from Peru in order to estimate the Li isotope fractionation factor between muscovite and silicate melt.

### Results

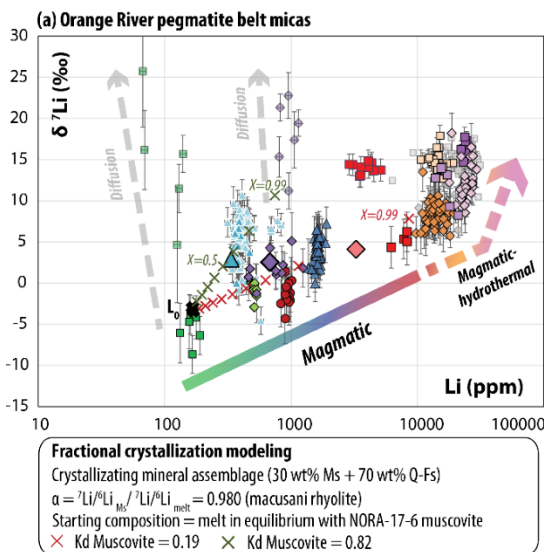
Our results indicate a significant variability of the  $\delta^7\text{Li}$  composition of micas from pegmatites of the Orange River belt from about -10 to 25 ‰ (Fig. 1a). Some muscovite crystals with relatively low Li concentrations (< 1000 ppm), were likely affected by kinetic diffusive effects, reflecting preferential losses of  $^6\text{Li}$  compared to  $^7\text{Li}$ , inducing substantial increase of  $\delta^7\text{Li}$  up to 25 ‰. However, most micas appear to be unaffected by such processes and their Li concentrations and  $\delta^7\text{Li}$  value globally correlate. Magmatic muscovite from barren pegmatites has a lower range of  $\delta^7\text{Li}$  values than that from Li-Ta-Be mineralized pegmatites. This might be the effect of mica crystallization at source level or during melt ascent, as  $^7\text{Li}$  is expected to favor melts over micas during equilibrium fractionation. Coupling between  $\delta^7\text{Li}$  and Li concentrations can be traced until the magmatic-hydrothermal stage as metasomatic micas, replacing the primary mineral assemblage within Li-Ta-Be pegmatite intermediate zones, have a heavier isotope signature than magmatic muscovite. Those metasomatic micas, characterized by skeletal cores of Li-muscovite compositions ( $\delta^7\text{Li}$

POSTDOC RESEARCHER: BALLOUARD Christophe  
 LABORATORY : GeoRessources/CRPG  
 PROJECT LEADER : MERCADIER Julien, MARROCCHI Yves

~8 ‰), are overgrown by lepidolite rims with  $\delta^7\text{Li}$  Li value up to 16 ‰ (Fig. 1b).

A correlation between  $\delta^7\text{Li}$  and Li concentrations is observed for the rhyolite glass from the Macusani tuff (Fig. 2). This can be modeled by about 70 wt% of open system equilibrium degassing (fluid-melt immiscibility) from a relatively Li-rich and high  $\delta^7\text{Li}$  melt (~20‰). The immiscible Li-rich and isotopically heavy fluid could have been extracted from the melt in a magmatic reservoir at depth. The difference of  $\delta^7\text{Li}$  value between the ‘undegassed’ melt and muscovite (~0 ‰) in the Tuff is of ~20 ‰, corresponding to an  $\alpha_{\text{muscovite/melt}}$  factor of 0.98 (Fig. 2). This value was used along with Li muscovite/melt partitioning coefficients to model the effect of fractional crystallization on muscovite compositions in the Orange River pegmatites (Fig. 1). The compositional range of muscovite from barren to Li-Ta-Be mineralized pegmatites can be reproduced by  $\leq 99$  wt% of fractional crystallization of an assemblage consisting of feldspar, quartz and muscovite. The metasomatic Li-micas could have crystallized from Li-rich and isotopically heavy immiscible aqueous media in isotopic equilibrium with the residual silicate melts, similar to the fluid/vapor exsolved from the macusani rhyolite

Figure 1. (a)  $\delta^7\text{Li}$  vs. Li concentrations diagram showing the compositions of magmatic to magmatic-hydrothermal micas from barren and rare-metal-mineralized pegmatites of the Orange River belt, including fractional crystallization modeling. Analyses shown in transparent are interpreted as reflecting kinetic fractionation (Li diffusion). (b) Core to rim transect of a magmatic-hydrothermal mica consisting of a Li-poor skeletal core overgrown by a Li-rich rim.



melt. This study highlights the use of *in situ* Li isotope studies to quantify the effects of magmatic differentiation along with immiscibility and metasomatic processes during the genesis of rare-metal pegmatites.

**Perspectives**

A refining of geochemical modeling will be done before manuscript preparation. We are also considering an experimental approach to better assess Li isotope mica-melt equilibrium fractionation. Other application cases considered for mica Li isotope analyses are the Variscan Beauvoir granite and Velay dome migmatites.

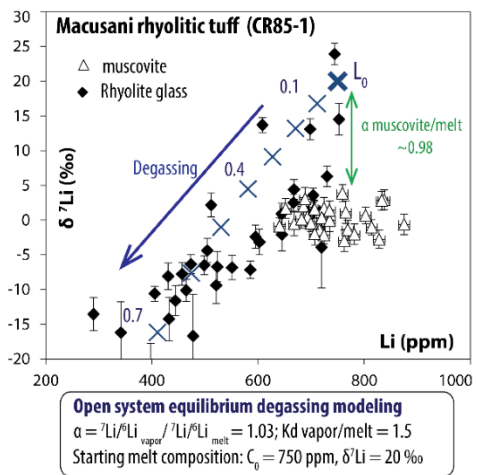
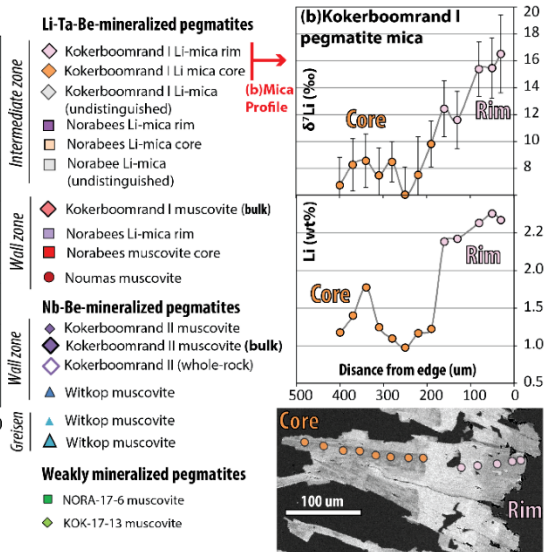


Figure 2.  $\delta^7\text{Li}$  vs. Li concentrations diagram showing the composition of rhyolite glass and muscovite from a tuff of Macusani, including melt degassing modeling.



## Li TRANSFER DURING CRUSTAL METAMORPHISM AND IMPLICATIONS FOR THE GENERATION OF RARE METAL ENRICHED MELTS

BALLOUARD Christophe – COUZINIE Simon –  
BOUILHOL Pierre – HARLAUX Matthieu\* –  
MERCADIER Julien – MONTEL Jean-Marc (\* :  
BRGM, Orléans)

### General framework

Most part of European hard-rock Li resources is associated with Late-Carboniferous peraluminous rare metal pegmatites and granites (RMPG) from the Variscan belt such as the Beauvoir leucogranite (Massif Central, France). GPMR can reach rare-metal (Li-Ta-Nb-Sn-Cs-Be) and F concentrations that are two orders of magnitude higher than common crustal granites. The extreme incompatible element enrichment of RMPG reflects a combination of processes such as fractional crystallization along with fluid immiscibility and metasomatism, and probably reflect specific partial melting conditions of peculiar sources.

### Objectives

Our objective is to trace the behavior of rare-metals and halogen, including Li and F, upon metamorphism and partial melting, in order to identify the favorable pressure-temperature conditions and protoliths for the generation of melts involved in the formation of RMPG

### Methods

Micas are the main hosts for Li as well as F in the deep crust, and can contain significant amount of Nb, Ta, Sn, W, Cs and Be. Moreover, the dehydration of muscovite and biotite are the main reactions controlling the partial melting of the crust, and the generation of peraluminous granitic magmas. Electron microprobe (EMP) and LA-ICP-MS analyses of micas as well as solid products of incongruent melting reactions (cordierite, garnet) were performed in para- and ortho-derived metamorphic rocks from greenschist facies to migmatites in order to trace the partitioning of rare-metals and halogens upon partial melting. Those analyses were coupled to geochemical modeling of the partial melting of different protoliths on isobaric P-T paths using *Perple\_X*. Such models are based on biotite/melt (Kd) partitioning parameters available for Li and F in the literature, and the Kd of muscovite, cordierite and garnet were calculated based on the biotite/mineral partition coefficients measured by EMP and LA-ICP-MS. The study area corresponds to the low pressure-high temperature (LP-HT) Velay anatectic dome (Massif central) formed and

exhumed during the late-orogenic extension of the Variscan belt from 320 to 300 Ma. Partial melting within the dome is contemporaneous with rare-metal magmatism in the Massif central and it is the host for Li-mica-topaz-bearing intrusions (i.e., Fabras granite). The dome thus represents the alimentation source for rare-metal enriched magmas.

### Results

The Li concentrations of biotite and peritectic cordierite from the Velay anatectic metapelites decrease with increasing temperature, estimated from ~700 to 840 °C based on pseudosection analyses (Fig. 1a). This reflects the incompatible behavior of Li and the progressive Li depletion of the melt during the biotite breakdown reaction. Metapelite anatexis at low pressure (<~5 kbar) yields melts that are relatively poor in Li (<~200 ppm), akin to those in equilibrium with biotite from regional cordierite-bearing granites (Figs. 1a). Such concentrations are largely below that of the melt in equilibrium with biotite from the topaz-bearing granite (Figs. 1a) (>5000 ppm). Lithium is readily incorporated in cordierite compared to biotite with partitioning coefficients from 2 to 3, whereas garnet does not incorporate significant amount of Li. Therefore, melting of a metapelite involving biotite breakdown at medium pressures (>~5 kbar), out of the stability field of cordierite, may increase by a factor two the Li concentration of the melt. Yet, the latter would remain relatively Li-poor. Moreover, decoupling is observed between Li and F, as the concentrations of F increase with temperature (Figs. 1 & 2a-b, d-e). Consequently, the Li-richest melts are produced at low temperature (<700°C) whereas F-richest melts are generated at high temperature close to the biotite-out isograd (>800 °C) (Fig. 2a-b). This entails that melting of metapelite is not amenable to generate melts with the geochemical signature of rare metals granites and pegmatites characteristically enriched in both F and Li.

In contrast, the biotite from peraluminous orthogneisses is substantially enriched in F-Li (Fig. 1), as well as in Sn-W-Nb-Ta, compared to that from metapelites. The partial melting of orthogneisses can yield melts with relatively high Li concentrations >600 ppm, up to that of the melt in equilibrium with the biotite from regional two-mica granites (Fig. 2c). Moreover, this Li-rich melt is also strongly enriched in F (and probably all mica-hosted rare-metals), because the complete destabilization of both muscovite and biotite occurs over a narrow range of temperature from 650 to 720 °C (Fig. 2f). Moreover, as F (and Li) is a fluxing element having the property to decrease the viscosity of liquids, this melt is likely mobile. Overall, peraluminous orthogneisses



POSTDOC RESEARCHER: BALLOUARD christophe  
 LABORATORY : GeoRessources/CRPG  
 PROJECT LEADER : MERCADIER Julien

identified in the Velay dome appear as favorable protoliths to generate melts that are pre-enriched in the elements found in economic concentrations in endogenous rare-metal deposits, although about 75 wt% of fractional crystallization from such anatectic melt remains needed to reach the composition of the parental melts of RMPG.

This study highlights the importance of protracted crustal differentiation by the remelting of older granites that formed and evolved during

previous orogens for the formation of rare-metal enriched silicate melts. In the case of the Velay dome, those older peraluminous granites are represented by a ca. 550 Ma old Cadomian batholith that originated from the partial melting of Neoproterozoic sediments in a back arc setting.

**Perspectives**

Manuscript finalizing and submission.

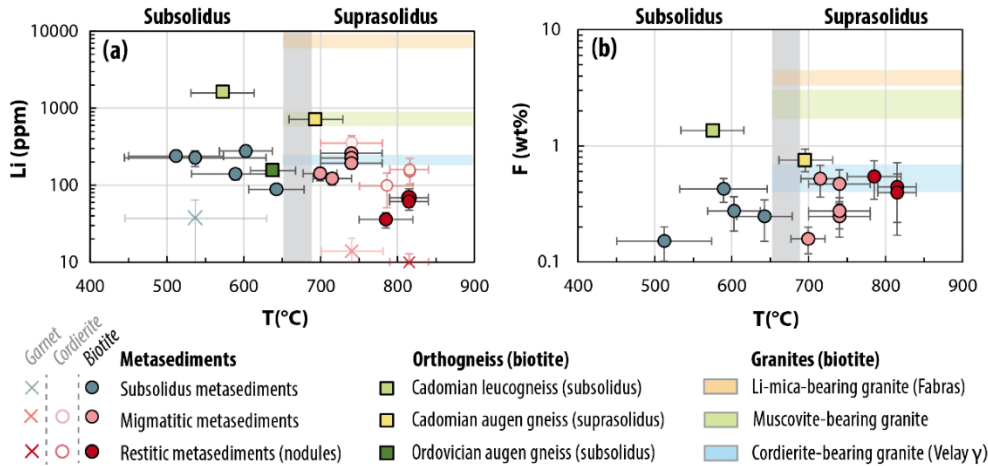


Figure 1. Evolution of the average Li – F compositions of biotite, cordierite, and garnet as a function of peak temperatures for para- and ortho-derived metamorphic rocks. Are also displayed the range observed in granites from the Velay dome. The grey fields represent the temperature range of muscovite breakdown in metapelites.

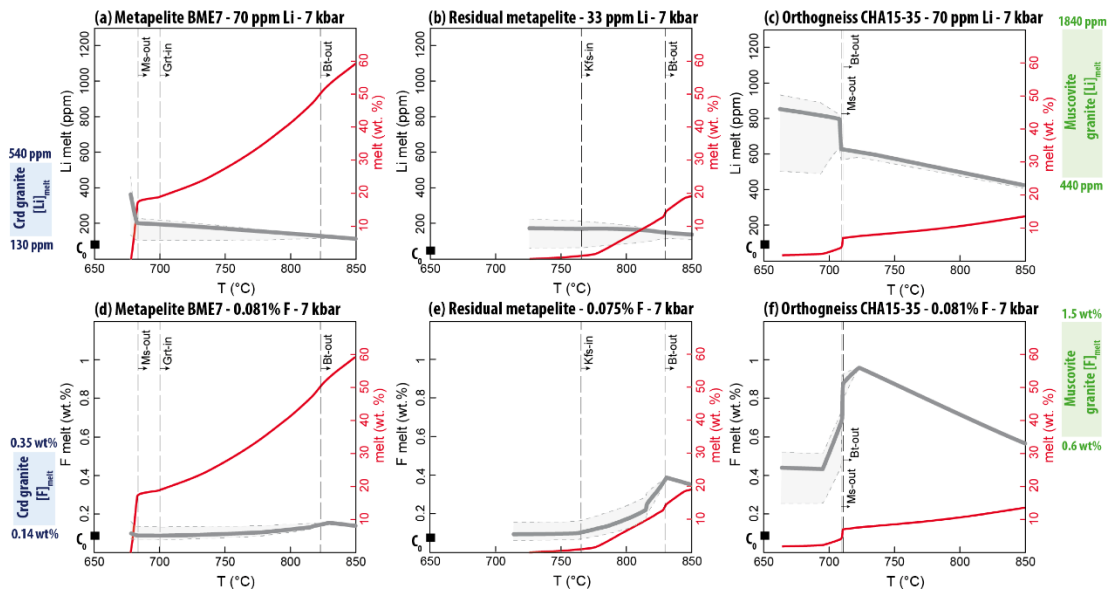


Figure 2. Lithium (a-b-c) and F (d-e-f) concentrations in melt vs. temperature diagrams comparing results of batch melting modeling for a metapelite, a residual metapelite and a leucogneiss from the Velay dome at 7 kbar. Melt volumes are shown as red curves. Blue and green fields represent the range of Li and F compositions of melts in equilibrium with the biotite of the cordierite-bearing and muscovite-bearing granite, respectively. C<sub>0</sub> represents the initial composition of the protoliths.

## **GEOCHRONOLOGY OF Li-MICA FROM PANASQUEIRA DEPOSIT AND ITS REGION: A VALIDATION OF THE K-Ar DATING**

### **General framework**

The S-W-(Cu) deposit of Panasqueira is a magmatic-hydrothermal system, which includes high-grade quartz-vein type mineralization (see Figure 1). In addition to petrological and mineralogical characterizations, geochronological data are needed to understand better the link between mineralization and the time of granite emplacement. One suitable dating technique on mica is the K-Ar method. During the last years, GeoRessources and the LabEx R21 provided substantial efforts in developing this method and its application on mica.

### **Objectives**

After the calibration of the argon desorption line last year, the following objective relies on the elaboration of the protocol for potassium analysis. The second objective of this work is the separation of mica from granites and their preparation for K-Ar dating. Then, those protocols were applied to a selection of mica from the Panasqueira Sn-W deposit.

### **Methods**

The K-Ar dating relies on coupling two distinct analytical techniques for argon and potassium measurements. Argon is quantified using a desorption line connected to a mass spectrometer and potassium by optical emission spectrometry (ICP-OES).

The argon desorption line has been calibrated regarding pressure dependence

and mass discrimination (different ionization conditions depending on the mass). It is also calibrated against a reference sample widely used in the literature for K-Ar dating: the Heidelberg biotite HD-B1 from the Bergell granodiorite [1]. This calibration has been verified using two other reference materials: Odin's glauconite GL-O [2] and the muscovite BMus/2 from the Bärhalde granite [3].

A defined and identical procedure must be applied to potassium (and argon) measurements to compare the ages. Two approaches were studied for potassium measurements that mainly rely on the choice of the laboratory where the analysis is made. A selection of samples was sent to two laboratories (GeoRessources and SARM), and the results were compared. Each laboratory has its protocol defined for reaching the most reliable, reproducible and precise measurements. Among the samples selected for potassium measurement tests were two reference samples: HD-B1 and BMus/2. The obtained %K<sub>2</sub>O contents were compared with literature data.

The so-defined protocols for argon and potassium measurements are applied to a selection of 5 micas from the Panasqueira deposit. Among this selection, two micas are dated to this day, following the so-defined procedure. The first sample PAN XVII-3 originates from a large selvage along a quartz vein [4]. The second PAN 181-2G is also a large mica selvage along a quartz vein that contains wolframite.

On the rest of the selection, argon measurements have been performed, and potassium analysis is currently in progress.

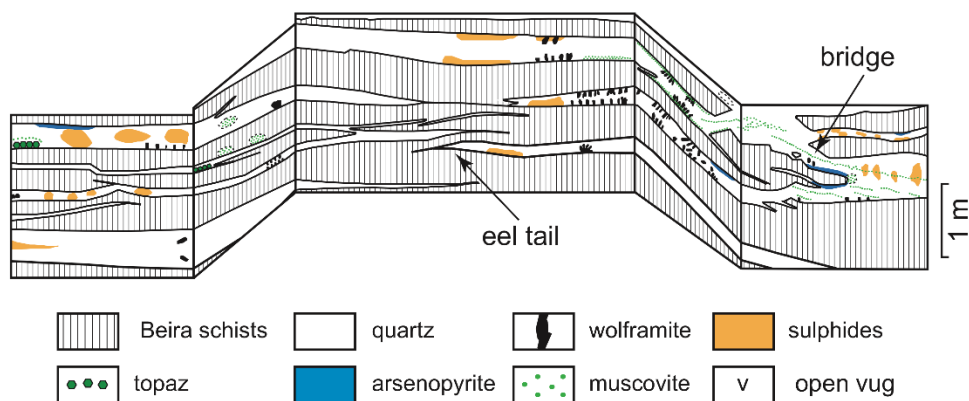


Figure 1 – Typical features of the Panasqueira vein system (slope “Bank”, C. Marignac ‘s observations in 1970).

	%K <sub>2</sub> O - SARM	%K <sub>2</sub> O – GeoRessources	%K <sub>2</sub> O - Lit	Age (Ma)	Age - Lit (Ma)
HD-B1 *	9.52 ± 0.14	9.39 ± 0.23	9.58 ± 0.06	-	24.21
BMus/2	10.13 ± 0.15	9.69 ± 0.24	10.2	<b>327.0 ± 5.4</b>	328.5 ± 1.1
GL-O	7.95 ± 0.12	7.56 ± 0.19	7.95	<b>95.7 ± 1.0</b>	95.0 ± 1.1
PANXVII-3	10.19 ± 0.15	10.02 ± 0.06	-	<b>295.9 ± 5.0</b>	296.0 ± 2.0
PAN181-2G	10.50 ± 0.16	10.26 ± 0.26	-	<b>292.0 ± 5.0</b>	-

Table 1 – Ages obtained using the so-defined protocols for Ar and K measurements for two reference materials and two micas from the Panasqueira deposit. Comparison with literature data if available. HD-B1 is a standard material for quantitative calibration of the mass spectrometer for argon measurement. Then, no age is determined on this sample, as the age from the literature is used for calibration.

Micas from the veins were separated by hand. For some samples, it was necessary to gently crush the granite to liberate the micas prior to hand separation. An internship student has partially completed this work as part of his M1 degree.

## Results

The SARM outputs appear as the most precise and reliable results on %K<sub>2</sub>O. They are also more consistent with the literature data. According to Table 1 and ages uncertainties, no significant discrepancy could be found between the ages determined on reference material BMus/2 and GL-O and literature data. This result tends to validate the calibration of the mass spectrometer (pressure, mass discrimination and quantitative) for argon measurements and the protocol for potassium analysis.

The age obtained on PAN XVII-3 is very close to the age from Carocci et al. [4] of 296.0 ± 2.0 using the Ar/Ar method and from older

data published by Snee et al. [5]. Finally, the age of PAN 181-2G of 292.0 ± 5.0 cannot be differentiated from the PAN XVII-3 mica considering uncertainties.

## Perspectives

The dating of micas from the Panasqueira veins is a new opportunity to understand better the timing of ore deposition, especially Sn-W. Further analysis are already planned on lepidolite from the Segura Li-Nb-Ta granitic dykes and mica from pegmatites (Medelin) in the Panasqueira region to contribute to a renewed temporal chart for these systems.

- [1] U. Fuhrmann, H. J. Lippolt, and J. C. Hess, *Chemical Geology*, 1987.
- [2] G. S. Odin, *International J. of Rad. App. and Instru. Part D*, 1990.
- [3] K. L. Rittmann, Univ. de Heidelberg, 1984.
- [4] E. Carocci et al., *Economic Geology*, 2020.
- [5] L. W. Snee, J. F. Sutter, and W. C. Kelly, *Economic Geology*, 1988.

Kristijan RAJIC<sup>1</sup>, Antonin RICHARD<sup>2</sup>, Hugues RAIMBOURG<sup>1</sup>, Romain MILLOT<sup>3</sup>

1: ISTO Université d'Orléans/CNRS/BRGM UMR7327, 1A Rue de la Ferollerie, 45100 Orléans, France

2: Université de Lorraine, CNRS-CREGU, UMR 7359 GeoRessources, 54506 Vandoeuvre-lès-Nancy, France

3: B.R.G.M., BP 6009, 45060 Orléans cedex 2, France

## Enjeux scientifiques

This project aims at implementing and applying in French laboratories (GeoRessources ISTO, and BRGM) a method for the determination of lithium isotopes in fluid inclusions. As lithium is a fluid-mobile element showing relatively large isotopic fractionation between the two stable isotopes <sup>7</sup>Li and <sup>6</sup>Li between different crustal reservoirs, Li isotopes have been widely used to trace deep crustal fluids (from fluids origins and fluid–rock interactions points of view). Here, the targeted natural samples have been collected from subduction zones, which are places of extensive circulation of deep crustal fluids, some of them being key ingredients for the formation of world class mineral resources.

## Etat de l'art

Fluids have an important role during subduction-related processes as regarding global cycling of chemical elements as well as deformation processes along the plate boundary interface. The progressive dehydration of the slab is well described based on metamorphic phase reactions. Recently, it was proposed that Li can be used as a prominent geochemical tracer for studying subduction slab dehydration. In exhumed accretionary prisms, metasedimentary units contain a record of vigorous fluid circulation in form of high abundance of quartz and calcite (and minor chlorite and albite) veins which gives us a chance to study interplay between fluid circulation and deformation.

The Kodiak accretionary complex of Alaska, Shimanto belt of Japan and Internal domains of Alps (Schistes Lustrés and Flysch Helminthoid) represent well exposed terrains interpreted as paleo-accretionary complexes. Across each complex, we have chosen two units – lower- and higher-grade, with different deformational style and peak temperatures (ca. 250°C and ca. 330°C, respectively). For the purpose of this study, we sampled syn-deformation veins, quartz-dominantly, to perform several methods to study fluids and fluid-rock interaction.

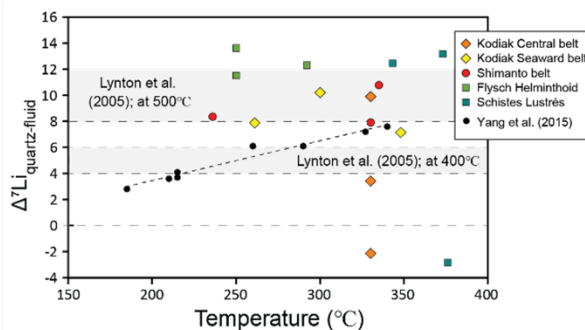


Fig. 1.  $\Delta^7\text{Li}_{\text{quartz-fluid}}$  from this study as well as from Yang et al. (2015) plotted as a function of temperature. Light gray shaded fields represent experimentally derived values from Lynton et al. (2005), with  $\Delta^7\text{Li}_{\text{quartz-fluid}}$  from +4 to +6‰ at 400°C and from +8 to +12‰ at 500°C.

## Approche méthodologique

We performed different methods to characterize fluid inclusions as well as host quartz, including LA-ICP-MS, cathodoluminescence (CL), EPMA, petrography of fluid inclusions and Raman spectroscopy. For the Li isotopes analyses we extracted the fluid from inclusions by crush-leach technique of Banks et al. (2000). The extracted fluid inclusion leachates and residue quartz have been analyzed by MC-ICP-MS at BRGM.

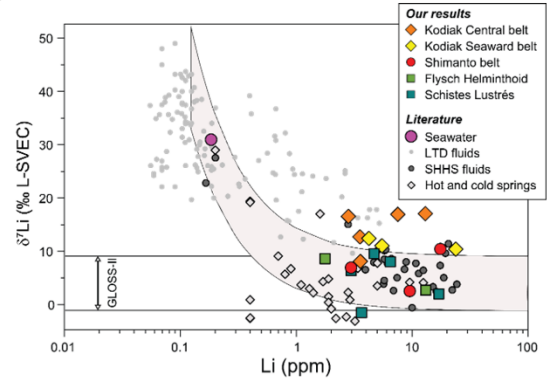


Fig. 2. The  $\delta^7\text{Li}$  value vs lithium concentrations of fluid inclusion leachates as well as values of seawater, interstitial pore fluids and the range of global subducting sediments (GLOSS-II; Plank, 2014). A gray area represents a binary mixing model between interstitial pore fluids and GLOSS-II.

## Résultats

The isotopic fractionation between quartz and fluid in examined veins,  $\Delta^7\text{Li}_{\text{quartz-fluid}}$  ranges from +7.15‰ to +13.63‰, without any temperature dependence (Fig. 1). The lack of temperature-dependent lithium isotopes fractionation between quartz and fluid may be result of (i) a disequilibrium crystallization of quartz from fluid, or as a result of (ii) dissolution-precipitation reactions between fluid inclusions and quartz.

Elevated lithium concentrations of FI leachates in comparison to interstitial pore fluids and seawater point to significant fluid-rock interaction and leaching of lithium from the host rock, where lithium is principally contained in chlorite. Variations likely resulted by different mineral reactions occurring along prograde path at three sites and consequent loss (in the Shimanto case) or retention of lithium (in the Kodiak case) in chlorite. In the Western Alps,  $\delta^7\text{Li}$  of fluids is similar to of the host rock, pointing to the dissolution of lithium-bearing minerals what causes a decrease in  $\delta^7\text{Li}$  of fluids (Fig. 2).

## Bilan – Perspectives de développement

All results will be presented at the EGU meeting (2023, Vienna) are processed and sufficient to begin with the preparation of the original manuscript to be published in scientific journal. Kristijan Rajic will defend his PhD thesis during spring 2023.

Kristijan RAJIC, Antonin RICHARD, Hugues RAIMBOURG, Romain MILLOT  
LABORATORY: GeoRessources, ISTO – Orléans, BRGM - Orléans  
PROJET LEADER: Antonin RICHARD

## LITHIUM ISOTOPES IN FLUID INCLUSIONS AS TRACERS FOR CRUSTAL FLUIDS

**RAJIC Kristijan (PhD student)**

**RICHARD Antonin – RAIMBOURG Hugues – MILLOT Romain**

### General framework

This project aims at implementing and applying in French laboratories (GeoRessources ISTO, and BRGM) a method for the determination of lithium isotopes in fluid inclusions developed previously by the Project Leader at the Geological Survey of Finland. As lithium is a fluid-mobile element showing relatively large isotopic fractionation between the two stable isotopes  $^7\text{Li}$  and  $^6\text{Li}$  between different crustal reservoirs, Li isotopes have been widely used to trace deep crustal fluids (from fluids origins and fluid–rock interactions points of view). Here, the targeted natural samples have been collected from subduction zones, which are places of extensive circulation of deep crustal fluids, some of them being key ingredients for the formation of world class mineral resources.

Fluids have an important role during subduction-related processes as regarding global cycling of chemical elements as well as deformation processes along the plate boundary interface. The progressive dehydration of the slab is well described based on metamorphic phase reactions. Recently, it was proposed that Li can be used as a prominent geochemical tracer for studying subduction slab dehydration. In exhumed accretionary prisms, metasedimentary units contain a record of vigorous fluid circulation in form of high abundance of quartz and calcite (and minor chlorite and albite) veins which gives us a chance to study interplay between fluid circulation and deformation.

### Objectives

The Kodiak accretionary complex of Alaska, Shimanto belt of Japan and Internal domains of Alps (Shistes Lustrés and Flysch Helmintoid) represent well exposed terrains interpreted as paleo-accretionary complexes. Across each complex, we have chosen two units – lower- and higher-grade, with different deformational style and peak temperatures (ca. 250°C and ca. 330°C, respectively). For the purpose of this study, we sampled syn-deformation veins, quartz-dominantly, to perform several methods to study fluids and fluid-rock interaction.

In a first stage, we studied, using in-situ analyses, the composition of the fluid trapped in fluid inclusions,

which we consider as representative of the fluid that was present at depth. In second stage, we study the Li isotopic signature of the fluid contained in inclusions and of the quartz at different depth of subduction zones. In parallel, we describe main lithium-bearing minerals and the changes in lithium concentrations along the prograde metamorphic path.

### Methods

We performed different methods to characterize fluid inclusions as well as host quartz, including LA-ICP-MS, cathodoluminescence (CL), EPMA, petrography of fluid inclusions and Raman spectroscopy. For the Li isotopes analyses we extracted the fluid from inclusions by crush-leach technique of Banks et al. (2000). The extracted fluid inclusion leachates and residue quartz have been analyzed by MC-ICP-MS at BRGM.

### Results

In lower-grade veins, two generations of primary fluid inclusions have been observed: 1-phase  $\text{CH}_4$ - and 2-phase  $\text{H}_2\text{O}$ -rich with  $\text{CH}_4$  vapor bubble. Conversely, only 2-phase  $\text{H}_2\text{O}$ -rich inclusions are observed in higher-grade quartz, with  $\text{CO}_2$  and  $\text{CH}_4$  in vapor bubble. LA-ICP-MS results revealed the presence of B, Na, K, Mg, Rb, Sr, Cs and Ba are within fluid, whereas Li, Ti and Al are mostly hosted in crystal lattice.

In the host rock, chlorite represents the main mineral host for lithium. In the Kodiak complex, chlorite preserves high concentrations of lithium (~240 ppm), whereas in the Shimanto belt, significant loss of lithium is observed as temperature rises (from ~320 ppm in chlorite at 250°C down to ~120 ppm at 330°C).

$\delta^7\text{Li}$  values of the leachates from three localities show distinct  $\delta^7\text{Li}$  values: (1) Kodiak accretionary complex +8.1 to +17.07 ‰, (2) Shimanto belt +2.53 to +10.39 ‰, and (3) The Alps -1.54 to +9.54 ‰. The Li isotopic signature of leachates is independent of other fluid tracers or parameters, such as temperature or salinity. Quartz is in general isotopically heavier than that of paired FI leachates, with  $\delta^7\text{Li}$  between +10.93 and +22.61‰ (Fig. 1).

Contrasting  $\delta^7\text{Li}$  of FI leachates from Kodiak and Shimanto is explained by lithium loss/retention in chlorite: the higher  $\delta^7\text{Li}$  of fluids in Kodiak is explained by the chlorite crystallization as it preferentially consumes  $^6\text{Li}$  and the fluid remains enriched in  $^7\text{Li}$ . Conversely, fluids from Shimanto are isotopically lighter than from Kodiak, consistent with lithium loss in chlorite as temperature increases.

Kristijan RAJIC, Antonin RICHARD, Hugues RAIMBOURG, Romain MILLOT  
 LABORATORY: GeoRessources, ISTO – Orléans, BRGM - Orléans  
 PROJET LEADER: Antonin RICHARD

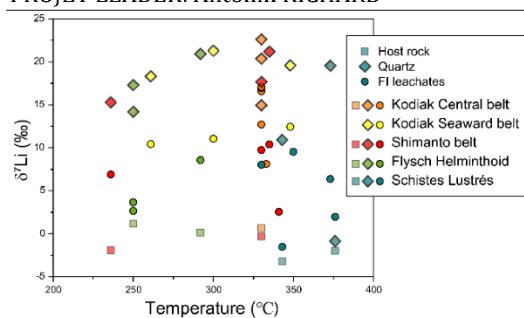


Figure 1. The  $\delta^7\text{Li}$  results of metasediments, host quartz and fluid inclusion leachates as a function of peak-metamorphic temperature.

The isotopic fractionation between quartz and fluid in examined veins,  $\Delta^7\text{Li}_{\text{quartz-fluid}}$ , ranges from +7.15‰ to +13.63‰, without any temperature dependence (Fig. 2). The lack of temperature-dependent lithium isotopes fractionation between quartz and fluid may be result of (i) a disequilibrium crystallization of quartz from fluid, or as a result of (ii) dissolution-precipitation reactions between fluid inclusions and quartz.

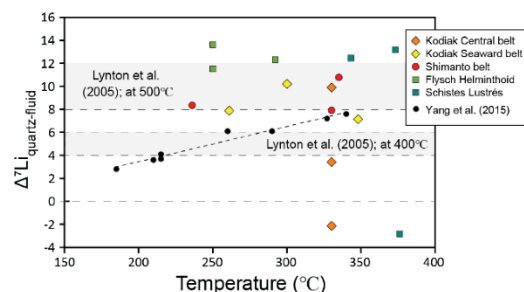


Figure 2.  $\Delta^7\text{Li}_{\text{quartz-fluid}}$  from this study as well as from Yang et al. (2015) plotted as a function of temperature. Light gray shaded fields represent experimentally derived values from Lynton et al. (2005), with  $\Delta^7\text{Li}_{\text{quartz-fluid}}$  from +4 to +6‰ at 400 °C and from +8 to +12‰ at 500 °C.

Elevated lithium concentrations of FI leachates in comparison to interstitial pore fluids and seawater point to significant fluid-rock interaction and leaching of lithium from the host rock, where lithium is principally contained in chlorite. FI leachates record a wide range of  $\delta^7\text{Li}$  (-1.54 to +17.07‰) in fluids from subducted sediments, and show contrasting behavior between the three studied sites. Such variations likely resulted by different mineral reactions occurring along prograde path at three sites and consequent loss (in the Shimanto case) or retention of lithium (in the Kodiak case) in

chlorite. In the Western Alps,  $\delta^7\text{Li}$  of fluids is similar to of the host rock, pointing to the dissolution of lithium-bearing minerals what causes a decrease in  $\delta^7\text{Li}$  of fluids.

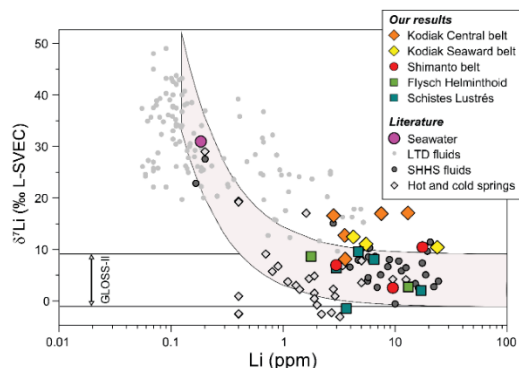


Figure 3. The  $\delta^7\text{Li}$  value vs lithium concentrations of fluid inclusion leachates as well as values of seawater, interstitial pore fluids and the range of global subducting sediments (GLOSS-II; Plank, 2014). A gray area represents a binary mixing model between interstitial pore fluids and GLOSS-II. Majority of results fall into mixing field, indicating the leaching of lithium from solid material and shifting of  $\delta^7\text{Li}$  value of fluids towards the protolith. Reference data: Seawater (Millot et al., 2004); LTD fluids: low-temperature diagenetic fluids (Scholz et al., 2010); SHHS fluids: sediment-hosted hydrothermal systems (Chan et al., 1994; James et al., 1999); Hot and cold springs (Barnes et al., 2019).

### Perspectives

All mentioned results will be presented at the EGU meeting (2023, Vienna) are processed and sufficient to begin with the preparation of the original manuscript to be published in scientific journal. Kristijan Rajic will defend his PhD thesis during spring 2023.

Yves Marrocchi<sup>1</sup>, Julia Neukampf<sup>1</sup> and Johan Villeneuve<sup>1</sup>

<sup>1</sup>: Université de Lorraine, CRPG-CNRS, UMR 7358 CRPG, 54500 Vandoeuvre-lès-Nancy, France

## General framework

Lithium is a fundamental element because it allows tracing the degree, kinetic and mode of mass transport in geological samples. Because of its small ionic radius, it diffuses very rapidly in minerals. Lithium zonation within magmatic minerals is therefore a powerful tool to quantify crystallization kinetics, isotopic disequilibrium episodes, and cooling rates. In addition to magmatic systems, lithium isotopes can also be used to obtain quantitative information on the conditions and kinetics of deposition of mineralization but also its biological effects on aquatic organisms.

## Objectives

Addressing these scientific questions requires the ability to measure lithium zonations and concentrations at very small scales. Until now, the in situ techniques used involved beam sizes larger than 30 microns (ion probe and ICPMS laser). This only allows targeting a limited number of minerals. This technical limitation can now be overcome with the installation of a radio frequency source on the CRPG 1280 HR2 ion probe that allows the generation of smaller primary beams than previously (~5 microns vs. 30 microns). The possibility to use a small primary beam allows to quantify the small scale distribution of lithium by determining its isotopic variations with precision.

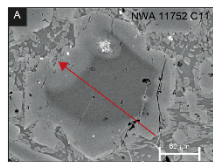
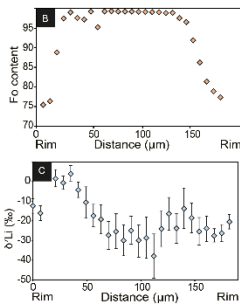


Figure 1. A- Backscattered electron image of a zoned olivine grains in a chondrule from the ordinary chondrite NWA 11752. B- Fo of the content of the zone grains from rim to rim. C- Lithium isotopic composition profile with isotopically light core and isotopically heavy rim. This type of isotopic variations was inaccessible before our analytical development.



## Methods

We determined the lithium isotopic compositions of different minerals (e.g., olivine, low-Ca pyroxene, quartz, micas, glass) by secondary ion mass spectrometry (SIMS) using the multi-collector CAMECA IMS 1280 HR2 at CRPG. Minerals were sputtered with a ~5 nA primary O beam set in Gaussian mode and accelerated at 13 kV. Secondary positive <sup>7</sup>Li ions were accelerated at 10 kV and analyzed in monocollection mode on the axial electron multiplier (EM). Under these conditions, internal precisions of ± 1 to 5 ‰ (2SE, depending on the Li content) was obtained on the <sup>7</sup>Li for a spot size of ~5 µm.

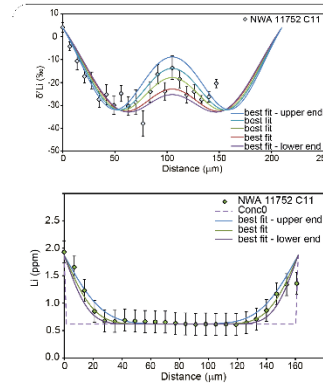


Figure 2. Top panel: Lithium isotopic profile within a chondrule olivine grain. Lines represent the diffusion models with the best fit for given parameters (e.g., temperature, oxygen fugacity, diffusion coefficient...). Low panel: Lithium concentration within the same grain. Lines represent the diffusion models with the best fit for the same parameters.

## Results

For illustrating the analytical development, we will present results obtained on type II chondrules from primitive meteorites. Chondrules are submillimeter-sized silicate spheroids representing the major high-temperature components of primitive meteorites (chondrites). Depending on the valence state of iron, chondrules are classified into type I and type II chondrules, with the limit between type I and II chondrules defined to be  $Mg\# \equiv 100 \times Mg/(Mg+Fe) = 90$ . Recent experimental and isotopic constraints suggest a genetic link between both types of chondrules with type II being derived from type I chondrules by oxidation. If type II chondrules derived from type I chondrules by oxidation, diffusive effects must have been recorded within the chondrule minerals. To investigate this process, we combined the major element compositions (measured by EPMA, Fig. 1) and Li isotopic composition in zoned olivine grains in type II chondrules from the ordinary chondrite NWA 11752 (LL3.05; Fig.1). They show that the chondrules have olivine grains with high magnesian olivine relicts in their cores with an initial composition of Fo97-99 whereas the surrounding olivine is fayalitic with a composition of Fo69-97 (Fig. 1). The boundaries between relict olivine and the fayalitic overgrowth show zoning in Fe-Mg. This zonation points to disequilibrium diffusion and records a rapid change in conditions during the chondrule formation (Fig. 2). The increase in Li concentration indicates diffusional exchange between the mesostasis and the olivine grains and inter-diffusional exchange between the relict grains and the fayalitic overgrowths. This is supported by the isotopic fractionation from rim to core which is up to 42‰ for <sup>7</sup>Li. Taken together, this supports models where type I chondrules represent the main precursor material involved in the formation of type II

## Summary and perspectives

Thanks to this analytical development, we have now the possibility to measure Li elemental and isotopic profiles with a spatial resolution of 5 microns. This allows diffusion processes to be investigated and modelled for different geological systems. Applied to chondrule formation, it allows genetic relationships between type I and type II chondrules to be assessed. These specific types of measurements and models can now be applied to other geological systems, for instance considering magmatic or mineralization processes.

JULIA NEUKAMPF  
 LABORATORY: CRPG  
 PROJET LEADER: YVES MARROCCHI

## DEVELOPMENT OF HIGH-RESOLUTION ANALYSIS OF LITHIUM IN MINERALS OF GEOLOGICAL INTEREST: APPLICATIONS TO CHONDRULE FORMATION.

MARROCCHI Yves - NEUKAMPF Julia - VILLENEUVE Johan

### General framework

Lithium is a fundamental element because it allows tracing the degree, kinetic and mode of mass transport in geological samples. Because of its small ionic radius, it diffuses very rapidly in minerals. Lithium zonation within magmatic minerals is therefore a powerful tool to quantify crystallization kinetics, isotopic disequilibrium episodes, and cooling rates. In addition to magmatic systems, lithium isotopes can also be used to obtain quantitative information on the conditions and kinetics of deposition of mineralization but also its biological effects on aquatic organisms.

### Objectives

Addressing these scientific questions requires the ability to measure lithium zonations and concentrations at very small scales. Until now, the *in situ* techniques used involved beam sizes larger than 30 microns (ion probe and ICPMS laser). This only allows targeting a limited number of minerals. This technical limitation can now be overcome with the installation of a radio frequency source on the CRPG 1280 HR2 ion probe that allows the generation of smaller primary beams than previously (~5 microns vs. 30 microns). The possibility to use a small primary beam allows to quantify the small scale distribution of lithium by determining its isotopic variations with precision.

### Methods

We determined the lithium isotopic compositions of different minerals (e.g., olivine, low-Ca pyroxene, quartz, micas, glass) by secondary ion mass spectrometry (SIMS) using the multi-collector CAMECA IMS 1280 HR2 at CRPG. Minerals were sputtered with a ~5 nA primary O<sup>-</sup> beam set in Gaussian mode and accelerated at 13 kV. Secondary positive <sup>6,7</sup>Li<sup>+</sup> ions were accelerated at 10 kV and analyzed in monocollection mode on the axial electron multiplier (EM). The dead-time of the axial EM was determined at the beginning of the session and set at 74 ns. The mass resolving power was set at M/ΔM = 3,000. Automatic centering of the transfer deflectors and mass was implemented in the analysis routine. A 5 × 5 μm<sup>2</sup> raster was applied to

the primary beam to ensure flat-bottomed pits. Under these conditions, internal precisions of ± 1 to 5 ‰ (2SE, depending on the Li content) was obtained on the δ<sup>7</sup>Li for a spot size of ~5 μm.

### Results

For illustrating the analytical development, we will present results obtained on type II chondrules from primitive meteorites. Chondrules are submillimeter-sized silicate spheroids representing the major high-temperature components of primitive meteorites (chondrites). Depending on the valence state of iron, chondrules are classified into type I and type II chondrules, with the limit between type I and II chondrules defined to be Mg# ≡ 100 × Mg/(Mg+Fe) = 90.

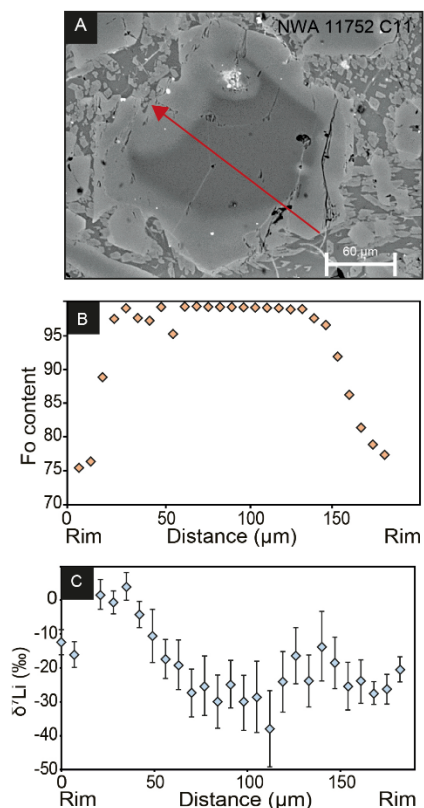


Figure 1. A- Backscattered electron image of a zoned olivine grains in a chondrule from the ordinary chondrite NWA 11752. B- Fo of the content of the zone grains from rim to rim. C- Lithium isotopic composition profile with isotopically light core and isotopically heavy rim. This type of isotopic variations was inaccessible before our analytical development.



JULIA NEUKAMPF

LABORATORY: CRPG

PROJET LEADER: YVES MARROCCHI

Recent experimental and isotopic constrains suggest a genetic link between both types of chondrules with type II being derived from type I chondrules by oxidation. Lithium (Li) and its isotopes is one of the most rapidly diffusing elements in minerals at high temperatures, making it a very powerful tool to estimate timescales of late-stage geological processes. Measuring the Li concentrations and isotopic compositions has the potential to provide isotopic and elemental profiles and give the opportunity to study the thermal history of chondrules and the conditions under which they formed. In particular, if type II chondrules derived from type I chondrules by oxidation, diffusive effects must have been recorded within the chondrule minerals. To investigate this process, we combined the major element compositions (measured by EPMA, Fig. 1) and Li isotopic composition in zoned olivine grains in type II chondrules from the ordinary chondrite NWA 11752 (LL3.05; Fig.1). In the three investigated chondrules, traverses (rim to rim or rim to core) were measured. They show that the chondrules have olivine grains with high magnesian olivine relicts in their cores with an initial composition of Fo97-99 whereas the surrounding olivine is fayalitic with a composition of Fo69-97 (Fig. 1). The boundaries between relict olivine and the fayalitic overgrowth show zoning in Fe-Mg. This zonation points to disequilibrium diffusion and records a rapid change in conditions during the chondrule formation.

All three olivine grains display an increase in Li concentration (up to 1.8 ppm, Fig. 2) towards their rims. Additionally, they exhibit an isotopically light core ( $\delta^7\text{Li} = -3.9$  to  $-38.3\text{‰}$ , Fig. 2) with a significantly heavier intermediate zone ( $\delta^7\text{Li} = 4.0$  to  $-28.0\text{‰}$ ) and slightly lighter rim ( $\delta^7\text{Li} = -2.9$  to  $-16.1\text{‰}$ ; Fig. 2). Within the olivine grains the  $\delta^7\text{Li}$  composition varies largely but is similar between the grains.

The increase in Li concentration at the rims of the olivine not only hint at a diffusional exchange between the mesostasis and the olivine grains but at inter-diffusional exchange between the relict grains and the fayalitic overgrowths. This is supported by the isotopic fractionation from rim to core which is up to 42‰ for  $\delta^7\text{Li}$ . The  $\delta^7\text{Li}$  profiles show that  $^6\text{Li}$  (the lighter and faster diffusing element) is more depleted in the isotopically heavier rim indicating that it was diffusing towards the core and/or into the mesostasis. The relicts were relatively homogeneous in their isotopic composition and from an isotopically distinct reservoir compared to the rims at the onset of diffusion. The isotopic fractionation occurred between the boundary layer near the edge of the relict and the rim of the fayalitic

overgrowth. The  $\delta^7\text{Li}$  composition of the olivine grains suggest that the relict grains have a different origin compared to the fayalitic overgrowth stemming from two different reservoirs in the solar system or heterogeneities within the same reservoir. Taken together, this supports models where type I chondrules represent the main precursor material involved in the formation of type II.

### Perspectives

Thanks to this analytical development, we have now the possibility to measure Li elemental and isotopic profiles with a spatial resolution of 5 microns. This allows diffusion processes to be investigated and modelled for different geological systems. Applied to chondrule formation, it allows genetic relationships between type I and type II chondrules to be assessed. These specific types of measurements and models can now be applied to other geological systems, for instance considering magmatic or mineralization processes.

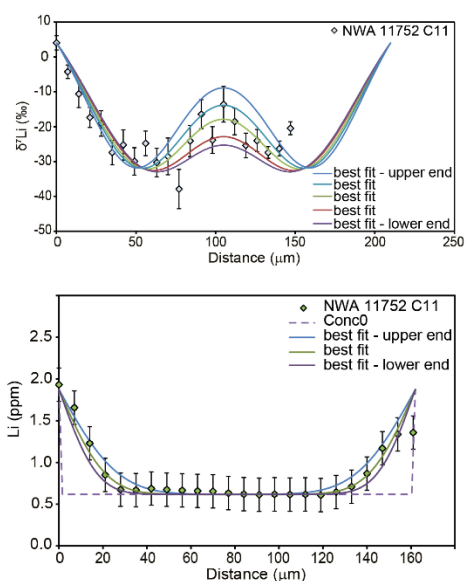


Figure 2. Top panel: Lithium isotopic profile within a chondrule olivine grain. Lines represent the diffusion models with the best fit for given parameters (e.g., temperature, oxygen fugacity, diffusion coefficient...). Low panel: Lithium concentration within the same grain. Lines represent the diffusion models with the best fit for the same parameters.

# Boron extraction from the Salar of Hombre Muerto in Argentina to produce lithium carbonate for lithium-ion batteries.

Abdoul Fattah KIEMDE<sup>1</sup>, Jerome MARIN<sup>1</sup>, Victoria FLEXER<sup>2</sup>, Alexandre CHAGNES<sup>1</sup>

1: CNRS, GeoRessources, Université de Lorraine, 54000 Nancy, France

2: CIDMEJu (CONICET-Universidad Nacional de Jujuy), Jujuy, Argentina

## Context

The brine of the salar of Hombre Muerto in Argentina contains sodium, boron, lithium, calcium, potassium, magnesium, chloride and sulfate. Lithium extraction from that brine is very challenging due to the high concentrations of impurities. Recently, an electrodialysis process was developed by Flexer et al. to produce lithium carbonate but the purity of the latter remains too low. In particular, it is necessary to remove boron to increase the purity of lithium carbonate and to enhance magnesium salt filtration during the process. Therefore, this work focuses on the formulation of new extraction solvent for the selective recovery of boron and its valorization.

## Goals

Boron recovery from aqueous solutions is well known, and many technologies such as adsorption, chemical precipitation, electrodialysis, ions exchange resins, solvent extraction and reverse osmosis were reported in literature to recover boron from brines. Among these technologies, solvent extraction is particularly interesting as it is a mature unit operation used in pharmaceutical and hydrometallurgy. Alcohols are usually used in solvent extraction to extract boron from various aqueous solutions. In this work, we investigate the implementation of a solvent extraction stage before electrodialysis relying on the use of alcohols to extract and valorize boron as borax from the salar of Hombre Muerto brine.

Aliphatic alcohols including mono-hydroxy alcohols [2-butyl-1-octanol (BOc), 1-octanol (Oc), 2-ethyl-1-hexanol (EH)] and di-hydroxy alcohols [2-methyl-2,4-pentanediol (MPD), 2-butyl-2-ethyl-1,3-propanediol (BEPD), 2-ethyl-1,3-hexanediol (EHD)] were employed as extractants at 1 mol.L<sup>-1</sup> diluted in kerosene, sulfonated kerosene, as well as mixtures of kerosene and 60% (wt) toluene or *m*-xylene.

## Methodology approach

A synthetic solution representative to the salar of Hombre Muerto brine was used to investigate the influence of the nature of the alcohols and the diluent on the extraction efficiency of boron and the selectivity towards K, Li, Mg, Ca and Na. The extraction experiments were conducted by contacting the synthetic brine and the organic phases in 50 ml centrifuge tubes at 35 ° C. The effect of alcohols and the diluents on the extraction efficiency of boron were investigated in order to find the best solvent. Then, the influence of the organic to the aqueous phase volume ratio (O/A; O and A stand for the organic phase volume and the aqueous phase volume, respectively) and the pH were studied for the optimization of boron extraction parameters.

Table 1. Influence of the diluent on extraction efficiencies of boron ( $E_B$ ) by alcohols (O/A = 1, pH = 1, 35 ° C, [alcohol] = 1 mol.L<sup>-1</sup>, ns: not soluble, i.e. solubility < 1 mol.L<sup>-1</sup>)

	Diluent			
	Kerosene	sulfonated kerosene	40% (wt) kerosene + 60% (wt) toluene	40% (wt) kerosene + 60% (wt) xylene
Alcohol	$E_B$ (%)	$E_B$ (%)	$E_B$ (%)	$E_B$ (%)
BOc	22.2	23.5	22.2	21.7
EH	23.4	17.4	17.4	22.1
Oc	10.4	9.4	9.9	14.0
EHD	ns	ns	97.2	96.2
BEPD	ns	ns	93.7	93.6
MPD	ns	54.8	89.7	88.8

## Results

There is no significant influence of the diluent on the extraction efficiencies of boron when mono-hydroxy alcohols are used as extractants (Table 1). It is difficult to conclude for di-hydroxy alcohols as they are only soluble in kerosene-aromatic mixtures excepting for MPD. Indeed, the extraction efficiency of MPD is strongly affected by the diluent since the presence of aromatics in the diluent increases the boron extraction efficiency from 55% to ~89%. The presence of two hydroxyl groups in the diols seems to enhance the extraction efficiency of boron. Therefore, 1 mol.L<sup>-1</sup> MPD diluted in sulfonated kerosene was used to investigate the effect of pH on the extraction properties of boron and other elements present in brines at O/A=4. As shown in Fig 1, boron extraction efficiency remained stable between pH 1 and 5.5, and then, decreased slightly at pH greater than 5.5. Furthermore, calcium and magnesium were co-extracted at pH greater than 7.3. As a conclusion, pH=5.5 and O/A=4 led to the best extraction efficiency (93%) without significant co-extraction of impurities.

## Assessment - Development prospects

MPD diluted in sulfonated kerosene will be used in mixers-settler to remove boron from the brine and produce borax for further valorization. Boron stripping from the organic phase could be performed by using sodium hydroxide and boron could be crystallized as borax from the stripping solution. The next part of this study will focus on the implementation of the solvent extraction operation in the electrodialysis process.

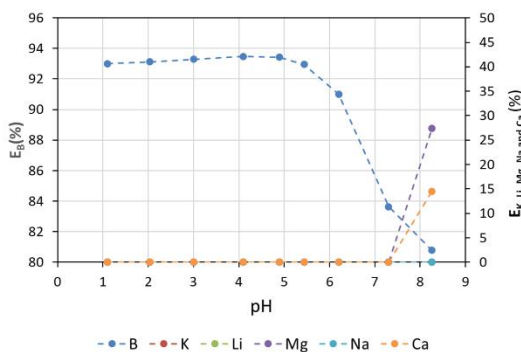


Fig 1. Influence of pH on boron and impurities extraction efficiencies from synthetic brine by MPD diluted in sulfonated kerosene ([MPD] = 1 mol.L<sup>-1</sup>, O/A=4, 35 ° C).

## BORON EXTRACTION FROM THE SALAR OF HOMBRE MUERTO IN ARGENTINA TO PRODUCE LITHIUM CARBONATE FOR LITHIUM-ION BATTERIES

Abdoul Fattah KIEMDE  
 Alexandre CHAGNES  
 Victoria FLEXER

### General framework

The salar of Hombre Muerto brine is rich in lithium, potassium, calcium, sodium, magnesium, boron, chloride and sulfate. Lithium recovery process from that brine is challenging due the high concentration of impurities. Currently, lithium extraction process is based on evaporation and precipitation, that makes that technology less efficient and sustainable for huge lithium production in long term. An electro dialysis process developed by Nieto et al. (2019 and 2020) allows precipitating lithium as low-grade lithium carbonate (purity=97.5%) without using any chemicals. For its use in the production of lithium-ion battery, the grade has to be increased. More especially, it appears important to remove boron and valorize these elements in other industries.

### Objectives

Boron recovery from aqueous solutions is well known, and many technologies such as adsorption, chemical precipitation, electro dialysis, ions exchange resins, solvent extraction and reverse osmosis were used in the past. Nowadays, solvent extraction is a mature process used in pharmaceutic and hydrometallurgy. Alcohols are the most reported molecules to extraction boron from brine. In this work, we investigate the implementation of a solvent extraction stage before electro dialysis relying on the use of alcohols to extract and valorize boron as borax from the salar of Hombre Muerto brine. The boron recovery was carried out from a synthetic solution representative of the brine.

Table 1. Influence of the diluent on extraction efficiencies of boron ( $E_B$ ) by alcohols ( $O/A = 1$ ,  $pH = 1$ ,  $35\text{ }^\circ\text{C}$ , [alcohol] =  $1\text{ mol}\cdot\text{L}^{-1}$ , ns: not soluble, i.e. solubility  $< 1\text{ mol}\cdot\text{L}^{-1}$ )

Alcohol	Diluent			
	Kerosene	sulfonated kerosene	40% (wt) kerosene + 60% (wt) toluene	40% (wt) kerosene + 60% (wt) xylene
	$E_B(\%)$	$E_B(\%)$	$E_B(\%)$	$E_B(\%)$
BOc	22.2	23.5	22.2	21.7
EH	23.4	17.4	17.4	22.1
Oc	10.4	9.4	9.9	14.0
EHD	ns	ns	97.2	96.2
BEPD	ns	ns	93.7	93.6
MPD	ns	54.8	89.7	88.8

The extraction efficiency of boron and the selectivity towards the impurities were determined in this work in order to select the best alcohol and design a process to recover boron and implement it the global process of lithium production combining electromembrane processes and precipitation-crystallization stages.

### Methods

Mono-hydroxy alcohols, i.e 2-butyl-1-octanol (Boc), 1-octanol (Oc), 2-ethyl-1-hexanediol (EH), and di-hydroxy alcohols, i.e 2-methyl-2,4-pentandediol (MPD), 2-butyl-2-ethyl-1,3-propanediol (BEPD), 2-ethyl-1,3-hexanediol (EHD), were employed as extractant at  $1\text{ mol}\cdot\text{L}^{-1}$  diluted in kerosene, sulfonated kerosene, and a mixture of kerosene and toluene 60% (wt) or *m*-xylene 60% (wt).

The extraction experiments were conducted by mixing the synthetic brine and the organic phase in 50 ml centrifuge tube in a shaker under 200 rpm and  $35\text{ }^\circ\text{C}$ . The effect of both alcohols and diluents were investigated in order to find the best solvent. Then, the influence of the organic to the aqueous phase volume ratio (O/A; O and A stand for the organic phase volume and the aqueous phase volume, respectively) and the pH were studied for the optimization of boron extraction parameters.

### Results

There is no significant influence of the diluent on the extraction efficiencies of boron when mono-hydroxy alcohols are used as extractants (Table 1). It is difficult to conclude for di-hydroxy alcohols as they are only soluble in kerosene-aromatic mixtures excepting for MPD, which is soluble in sulfonated kerosene as well as in mixtures of kerosene and 60% (wt) toluene or *m*-xylene. However, the extraction efficiency of boron by the di-hydroxy alcohol MPD is strongly affected by the diluent since the presence of aromatics increases the boron extraction efficiency from 55% to ~89% whereas no significant enhancement was observed for the mono-alcohols.

Abdoul Fattah KIEMDE

LABORATORY: GeoRessources

PROJET LEADER: Alexandre CHAGNES

As depicted in Table 1, di-hydroxy alcohols are most efficient than mono-hydroxy alcohols. This difference may be attributed to the presence of two hydroxyl groups in the di-hydroxy alcohols molecules. As the presence of aromatic diluents is a serious drawback for their use in industry, sulfonated kerosene was chosen to investigate the effect of O/A ratio and pH on the extraction properties of boron and impurities. The increase of O/A ratio improves the extraction efficiency of boron whatever the alcohol used (Figure 1 (a)). Most importantly, only boron is recovered when O/A ranged from 1 to 7. At O/A greater than 4, boron extraction efficiency increases slightly. Then O/A=4 was set to study the influence of the pH. As shown in figure 1(b) boron extraction efficiency remains stable for pH=1-5.5 when MPD, EH, BOc, and Oc, are used as extractants. However, the extraction efficiency decreases slightly for MPD and sharply for BOc, EH and Oc between pH 5.5 and 8. This behavior may be explained by the presence of boric acid at acidic condition.

In addition, at pH=7 and 8, calcium and magnesium are co-extracted.

Then, for high selectivity boron extraction, the extraction experiment should be carried out at acidic conditions. MPD exhibits the best extraction efficiency of boron (93%) at pH=5.5 and O/A= 4.

### Perspectives

As MPD diluted in sulfonated kerosene is efficient for boron recovery from the synthetic brine, this solvent will be used to perform boron extraction from the salar brine by means of mixers-settlers. Thereafter, boron will be stripped from the organic phase by using sodium hydroxide and crystallized as borax. The physicochemistry of boron extraction will be investigated and a physicochemical model will be developed.

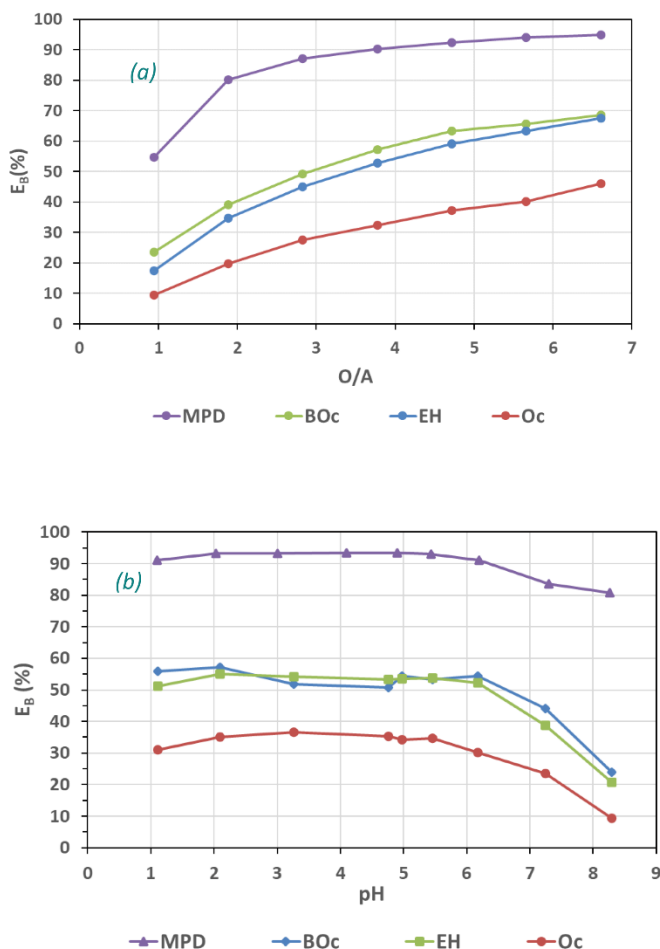


Figure 1. Boron extraction from synthetic brine by alcohols diluted in sulfonated kerosene, influence of the O/A ratio at pH=1 (a), influence of the pH at O/A=4 (b) ([alcohol]=1 mol.L<sup>-1</sup>, 35 °C).

## LITHIUM & ENVIRONMENTAL HEALTH: STUDY OF *IN VITRO* AND *IN VIVO* IMPACTS OF LITHIUM ON AQUATIC ENVIRONMENTS

COSSU-LEGUILLÉ Carole – MINGUEZ Laetitia

### General framework

The increasing demand for lithium, particularly to power the batteries in our computers and other electric cars and scooters, will inevitably lead to its release in aquatic ecosystems. However, its possible ecotoxicity on aquatic organisms is still poorly understood. The available data are scarce and very heterogeneous. One area where information is more abundant is the medical field, since lithium remains the treatment of choice for bipolar disorders. However, even in humans and other mammalian models, the toxic mode of action of lithium is still under debate. As the biological targets of lithium have been conserved through the evolution, its potential risk to aquatic organisms needs to be assessed.

### Objectives

The aim of this project was to determine and understand the biological effects of lithium on aquatic organisms.

### Methods

We started by a meta-analysis of the literature to highlight the scientific gaps on this topic. We conducted standardized bioassays to bring new knowledge on toxicity of different lithium forms to several aquatic organisms for which data are missing. We assessed long-term toxicity of Lithium on the freshwater bivalve *Dreissena polymorpha*, commonly used in ecotoxicological studies for its ability to accumulate high quantities of contaminants. A multi-biomarker approach

on different levels of biological integration was used, in order to identify the key events in the occurrence of an adverse effect and thus define the general health status of the bivalves. All the information acquired, combined with the results of a battery of standardized bioassays, will provide empirical data for risk assessment and the development of predictive approaches.

### Results

Our meta-analysis revealed that the Lithium chloride and sulfate salts were the most tested ones. A few data on other salts were available but mostly obtained by extrapolation and not true assessment. All the lithium forms were hypothesized for having the same toxicity. Most of the ecotoxicity data were obtained on fishes and the other trophic levels were poorly represented. Similarly, there is a clear lack of studies on the chronic effects of lithium on aquatic organisms, which can be major accumulators of this element.

Bioassays highlighted a higher sensitivity of primary producers to lithium, and different toxicity values depending on the tested lithium form. LiOH showed the strongest toxicity towards algae, bacteria and daphnids. These results underline that extrapolations of toxicity from one salt to another are not so obvious. Despite the presence of lithium mainly in its ionic form in the exposure media (i.e. > 90%), the contributed counterions would also play a role in the observed toxicities. It should be noted that this does not involve changes in pH.

The 28d-exposure of *D. polymorpha* to different lithium concentrations addressed the issue whether lithium has a dose-dependent effect on bivalve metabolism. The results confirm that both lithium concentration and exposure duration matter in the observed effects, but not in a linear way. This means that a strong interaction between dose and exposure

duration was observed on the physiology of bivalves. This could be related to the narrow therapeutic window of lithium, implying that small variations in concentrations in organisms lead to different physiological responses. Tissue concentrations were quantified in organisms every week (Figure 1). Results showed a rapid accumulation of lithium during the first week of exposure to reach a plateau whose value depends on the exposure concentration.

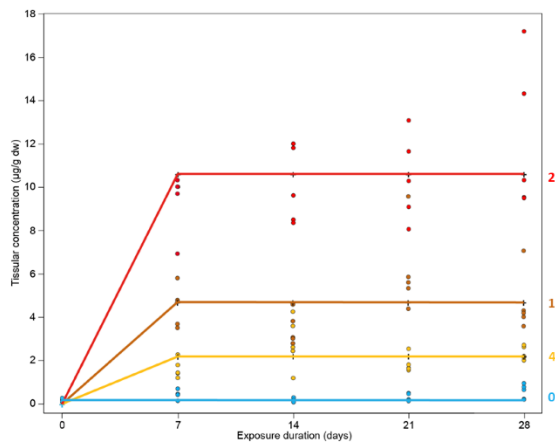


Figure 1: Tissue concentrations measured every week in bivalves exposed to 0, 40, 100 and 250 µg Li/L.

Lithium seemed also to impact mitochondrial respiratory chain enzyme activities at environmentally relevant concentrations. Higher filtration rate and lower respiration rate in exposed organisms, leading to overall higher scope for growth (SfG) values in lithium-exposed organisms were also observed after 28 days (Figure 2).

The physiology of energy balance given by SfG represents the energy available for growth and reproduction of an individual after all physiological demands of respiration and excretion have been met. The higher SfG observed in Li-exposed bivalves means they would use more energy for their somatic and gonadal growth than control individuals. All these effects around the energy balance in organisms could be related to serotonergic influences, known to be modulated by lithium in mammals.

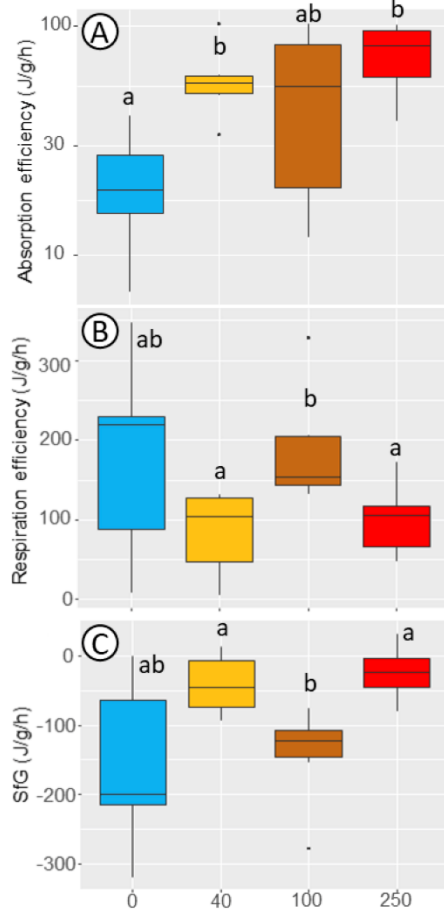


Figure 2: Absorption efficiency based on filtration rate (A), Respiration efficiency (B) and Scope for growth (SfG) (C) in *D. polymorpha*. Values are the median  $\pm$  95% CI.

### Perspectives

We will continue to complete our ecotoxicity dataset by exposing fish larvae, knowing to be potentially more sensitive to contaminants, to the four chosen lithium salts, and by performing chronic tests on *Daphnia* species.

Further studies on *D. polymorpha* will be performed. We will try especially to better understand its kinetics of accumulation and depuration, as well as the subcellular fractioning of lithium. We will also attempt to refine our understanding of the mechanisms of action of lithium by focusing in particular on energy metabolism and mitochondria and the consequences of these modifications for populations.

**MULTI-SCALE ANALYSIS OF THE IMPACT OF LITHIUM ON MICROORGANISMS**

**FIERLING Nicolas - BAUDA Pascale - BILLARD Patrick - BLAUDEZ Damien**

**General framework**

Due to its low abundance in the earth’s crust and its high technological importance, lithium (Li) is considered a strategic metal. The exponential demand in various fields (energy, technology, medicine...) and a low recycling rate leads to a significant release of this metal into the environment. Knowledge on the impact of this emerging contaminant on both individual microorganisms and communities is however limited.

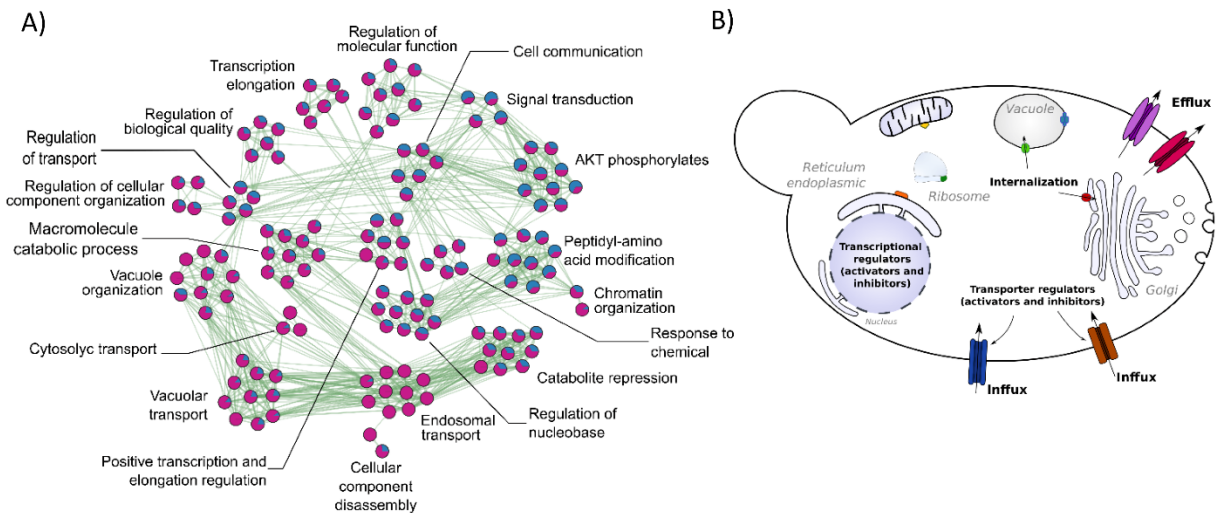
**Objectives**

The first objective of this PhD thesis is to deepen our knowledge on the response mechanisms of two model organisms (*Saccharomyces cerevisiae* and *Escherichia coli*) to Li exposure through different molecular approaches and to possibly identify Li-responsive biomarkers.

The second objective is to describe and understand the impact of Li on the microbial diversity and activities of soils.

**Results**

A first approach, described and illustrated in the previous report, combining different screenings of a *S. cerevisiae* mutant library in the presence of Li was performed. This approach was completed by the screening of the library in the presence of other metals to highlight Li-specific responses. Our results suggest that transport systems play a central role in Li tolerance (Figure 1A). In contrast, several pathways of transcriptional regulation could be important cellular targets of Li stress. Finally, among the 183 mutants identified from the screening, only three and six were specifically sensitive and resistant to Li, respectively.



**Figure 1: A) Summary of functional enrichment analysis network of yeast functions that when deleted confers a resistance or a sensitive phenotype to lithium. The proportion of genes involved in the resistance (magenta) and sensitive (blue) phenotype is represented by the pie charts inside each node. Green lines represent gene overlaps between two functions and the edge width being proportional to the number of shared genes. The enrichment map was built using Metascape and visualized with Cytoscape. B) Main cellular mechanisms involved in Li tolerance identified by the evolutionary engineering approach with Li hyper-tolerant yeast clones.**

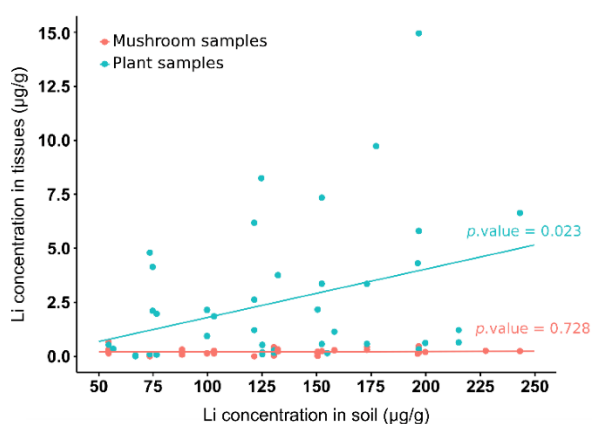
In conclusion, these Li-specific related mutants could be good candidate biomarkers; however further experiments will be needed to validate this finding.

The second approach consisted in performing an evolutionary engineering experiment with yeast and Li. The aim was to expose cells to an increasing range of Li concentrations to obtain hyper-tolerant clones. We investigated which mutations in the genome could be associated to Li hyper-tolerance. The advantage of this approach is to mimic the genetic adaptation that can occur in cells facing Li contamination. Among the proteins encoded by the genes that were mutated, we identified ion transporters, transporter regulators, ribosomal proteins, proteins with catalytic activity, membrane proteins and transcriptional regulators (Figure 1B).

Common genes involved in Li tolerance were found by both approaches. These datasets therefore demonstrate the robustness of our experimental designs. However, these approaches are also complementary since we were able to reveal new mechanisms contributing to Li tolerance by the evolutionary experiment. In conclusion, our data highlight the central role of transport systems in yeast tolerance to Li and that transcriptional regulatory mechanisms are important for both sensitivity and tolerance to Li.

At a wider scale, we have initiated the study of the effects of Li on microbial communities and activities. As a first step towards this objective, we have sampled and analyzed soils from areas naturally enriched in Li. We aimed at collecting samples with different concentrations of lithium. Based on geological and pedological maps, we collected samples at three locations in the Massif Central (Echassières & Ambazac) and in Czech Republic (Lysina). We have successfully

obtained a collection of soil samples harboring a gradient of Li concentrations (validation by ICP-MS). Samples of mushrooms and plants were also collected to determine some potential macroscopic biomarkers. The first results revealed the absence of a correlation between the concentration of Li in soils and the level of accumulation by plants (Figure 2). Moreover, mushrooms did not accumulate Li (<0.7 ppm). However, due to a low diversity of fungal species found at the sampling sites (dry conditions), more samples should be collected in the future.



**Figure 2: Relationships between Li concentrations found in soil and in biota (plants or mushrooms).** The lines represent linear regressions (Pearson's correlation test).

### Perspectives

Further mechanistic investigations will be performed to reveal the acute proteomic or transcriptomic response of cells to Li. Moreover, in order to further understand the impact of Li at the microbial community level, metabarcoding diversity analysis and functional approaches will be performed on selected soils exposed to Li in controlled conditions.





3 6.9410  
**Li**  
Lithium



# Beauvoir programme





Critical metals are the metals supply disruption of which can entail severe industrial and/or economic consequences for sectors such as renewable energy, mobility and defense. Since these metals are associated with significant supply risk, there is a strong interest in exploring their alternative sources. A good example is lithium. This metal was listed as a critical metal for the European Union in 2020. The currently used lithium comes from the Andean salars and from granites or lithiniferous silicate pegmatites (lepidoolite, or spodumene). There is currently no significant lithium production in Europe but several prospects are underway.

According to the studies of Deetman et al. (2018) and Mulvaney et al. (2021), the global demand for lithium could increase tenfold between 2015 and 2050, mainly due to the demand on materials required for the production of lithium-ion batteries for electric vehicles. The same authors report the possibility of depletion of current lithium resources by 2060-2090 (Mulvaney et al., 2021). The search for new resources is therefore essential to meet the future demand.

In the framework of a collaborative research program between LabEX RESSOURCES21 and Imerys, the granite massif of Beauvoir will be examined from the mineralogical, geochemical, and metallogenic perspectives. The work focuses on the formation of intrusion (age, nature of magmatic processes leading to the formation of hyper-differentiated granites), the mineralogy of critical or strategic metal carriers, such as Li, Nb-Ta, Sn-W, and the most efficient methods of separating the rare metal-carrying phases.

The Beauvoir site is located in the Échassières district, Auvergne-Rhône-Alpes region, 470 km from Nancy (Figure 1), in the north-east of the French Massif Central.

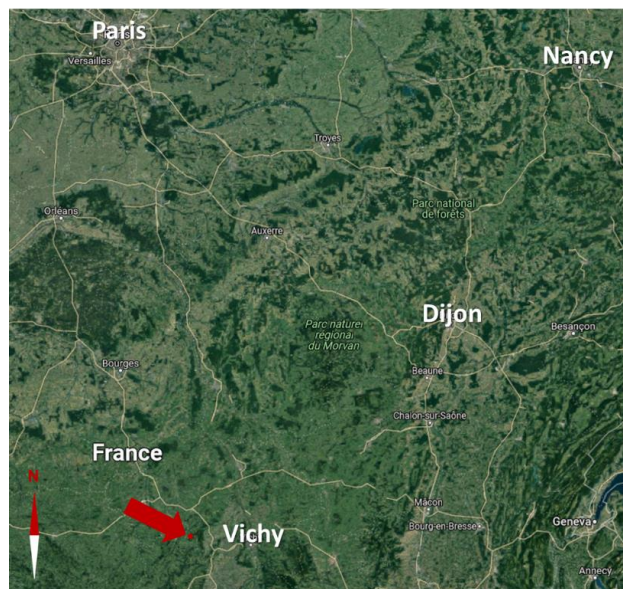


Figure 1 – Geographic location of the Beauvoir site

Beauvoir site has been exploited by Imerys for kaolin production for several decades. The site comprises a quarry and a plant that employs size- and gravity-based separation. These methods are among the “greenest” separation techniques because they do not require the use of reagents.

In January 2022, seven researchers, four doctoral researchers and two engineers affiliated to CNRS, GéoRessources, and CRPG – members of the Université de Lorraine belonging to LabEX RESSOURCES21 visited the site for the first meeting between the scientific and the industrial teams (Figure 2).



Figure 2 – The scientific team of LabEX RESSOURCES21 and the industrial team of Imerys working on the Beauvoir project

### Geological setting

Owing to the works conducted by the teams of the GPF scientific drilling campaign (synthesis in the special issue of *Geology of France* (1987), and Cuney et al. (1992)), the subsoil structure of Beauvoir was proposed in accordance with the schematic representation given in the Figure 3.

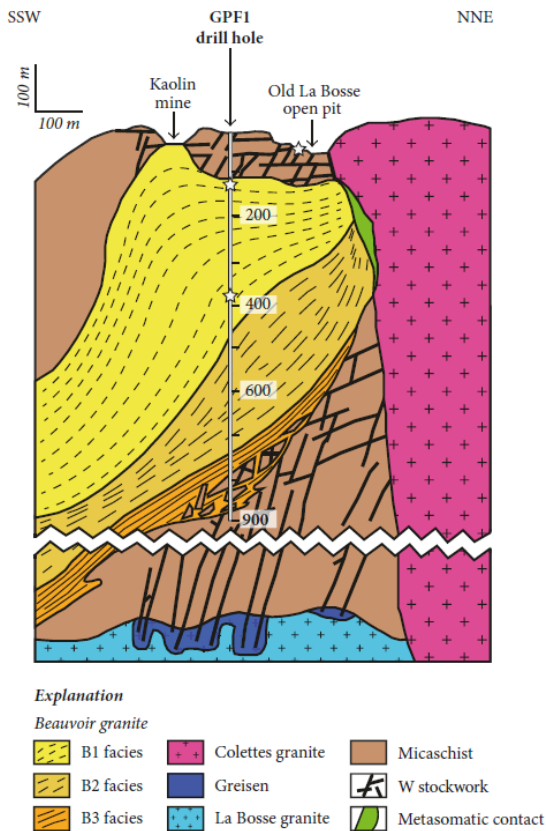


Figure 3 – Schematic representation of the Beauvoir granite (Géologie de la France, Aïssa et al. (1987) et Cuney et al. (1992))

### The project

The LabEX RESSOURCES21 scientific team is composed of ten permanent researchers, two post-doctoral and five doctoral researchers. The project comprises three major axes:

#### *First axis – Geology*

The actions of this axis of the project are aimed at establishing the relationship between the distribution and the content of rare and critical metals and magmatic and hydrothermal phenomena, along with the use of geological dating methods to understand the formation of pluton over time.

#### *Axe 2 – Characterization*

The actions of the second axis of the project are dedicated to: (1) the development of portable tools designed to detect and quantify in a fast and practical manner the rare and critical metals and (2) the establishment of the relationship between geochemistry and mineralogy of the studied rocks.

#### *Axis 3 – Processing options for metal recovery*

The third axis is dedicated to the development of a processing route suitable for the recovery of lithium-bearing minerals and phases-carriers of other rare metals such as, for example, Nb and Ta, using gravity and flotation separation methods, coupled with modelling tools.

### The visit to the Beauvoir site

Despite the difficult sanitary situation in January of 2022, the scientific team was welcomed on site for one and a half days in strict compliance with all health and safety regulations.

On the first day of the mission, the scientific team (divided into three groups in accordance with the scientific interests) visited the kaolin quarry (Figure 4) and the drill core storage facility.



Figure 4 – Kaolin quarry. Beauvoir, Imerys.

The geologists and engineers of Imerys presented the general drilling plan for the years of 2021-2022, the equipment installed on the site, the various aspects of the sampling procedure, how geological anomalies are treated and the methods used to capture the representative images of the cores. The acquisition of the core images is conducted in a closed black box, where the cores are exposed to light with constant characteristics, as well as UV light. Each core is characterized with three images: wet core, dry core and core under UV light. If necessary, color tablets are introduced for reference.

At the drill core storage facility, doctoral and post-doctoral researchers were able to make their first pre-selection of samples for their future studies.

The following half-day was dedicated to the exchange between the industrial and the scientific team. The doctoral and post-doctoral researchers presented their research projects and their strategies to achieve the set objectives. Between the presentations, short Q&A sessions with the members of industrial team took place.

The visit concluded with the demonstration made by the representatives of the «characterization» axis, which consisted in presenting the portable tools and showing their use directly on the drill cores coming from the new drilling campaign; LIBS (Laser-Induced Breakdown Spectroscopy) was presented by Naila Mezoued (Figure 5) and the XRF (X-ray fluorescence) by Jean Cauzid.

#### **Acknowledgement**

The scientific team wishes to thank Imerys and the geologists and engineers of the Beauvoir site for the excellent welcoming visit.

**Article written by:** Michel Cathelineau, Alexandre Chagnes and Olga Chernoburova



Figure 5 – Demonstration of the portable tools (LIBS) by Naila Mezoued

#### **References**

- Cuney, M., Marignac, C., Weisbrod, A., 1992. The Beauvoir topaz-lepidolite albite granite (Massif Central, France); the disseminated magmatic Sn-Li-Ta-Nb-Be mineralization. <https://doi.org/10.2113/GSECONGEO.87.7.1766>
- Deetman, S., Pauliuk, S., van Vuuren, D.P., van der Voet, E., Tukker, A., 2018. Scenarios for Demand Growth of Metals in Electricity Generation Technologies, Cars, and Electronic Appliances. *Environ. Sci. Technol.* 52, 4950–4959. <https://doi.org/10.1021/acs.est.7b05549>
- Harlaux, M., Mercadier, J., Bonzi, W., Kremer, V., Marignac, C., Cuney, M., 2017. Geochemical Signature of Magmatic-Hydrothermal Fluids Exsolved from the Beauvoir Rare-Metal Granite (Massif Central, France): Insights from LA-ICPMS Analysis of Primary Fluid Inclusions. <https://doi.org/10.1155/2017/1925817>
- Mulvaney, D., Richards, R.M., Bazilian, M.D., Hensley, E., Clough, G., Sridhar, S., 2021. Progress towards a circular economy in materials to decarbonize electricity and mobility. *Renew. Sustain. Energy Rev.* 137, 110604. <https://doi.org/10.1016/j.rser.2020.110604>

## THE MAGMATIC-HYDROTHERMAL SYSTEM OF THE BEAUVOIR GRANITE AND ITS IMPACT ON THE DISTRIBUTION OF CRITICAL METALS

### General framework

The Beauvoir granite belongs to the Echassières granitic complex, which is located in the northern part of the French Massif Central and was emplaced within the micaschists of the Sioule metamorphic series as a result of the late-Variscan orogeny evolution (ca. -420 to -290 Ma). This highly differentiated topaz-lepidolite-albite granite is characterised by Sn-Li-Ta-Nb-Be mineralisation and represents one of the best examples of peraluminous high-phosphorus rare-metals granite (PHP-RMG) worldwide (Cuney et al. 1992), which are the most important hard-rock Li resources in Europe.

### Objectives

While it appears that purely magmatic processes (partial melting, fractional crystallisation, etc.) are responsible for the high Sn-Li-Ta-Nb-Be concentrations in the Beauvoir granite, the impact of the magmatic-hydrothermal system on the multiscale distribution of metals is not as well quantified. This is however key to understanding the mineralogical, textural and geochemical evolution of the granite from its crystallisation to its exhumation, especially since the hydrothermal mobility of metals has been highlighted in the works of Harlaux et al. (2017). It therefore appears relevant to further characterize the Beauvoir magmatic-hydrothermal system through two major axes: (1) tracing the origin of hydrothermal fluids (magmatic, metamorphic, and meteoric) and (2) quantifying of the behavior of

metals during magma-fluid (immiscibility), fluid-fluid (mixing and immiscibility) and fluid-rock interactions.

### Methods

In addition to petrographic observations, the study of fluid inclusions (FIs) has been further carried out through microthermometry and Raman spectroscopy analyses. Microthermometric measurements are realized on a Linkam THMS600 heating-cooling stage connected to an Olympus BX51 microscope and to a cooling circuit for measuring temperatures higher than 200 °C. This system allows the determination of the temperatures of phase transition within an interval ranging from -200 °C to 600 °C. FIs are also analysed by Raman spectroscopy using a LabRAM HR800 spectrometer (HORIBA Scientific, Jobin-Yvon). Solids trapped within the FIs can be identified while searching for a match for their spectrum in a database and the relative proportions of trace volatiles present in the vapour phase can be determined using an in-house calibration. Altogether, these experiments will allow us to classify fluid inclusions and learn more about the fluids chemistry and the P-T conditions of fluid circulations. In parallel, the different generations of apatite were identified, petrographically characterised and analysed by SIMS (secondary ion mass spectrometry) in order to determine the variation of their oxygen isotopic composition.

### Results

Microthermometric measurements correlates with those of previous works (Aïssa et al. 1987; Harlaux et al. 2017) and can be used to classify FIs from the

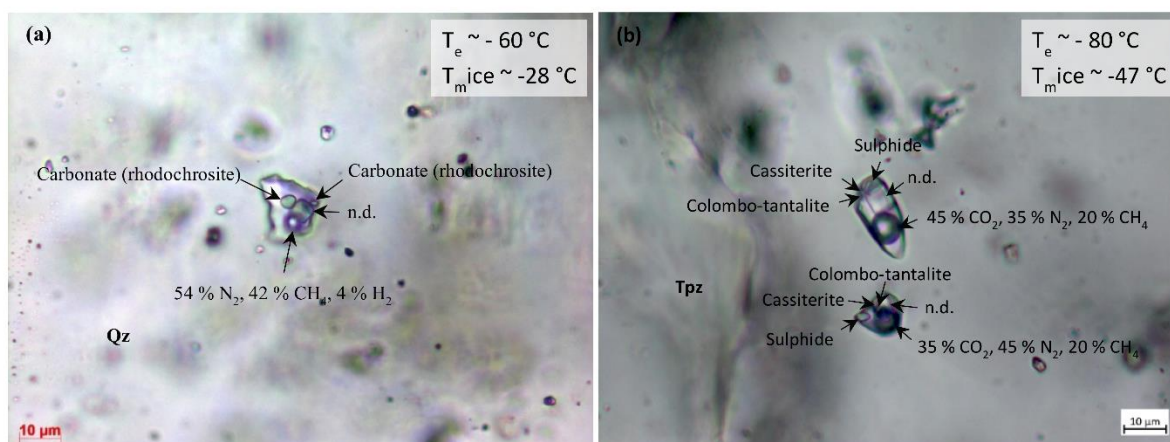


Figure 1. Microthermometry and Raman spectroscopy results of fluid inclusions trapped in (a) globular quartz of the transition zone between B1 and B2 facies (-450 m); (b) magmatic topaz from the B1 facies (-390.9 m)

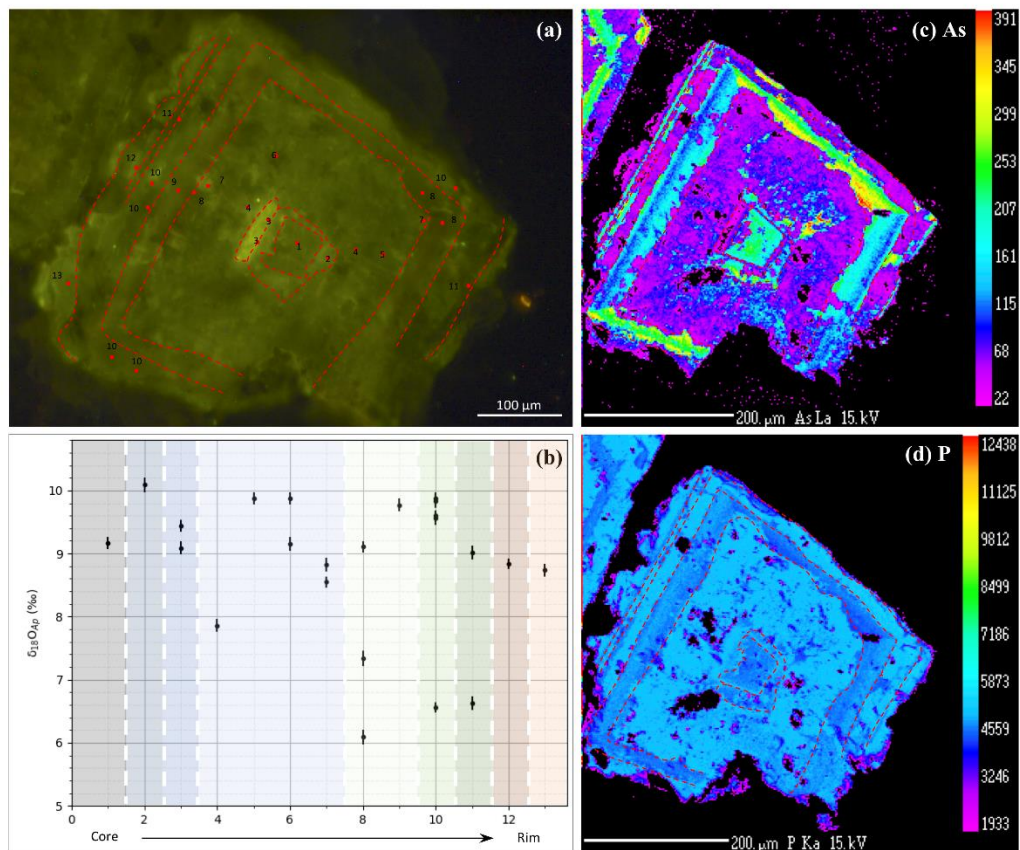


Figure 2. (a) CL image of an apatite crystal associated with fluorite in the B2 facies (-486.52 m) and location of SIMS analyses; (b)  $\delta^{18}\text{O}$  variations from the core to the rim of the crystal (Colours refer to the growth bands represented on figure a); (c) and (d) X-ray mapping of As and P concentrations respectively (expressed in ppm)

earliest fluids to the latest hydrothermal circulations (Figure 1). The goal being to better understand the metal distribution via fluids during the evolution of the magmatic-hydrothermal system, establishing a relative chronology of fluid circulations is therefore essential. We focus first on magmatic fluids, identified as the earliest fluids circulating in the Beauvoir granite. Raman spectroscopy data show in particular the presence of cassiterite (Sn) and colombo-tantalite (Ta-Nb) in magmatic FIs trapped in magmatic topaz from the B1 facies (Figure 1). If we show that they are daughter crystals, it would support the idea of high hydrothermal mobility of metals highlighted by Harlaux et al. (2017). Finally, oxygen isotopic data show variations that can be significant between the different generations of apatite and within some generations, even if values within most generations are generally quite consistent. In the case of apatite associated to fluorite,  $\delta^{18}\text{O}$  of apatite values range from 6 to 10 ‰, the lowest values being found at the

rim of the crystal where the concentrations of As and P respectively increase and decrease. They show a slight correlation with cathodoluminescence domains, which seem to be essentially linked to variations in elemental concentrations, in particular in P and As (Figure 2).

### Perspectives

We would like to continue the study of FIs not only through microthermometric and Raman spectroscopy analyses but also through the determination of their major and trace elements composition by LA-ICP-MS.  $\delta^{18}\text{O}$  in apatite will be interpreted in the light of other parameters such as the temperature of fluid circulation to have access to the O isotopic composition of the fluids or U-Pb dating results.

### References

- Aïssa et al. (1987) *Géologie profonde de la France*, 1.2-3: 335–350.
- Cuney et al. (1992) *Economic Geology*, 87.7: 1766–1794.
- Harlaux et al. (2017) *Geofluids*, 1-25.

ESTEVEES Nicolas

LABORATORY: Centre de Recherches Pétrographiques et Géochimiques (CRPG)

PROJET LEADER: BOUILHOL Pierre ; France Lydéric ; Cuney Michel

## THE ROLE OF MAGMATIC DIFFERENTIATION IN MAKING RARE-EARTH METAL GRANITES : PETROGENETIC EVOLUTION OF THE BEAUVOIR GRANITE

ESTEVEES Nicolas

BOUILHOL P. – FRANCE L. – CUNEY M.

### General framework

Magmatic differentiation is known to enrich residuals melts in incompatible elements through crystal fractionation. At the paroxysm of this differentiation, we find the group of rare metal granite, known for their economic potentials in Li, Nb-Ta, Sn-W (Cuney et al., 1992). If the evolution from a mafic-intermediate to granitic composition is well explained, the genesis of rare metals granites is for instance, poorly constrained.

### Objectives

Two main hypotheses are brought forward to explain the petrogenesis rare metal magmas, the first invoking residuals liquids after more of 99% of a granitic reservoir (Zoheir et al., 2020), whereas the second is based on specific source related processes (whether chemical and/or melting reactions, *e.g.* Michaud et al., 2021). Through sampling of the historical Beauvoir GPF drill, the objectives are to constrain the source of this granite and to highlight differentiation processes that led to the enrichment of this body. Associated with these two studies, another goal is to know the duration of this magmatic construction through high resolution zircon U/Pb dating, and in other word, how long does it take to reach economic concentration in these incompatible elements.

### Methods

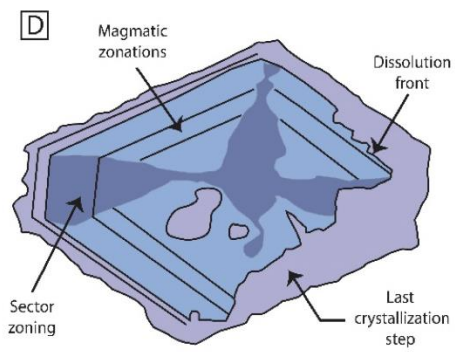
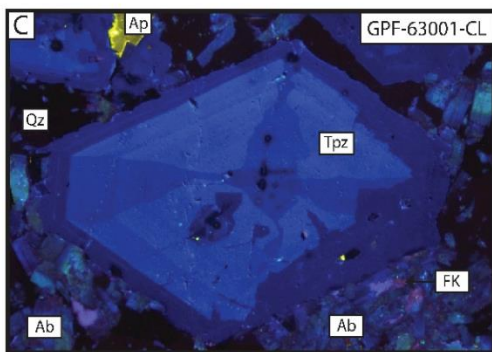
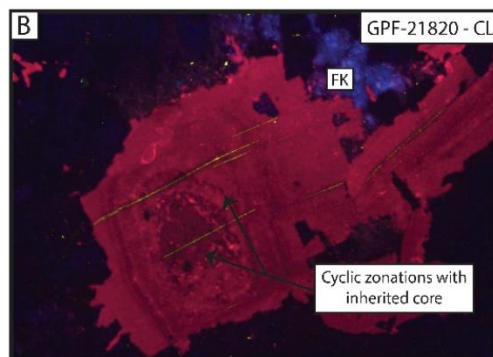
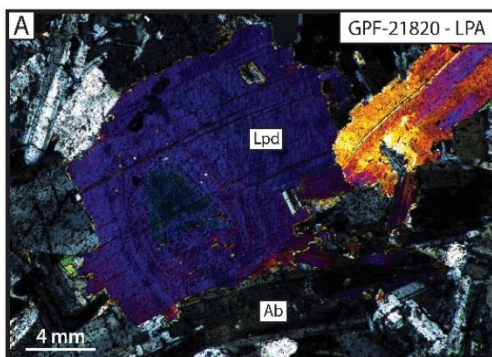


Figure 1. A et B) Lepidolite with cyclic zonation in LPA (A) and under CL image (B). C) Topaz from GPF-63001 (B2) under CL image and his interpretative scheme (D).

ESTEVEES Nicolas

LABORATORY: Centre de Recherches Pétrographiques et Géochimiques (CRPG)

PROJET LEADER: BOUILHOL Pierre ; France Lydéric ; Cuney Michel

In order to find the source of these magma, an isotopic study (Sr, Nd and Pb) is currently underway on both Beauvoir samples and potential protolith (mainly ortho- and paragneiss). In association with the University of Geneva, zircons from 14 samples of Beauvoir granite will be analyzed for HR-ID-TIMS. These high-resolution dating will provide the more accurate crystallization age of the Beauvoir granite. To constrain the magmatic differentiation process, thin sections are first analyzed under cathodoluminescence spectroscopy (CL), in order to track zonation in minerals, allowing selecting specific phases that recorded the differentiation process. This first step will be followed by EPMA analyses and LA-ICPMS, allowing to quantify the differentiation in terms of elemental budget

### Results

CL analyses show complex magmatic textures like oscillatory zoning or dissolution events in both lepidolite and topaz (Figure 1). These features are directly associated to different magmatic batches, owing both oscillatory zoning and partial dissolution. Mineralogical composition of mica (Figure 2) also reveals different

magmatic intrusions. Indeed, from the bottom to the top of the body (for B3 and B2), composition of less differentiated mica of each sample evolves from a zinwalditic to trilithionitic composition (less to more differentiated). This magmatic differentiation reflects increasingly differentiated intrusions (or sills) in the magmatic body. Finally, each intrusion differentiates itself toward a polyolithionitic composition, with lepidolite more and more enriched in Lithium. The Beauvoir granite would thus be regarded as a sill stack which crystallization leads to enrichment in rare metals from bottom to the top of the pluton.

### Perspectives

Perspectives of this work are to continue isotopic studies to constrain both sources and timing, and finish to understand the differentiation process via an elemental quantification with LA-ICPMS.

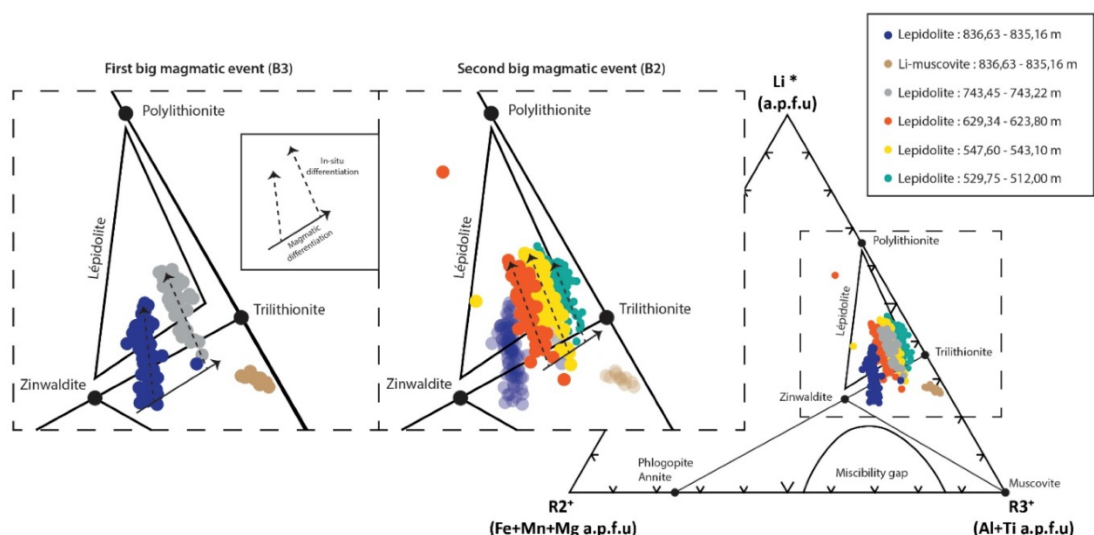


Figure 2. Composition of white mica of the Beauvoir granite (B3 and B2, from Jacquot, 1987) in the ternary diagram of Foster (1960). We see an evolution of lepidolite's composition for each magmatic event from



Naila MEZOUE  
GeoRessources  
Cécile FABRE and Jean CAUZID

---

## PORTABLE, QUICK AND QUANTITATIVE ANALYSIS OF LIGHT ELEMENTS (Li, Be, F) IN RARE METAL BEARING FELSIC ROCKS: THE BEAUVOIR CASE STUDY

### General framework

Lithium is a light element, essential to manufacturing batteries for both low-pollution vehicles and electronic devices of all kinds (phones, laptops, etc.). In fact, it is currently considered one of the most critical and strategic raw materials for Europe to achieve its low-carbon future ambition and secure a sustainable digital supply chain. As a consequence, renewed interest is given to projects developing new methods of exploration and exploitation of this high-demand mineral.

### Objectives

Lithium, in particular, is an element hard to detect and quantify using conventional analytical techniques which are also time-consuming and costly procedures during prospecting. Applying handheld spectroscopic analysis devices such as pLIBS, pXRF, or IR allows us to gather a considerable amount of qualitative and quantitative data in real time, directly in the field or in a laboratory setting, and on multiple sample types. Therefore, innovative strategies using the different pieces of information acquired can be developed to explore new ore deposits. For this purpose, three major steps were defined:

- Operate portable LIBS device to quantify light elements on un-prepared in-situ samples, in the quarry.
- Combine and reconcile results from different portable spectroscopic devices (LIBS, XRF, VNIR-SWIR, and Raman) to provide reliable and rapid information on mineralogical composition, proportion and elements concentration.
- Design an on-site laboratory, using portable spectroscopic analytical tools, dedicated to optimizing time resources and analytical costs.

### Methods

The handheld LIBS device applies a high-energy laser pulse at the surface of the sample to generate a plasma plume. Then the plasma light emitted is collected and processed to obtain an atomic spectrum. The specific location of emission lines provides qualitative information about the elemental composition of the rock while quantitative

analysis of these elements requires individual calibration curves.

Thus, to quantify lithium content in the main Li-bearing mineral observed in Beauvoir granite, Lepidolite, we analyzed using the SciAps handheld LIBS Z300, numerous reference samples with known lithium concentrations ranging from 350 ppm to 3 w% Li. Only Li-bearing Micas samples were considered to limit chemical matrix effects during the ablation process. However, to represent best the homogeneous composition of the Beauvoir granite and determine lithium content in hole core portions, 9 samples (12cmX8cmX5mm) extracted from a previous drilling campaign (2018) were analyzed. Acquiring a significant number of shots per sample allows to i) reduce any shot-to-shot variability caused by the plasma fluctuation and ii) obtain a representative LIBS spectra while minimizing the effect of chemical heterogeneities due to the sample's texture.

The LIBS spectra can be processed using the internal software to correlate the Li signal to the actual Li concentrations using a univariate linear regression model or through external regression models (PLSR, iPLS ...) using statistical computing software.

### Results

The Li-Micas calibration curve is shown in figure 1. The lithium signal is mostly represented in 4 wavelength ranges at 460, 610, 670, and 812 nm which were used to build the curve. The triple peak at 460 nm appears to be correlated with the highest lithium contents samples. Small variations in lithium signal within the same sample reflect the impact of physical matrix effects such as texture, hardness, and surface homogeneity on the plasma ablation process. The model shows good performance and the lowest RMS Error (0.11 %Li) when using internal standards (Al, Si, K, Rb, Cs) to normalize the Li signal.

A second calibration curve was built using Beauvoir granite samples. For each sample, a large number of shots were averaged to obtain a representative signal of the Li content for each granite portion. Variations between high and low Li signal from one shot to another in the same sample illustrate the heterogeneous mineral composition of the granite (Feldspar, Quartz, and Lepidolite).

The Beauvoir Granite calibration curve was tested on 4 m of granite portion from drill hole EMI21\_S13). A vertical profile of 396 points, a point each cm, was

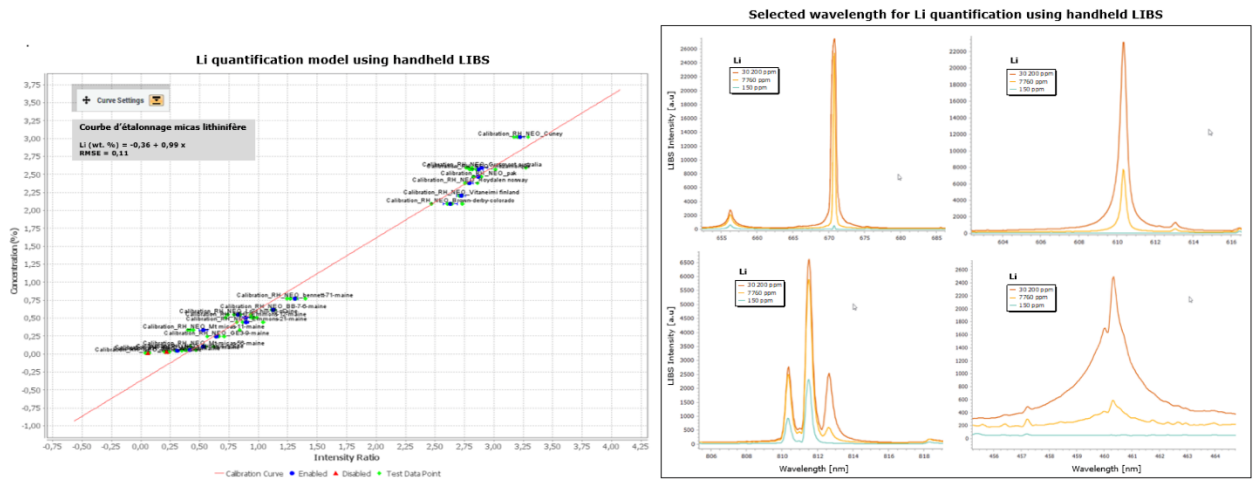


Figure 1. Li-Micas calibration curve using handheld LIBS.

### Beauvoir Granite calibration curve

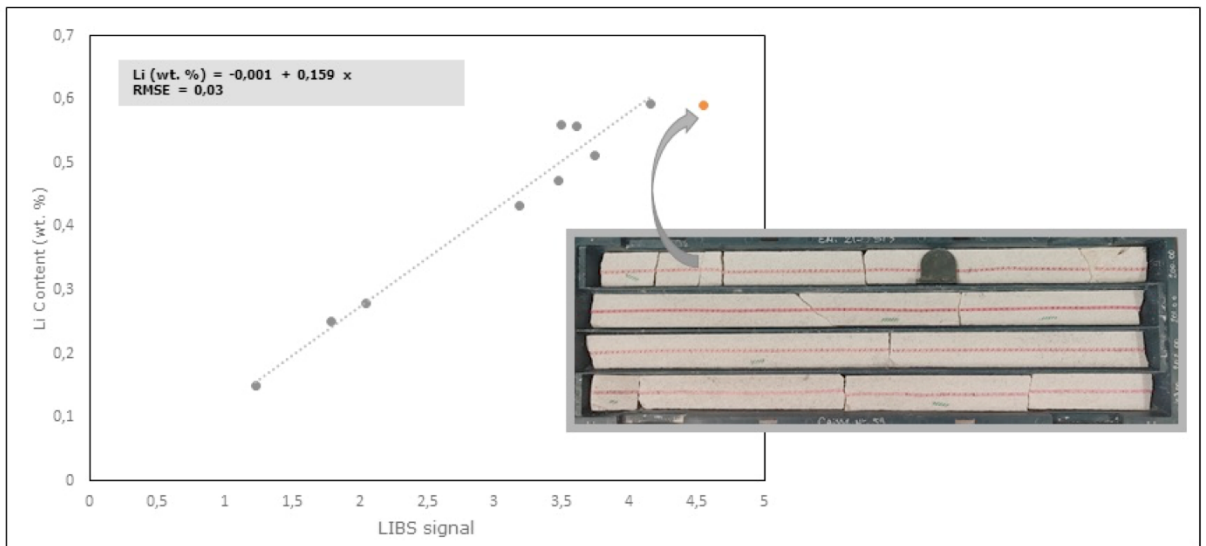


Figure 2. Beauvoir Granite calibration curve using handheld LIBS.

analyzed and then averaged to predict Li content. The result (figure 2) is promising, although, more tests are required to validate the model.

### Perspectives

Further work will be devoted to testing and validating the quantification models developed on various samples from the last drilling campaign (EMILI21) on Beauvoir granite. Thus, we will study the effect of facies and grain size variation as well as the impact of alteration and mineralized veins on lithium content prediction using handheld LIBS.

Additionally, acquisition parameters such as the number of analyses required and sampling steps will be optimized to guarantee a rapid and reliable field application.

The final part of this research will be focused on automatic mineral recognition and data reconciliation to provide a complete geochemical diagnosis of samples including elemental and mineral composition and proportion.

Steven KAHOU

LABORATORY: GeoRessources

PROJET LEADER: Michel CATHELINÉAU, Marie-Christine BOIRON

## QUANTITATIVE MINERALOGY OF THE BEAUVOIR GRANITE

KAHOU Steven

CATHELINÉAU Michel – BOIRON Marie-Christine

### General framework

The Beauvoir granite is a Carboniferous intrusion in the Sioule metamorphic series (Massif Central). Various scientific teams have studied the deposit to understand the magmatic genesis and mineralogy of this mineralized granite (Cuney et al. 1992), in particular, thanks to the GPF deep borehole and numerous works carried out between 1986 and 1990 and published in the following years. The albite-lepidolite-topaz granite of Beauvoir is the last intrusion in a peraluminous granitic complex of Variscan age composed of three successively emplaced units: the hidden granite of La Bosse, the two-micas granite of Colettes and the Beauvoir granite consisting of 3 units B1 to B3 (Cuney et al. 1992). The exposed part of the Beauvoir granite (unit B1) is currently quarried for kaolin. Compared to similar Li-F-rich igneous bodies, the Beauvoir granite is highly enriched in Sn (200-1400 ppm), Ta (20-400 ppm) and Be (20-300 ppm). The B1 granite, hololeucocratic, is composed of albite and abundant colorless lepidolite laths forming a framework filled with globular quartz and rare crystals of weakly perthitic and xenomorphic potassium feldspar.

### Objectives

The first approach of the project consisted in characterizing the lithium-bearing minerals (mainly lepidolite and, to a lesser degree, the Li-rich phosphates) and the Nb-Ta-Sn oxides (microlite, columbite-tantalite, cassiterite), from the cores available from the PER drillings. One of the objectives is to map the variability of Li (Rb, Cs, Fe) concentration in the lepidolite, and Sn, Ta-Nb concentrations in the oxides at the crystal scale.

The project's core links geochemistry and mineralogy to the needs of the teams working on separation processes. Several scales of mineralogical and textural variability are considered: the sample (the crystal, the population of crystals) and the geological site (vertical variation (drilling) and horizontal (lateral extrapolation between drillings)). All these detailed mineralogical data will also help the teams in charge of reconstructing the site's geological history and those developing the calibration of portable tools.

This study aims to generate sufficient knowledge to map the deposit in terms of metal carriers' textural and elemental properties in the mining areas. It is

crucial to compare the estimates of mineral phase proportions from *in situ* thin section mapping (microXRF) and the calculation of mineral phase proportion from total rock geochemistry on drill cores.

### Methods

Quantitative mineralogical analyses were carried out with a Bruker M4 Tornado Micro-XRF via 2D mapping of thin sections and drill cores. Mineral recognition was carried out using a Keyence VHX-100 digital optical microscope, an Olympus BX51 optical microscope, and a JEOL J7600F FEG scanning electron microscope which allows both EDS/WDS coupling. The chemical composition of the different minerals was measured with a CAMECA SX100 electron microprobe. The trace elements (Li, Be, etc.) were quantified using an Agilent 7900 quadrupole ICPMS coupled to an ESI New Wave 193 nm nanosecond excimer laser ablation system. The whole rock geochemical data have been obtained at the SARM-Nancy and provided by Imerys. The samples analyzed come from the PER drilling campaign carried out in 2018 (PER North, Centre, and South, with a maximum depth of 140 m).

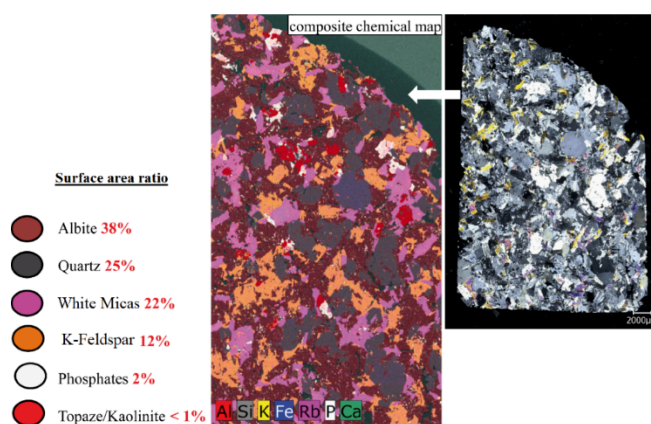


Figure 1. Micro-XRF composite chemical map showing the different minerals present in the rock as well as their surface area ratio.

### Results

First, the micro-XRF analyses made possible to estimate the surface proportion of minerals and thus determine their abundance. Taking, as an illustration, the C67 thin section (i.e. from the PER Centre borehole, 67 m depth), the combination of different elemental maps from the XRF analyses yields a composite chemical map in which the distinct minerals are easily identifiable as well as their proportion (Fig. 1). Based on this technique, the

Steven KAHOU

LABORATORY: GeoRessources

PROJET LEADER: Michel CATHELIN, Marie-Christine BOIRON

synthesis of the modal abundance of minerals from the 3 PER boreholes, and at different depths, is shown in the diagram in Figure 2. This diagram shows that albite is the most abundant mineral in the three boreholes (> 35%), followed by quartz, lithiniferous micas, microcline and phosphates. Topaz and oxides (i.e. cassiterite, columbite-tantalite and microlite) are present in minor to trace proportions.

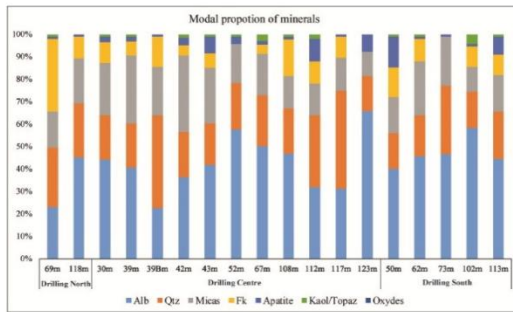


Figure 2. Diagram showing the modal proportion of minerals from the North, Central and South PER boreholes and at different depth.

The study's second objective is to calculate the relative proportions of minerals by knowing the individual composition of each mineral phase. Taking into account the relations between the quantities of an element and the sum of its bearers, graphical or numerical solutions may be obtained.

The QP diagram from Figure 3 shows that most of the points corresponding to the typical facies analyzed in petrography and geochemistry agree with the bulk geochemical data set from Imerys. Thus, the entire trend is covered from unaltered rocks to muscovitised and greisen alteration facies.

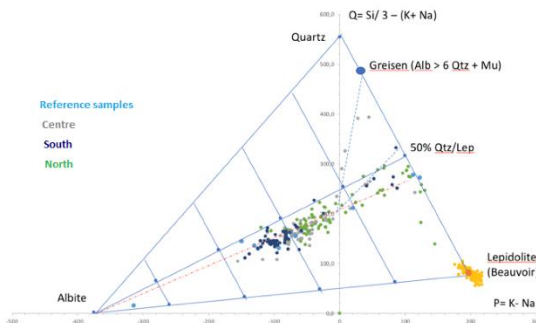


Figure 3. QP diagram showing the three PER boreholes North, Centre and South. Some reference samples are indicated by a blue point. The yellow points and the orange point correspond to the lepidolite analyzed and the average of the analyzed lepidolites, respectively.

The main trend corresponds to a "mix" for the fresh rocks between an albite pole on the one hand and a variable proportion of the quartz pole (40% of the quartz-lepidolite mix) + lepidolite (60% in the quartz-lepidolite mix). However, above values of about Q= 150, which corresponds to P= -80 (see Figure 3), the points continue to line up on the same axis, but this corresponds to the partial to total replacement of albite by a quartz-muscovite mixture (muscovitisation, or "true" greisen alteration if the relative amounts of muscovite and quartz in greisen is respected).

Perspectives

Based on the PER drillings, an initial inventory of the metal-bearing phases, their texture and their crystal-chemical variability was carried out. Based on the observation of drill cores coupled with the processing of geochemical data, sampling representative facies from the new drill holes will allow the inventory of typical facies to be completed. Finally, the quantitative approach to vertical variations in relative mineral abundance will be carried out by comparing estimates from micro-XRF mapping and the results of normative estimates or by algebraic resolution. Generalizing the quantitative mineralogy calculations to drilling data sets would lead to a mineralogical model block of the Beauvoir quarry.



79 196.97

**Au**

Gold

# Integrated project on Gold in french Guiana

Nina FERMET-QUINET<sup>1</sup>, Yann GUNZBURGER<sup>1</sup>, Rasool MEHDIZADEH<sup>1</sup>,

<sup>1</sup>: Université de Lorraine, CNRS-CREGU, UMR 7359 GeoRessources, 54000 Nancy, France

## Scientific issues

Mining activities are source of both positive (e.g., employment, infrastructure development) and negative (e.g., pollution, deforestation, social conflicts) impacts on territories. Although these impacts are now well known and studied at site level, all these activities, and their socio-economic and environmental effects on territory, are not systematically included in sustainable land use strategies. French Guiana is one of the most interesting case studies in the world due to (i) its geographical location in the Northern part of South America, (ii) its geo-ecological environment defined by its Amazonian Forest cover, (iii) its massive hydrographic network which is the place of a unique faunistic and floristic richness, and (iv) finally real legal and illegal mining activities linked to the presence of gold deposits (Fig.1). Therefore, the present work aims to develop a decision support tool for territorial planning that considers, coexistence between legal and illegal activities, but also vulnerabilities of the territory, different possible trajectories of territorial development (e.g., ecotourism) and local and geopolitical controversies at territory scale.

## State of the art

Present work aims to continue the work carried out by Scammacca (2020) resulting in the development of a methodology for assessing risks associated with mining industry at territory scale. Fig.1. enables to visualize issues associated with mining activities, particularly through superposition of the greenstone belt, source of the gold deposits, with the various mining authorization zones, and its location in the Amazon Park. Impacts of mining activity vary according to multiple criteria (e.g. deposit, extraction techniques, gold recovery methods). Thus Scammacca *et al.* (2021) proposed a typology of legal sites according to their size. One issue is to understand the illegal phenomenon through the resilient society of the *garimpeiros* and its economic functioning, which is defined by the intensity of illegal gold mining activities and their characteristics. Literature on this subject mainly concerns impacts in terms of deforestation and mercury contamination for the best known (Melun *et al.*, 2020) and social-economical studies (Le Tourneau, 2020).

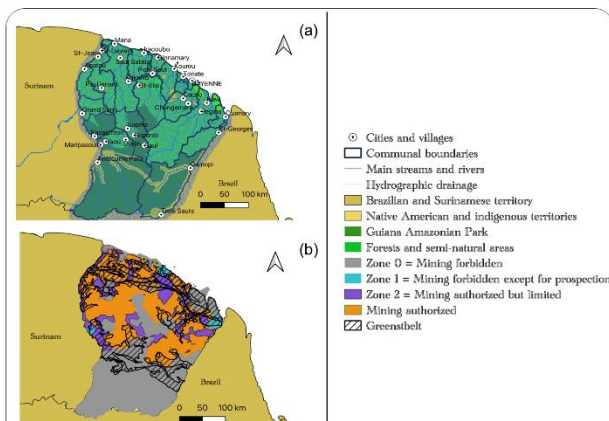


Fig.1. Land use maps of French Guiana : (a) simplified map of concerted development zones; (b) development plan for mining guidance. Data sources : <https://www.guyane-sig.fr>

## Methodological approach

To develop a typology of illegal sites from the point of view of impacts, we carried out: field missions, individual interviews with local stakeholders, and statistical analyses of data provided by the Observatory of Mining Activity in French Guiana (OAM). To identify and measure intensity of impacts of illegal gold mining activities on socio-economic and environmental development, it was necessary to understand the functioning of each typical site identified and their intrinsic characteristics. This work was carried out using photographs provided by the National Forestry Office of French Guiana, field missions and statistical tests on the OAM data.

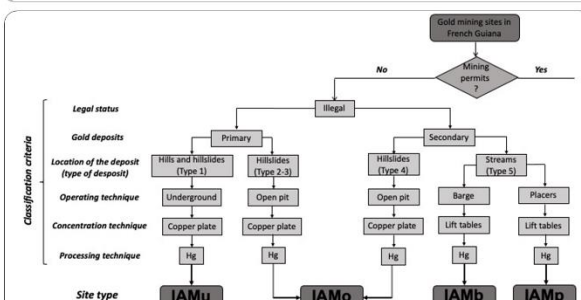


Fig 2. Proposed typology for French Guiana illegal artisanal mining (IAM) sites: underground (IAMu), open pit (IAMo), barges (IAMb), and placers (IAMp).

## Results

Analysis of data collected in the field through interviews and bibliography enabled us to identify 4 types of illegal sites based on six classification criteria: legal status, gold deposit, location of deposit, operating, concentration and processing techniques (Fig.2). Study of operating techniques of sites through statistical analyses of the different intrinsic characteristics of each site have shown that there is a root characteristic, which can explain the variation of the other characteristics and therefore the intensity of impacts. However, this root characteristic is specific to each type of site (e.g. number of wells for IAMu) and heterogeneity of data does not allow us to go further in the typology. Indeed, it does not allow illegal sites to be grouped under a typical characteristic as proposed by Scammacca *et al.* (2021) through site size. Given these results, it was decided to use a statistical approach based on existing relationships between the root characteristic and other intrinsic characteristics of each type of illegal sites.

## Assessment - Development perspectives

This approach allows to respond to the phenomenon of illegal mining activity by simulating different types of illegal sites based on real field data and thus to calculate their impacts on a territory. The final objective is to generate different mining development scenarios for a territorial objective and to compare them based on their risk scores. Therefore, several perspectives have been identified: (i) extend the random approach to legal sites, (ii) automate the methodology, (iii) produce a map to reflect perception of stakeholders on impacts and (iv) calculate risk scores of scenarios.

Nina FERMET-QUINET

LABORATORY: GeoRessources UMR7359

PROJET LEADERS: Yann GUNZBURGER & Rasool MEHDIZADEH

## MULTIDISCIPLINARY ANALYSIS OF MINING-RELATED RISKS IN THE CONTEXT OF TERRITORIAL PLANNING: DECISION SUPPORT TOOL DEVELOPED AND TESTED ON GOLD MINING IN FRENCH GUIANA.

FERMET-QUINET Nina, GUNZBURGER Yann, MEHDIZADEH Rasool

### General framework

French Guiana is a geo-ecological territory of 84,000 km<sup>2</sup> located in the NE of South America. Its borders are represented by the Maroni River to the W and the Oyapock River to the E, which separates it from Suriname and Brazil respectively. It is characterized by the presence of significant mineral resources, particularly gold in primary and secondary deposits. These deposits are exploited legally and illegally, producing between 2-5 and 3-5 tons of gold per year respectively. Impacts of legal and illegal gold mining activities, whether negative (*e.g.*, destruction of biodiversity, deforestation, mercury contamination, social protest) or positive (*e.g.*, direct and indirect employment, development of local activity) vary according to multiple criteria such as type of deposit targeted, number of workers, extraction techniques, and gold recovery methods.

### Objectives

Although impacts of mining activity at the mine scale are now well known, their repercussions at the territorial level are not systematically considered in territorial development planning. Consequently, the present work aims at developing a decision-support tool for territorial planning that considers coexistence between legal and illegal activities, but also vulnerabilities of the territory, different possible territorial development trajectories (*e.g.*, eco-tourism) and local and geopolitical controversies at the scale of the territory. To this end, we continue the work carried out by Scammacca (2020) which resulted in the development of a methodology for assessing positive and negative impacts and risks associated with mining industry at the scale of a territory. During the first year, particular attention was given to illegal mining activities and in particular the creation of a typology of site operations associated risks. This typology aimed at completing the typology of legal mines proposed by Scammacca *et al.* (2021) and be included in a scenario

comparison model which meets a certain territorial objective (*e.g.*, X ha deforestation). This tool should allow local stakeholders to discuss development of the mining sector through comparison of different territorial mining scenarios, according to their risk levels. This tool could also help both to clarify the issues involved in raising public awareness and to provide strategic assistance, supported by a risk analysis, to actors involved in the fight against illegal gold mining.

### Methods

To develop a typology of illegal sites from the point of view of their impacts, we carried out field missions, individual interviews with local stakeholders and statistical analyses of data provided by the *Observatoire de l'Activité Minière* (OAM) in French Guiana. To identify and measure intensity of impacts of illegal gold mining activities on socio-economic and environmental development, it was necessary to understand the functioning of each typical site identified, their root characteristics and their specific characteristics. The root characteristic corresponds to the major intrinsic characteristic of a site, *i.e.*, the one that varies the other specific intrinsic characteristics. This work was carried out using photographs of the illegal sites provided by the *Office National des Forêts* of French Guiana, field missions and statistical tests on the OAM's data using JMP software.

### Results

The results of data collected in the field through interviews and bibliography enabled us to identify 4 types of illegal sites based on six classification criteria: type of geological deposit, location of the deposit, exploitation, concentration, and processing methods (Fig. 1). The study of operating techniques of sites through photographs and identification of intrinsic characteristics of the different sites, as well as statistical tests, let to identify a root characteristic, as for the legal sites, which explains the variation of the other characteristics and therefore the intensity of impacts (Fig. 2). However, this root characteristic is specific to each type of identified sites (*e.g.*, shats for IAMu and motor pumps for IAMp) and heterogeneity of data does not allow us to go further in the typology. Indeed, it does not allow illegal sites to be grouped under a typical characteristic as proposed by Scammacca *et al.* (2021) through site size. Given these results, it was decided to use a statistical approach based on existing correlations between the root characteristic and other intrinsic

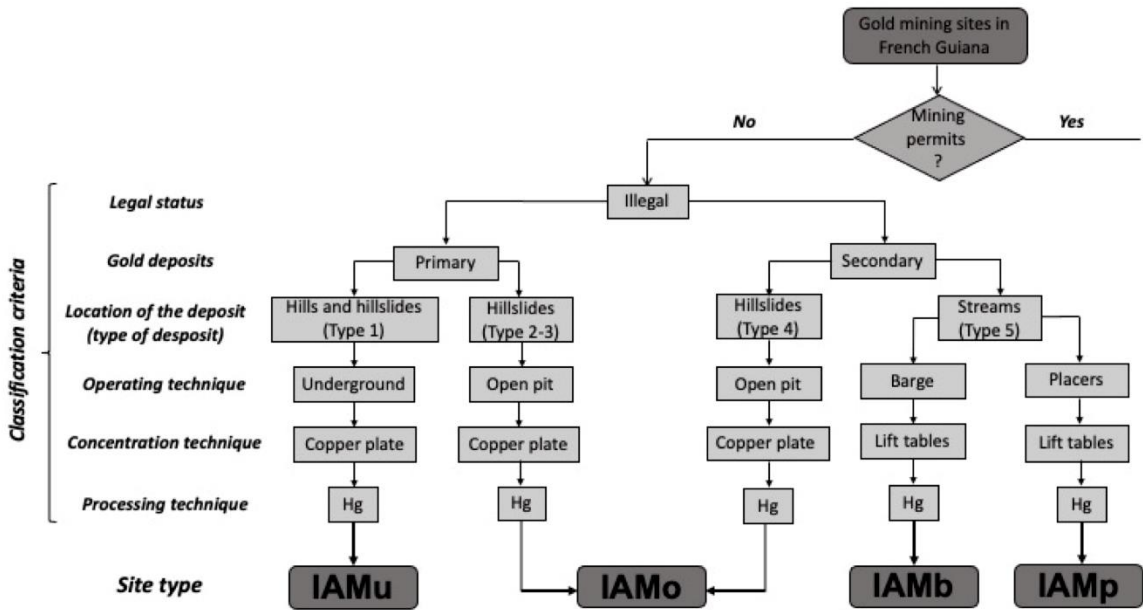


Figure 1. Proposed typology for French Guiana’s illegal sites. IAMu, IAMo, IAMB and IAMp corresponds respectively to underground, open pit, barges, and placers illegal mining.

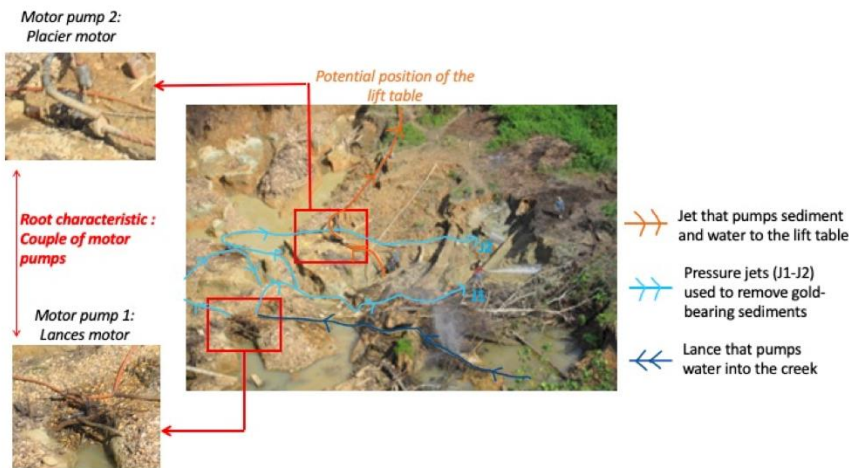


Figure 2. Schematic illustration of an illegal placer mining site, with some of its intrinsic characteristics. Its root characteristic corresponds to the pair of motor pumps. Picture was provided by the ONF of French Guiana.

characteristics of each type of illegal sites. This approach allows to estimate the characteristics of each illegal site through a statistical approach, to integrate (through a stochastic approach) illegal sites in scenario generation process and then to calculate their impacts on a territory.

**Perspectives**

Final objective is to generate different mining development scenarios based on a territorial objective and to compare them, based on their level of positive and negative risks. Therefore, in order to

achieve this objective, several perspectives have been identified: (i) extend the statistical approach to legal sites; (ii) generate a number of mining sites (legal and illegal) that meet different territorial objectives; (iii) calculate impacts of the scenario on the territory thanks to the existing correlations between the different types of sites and their impacts ; (vi) produce a stakeholders map to reflect their perception on impacts (v) calculate the risk score of different scenarios by integrating the perception of impacts and finally (vi) automate this entire methodology.



Thomas MONOT  
LRGP (Laboratory of Reactions and Chemical Engineering)  
PROJET LEADER: Baptiste LAUBIE

## GOLD HYPERACCUMULATION BY PLANTS AND AGROMINING IN FRENCH GUYANA

Thomas MONOT, Guillaume ECHEVARRIA, Baptiste LAUBIE, Marie-Odile SIMMONOT

### General framework

The growing demand for metals requires new processes to mine increasingly diluted and complex resources, while limiting their impact on the environment. Agromining is an attractive solution to achieve this double objective, by using hyperaccumulating plants capable of concentrating metals in the aerial parts, to produce marketable metal compounds. The aim of this project is to evaluate the potential for gold (Au) agromining in French Guyana.

### Objectives

The first step for agromining development is the identification of plant species capable of accumulating the metal of interest (*i.e.* gold). The exhaustive analysis of hundreds of species collected in herbaria is done with the help of a Field-Portable X-Ray Fluorimeter FPXRF (non-destructive and semi-quantitative method). Once the species are identified, they can be collected in the field and analysed by more conventional methods such as Inductively Coupled Plasma – Optical Emission Spectrophotometry ICP-OES (destructive and quantitative method).

The objective of this work is to verify that the analysis of gold in biomass and in their ashes is feasible with this type of apparatus, to define the possible interferences and the limits of detection (or even the limits of quantification).

### Methods

The FPXRF spectrometer used in this study is a NITON XL3t GOLDD from Thermo Scientific equipped with a radiation backscatter shield. To test the calibration for Au, two matrices are spiked with the ICP Au standard solution (Plasmacal Scp Science) to produce synthetic standards. Microcrystalline cellulose is used to simulate a plant matrix, and wood ash obtained from an industrial boiler is used to simulate plant ashes. In parallel, Au concentrations in

these samples are determined by ICP (ICP-OES ICAP 6300 DUO from Thermo Scientific).

### Results

Experiments show that the limit of quantification for gold is between 10 and 25 ppm with the FPXRF, depending on the calibration mode. The instrument has a linear response over a wide concentration range, both on organic material (biomass) and on mineral (ash) (Figure 1).

In contrast, measurements on plant samples (*Phyllanthus stipulatus*, Figure 2) collected in French Guyana (after selection *via* herbarium analysis), give a positive response to gold with FPXRF, while no trace is detected by ICP. This result is attributed to interferences between emissions rays of gold and zinc ( $L\alpha$  of gold and  $K\beta$  of zinc). Thus, when the matrix contains significant amounts of zinc, the device indicates the presence of gold.

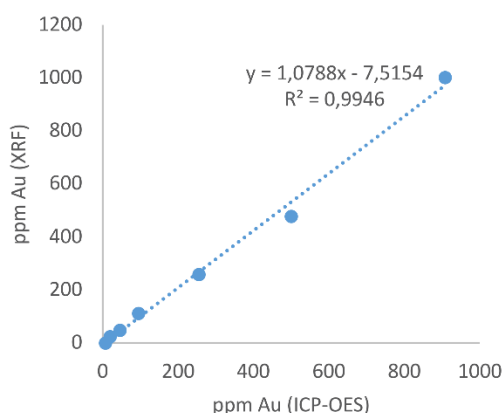


Figure 1. Gold calibration curve of FPXRF, with doped wood ashes.

### Conclusion

As it stands, the use of FPXRF does not allow the formal identification of gold hyperaccumulators. Quantification limits are high compared to the concentrations potentially present in plants (of the order of ppm) and the interferences strongly limit the use of this tool for the analysis of ashes, often rich in zinc.

Thomas MONOT

LRGP (Laboratory of Reactions and Chemical Engineering)

PROJET LEADER: Baptiste LAUBIE

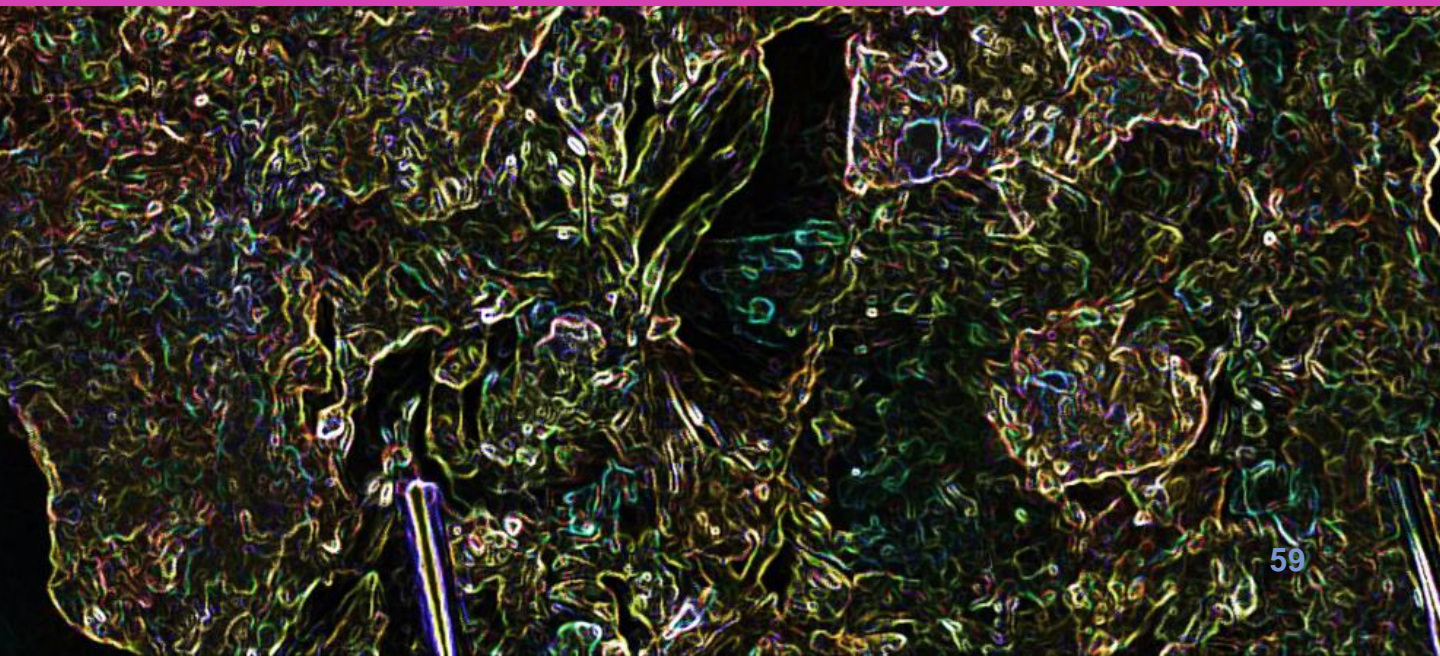
---



*Figure 2. Phyllanthus stipulatus, candidate for gold agromining, in French Guyana herbarium, in the field and after collection.*



**And more !**



Yujin JEGAL

LABORATORY: CRPG, GeoRessources

PROJET LEADER: Etienne Deloule, Julien Mercadier

## IN-SITU K-CA AND RB-SR DATING AND TRACING BY SIMS AND LA-ICP-MS

JEGAL Yujin

DELOULE Etienne, MERCADIER Julien

### General framework

Rb-Sr and K-Ca isotopic systems have been used in geosciences to date and trace geological processes. This isotopic system is particularly suited to K and Rb-rich minerals (e.g., micas and feldspars) which are complementary to minerals traditionally dated using U-Pb isotopic systems (e.g., zircon or monazite), which may be absent from certain geological contexts (e.g., hydrothermalism) and/or affected by post-crystallization alteration which affects this geochronometer. The conventional K-Ca and Rb-Sr dating methods based on physical separation and dissolution are encountered to limitations to date pure mineral separates and can be time-consuming and analytically challenging. In-situ methods applied at tens of micrometer scale directly on minerals like LA-ICP-MS (Laser Ablation Inductively coupled plasma mass spectrometry) and SIMS (Secondary Ion Mass Spectrometry) can be thus good alternative solutions. However, isobaric overlaps of  $^{87}\text{Rb}$  on  $^{87}\text{Sr}$ ,  $^{40}\text{Ca}$  on  $^{40}\text{K}$  cannot be solved by conventional in-situ mass spectrometry. The new generation of ICP-MS (Agilent 8900) where one reaction cell is situated between two quadrupoles (ICP-MS/MS) and SIMS IMS-1280-HR2 with high resolving power ( $\sim 40,000$ ) can cope with the isobaric interference by introducing reaction gases and high resolving power, respectively.

### Objectives

The project aims to develop and apply two isotopic systems (Rb/Sr and K/Ca) to date and trace geological processes by in-situ methods: SIMS and LA-ICP-MS. The first targeted isotopic system is Rb-Sr. Several limitations currently exist such as (i) the availability of reference materials (RMs) for the calibration of in-situ Rb/Sr mineral data, (ii) potential fractionation and matrix effects on Rb-Sr isotopic analysis (iii) the application of these developments to define their applicability of Rb-Sr system. Thus, the objectives are (i) to characterize and propose the Rb-Sr isotopic values of RMs suitable for in-situ Rb-Sr dating, (ii) to demonstrate the feasibility and capability of the two in-situ methods for measuring the Rb-Sr isotopic ratios and (iii) to apply in-situ Rb-Sr dating using the characterized RMs and optimized analytical conditions of LA-ICP-MS/MS to geological case studies.

### Methods

CRPG RMs in powder form and as mineral grains were characterized by multi-techniques: SEM-EDS, EPMA and ICP-MS at GeoRessources and CRPG, Nancy. The powder RMs were analyzed by ID-TIMS ( $^{87}\text{Sr}/^{86}\text{Sr}$  and Sr concentrations) and ID-MC-ICP-MS (Rb) at CRPG. The Rb-Sr isotopic compositions of CRPG RMs in mineral grain form and powder pellets were analyzed by LA-ICP-MS/MS (Agilent 8900 coupled to an ESI 193 nm) at GeoRessources and CAMECA IMS 1280-HR2 instruments at CRPG. RMs with a wide range of Rb-Sr and major element compositions and different physical properties were used either as primary calibration standards for mass bias correction or as secondary standards. Finally, Rb-Sr dating of mica-bearing samples by LA-ICP-MS/MS was carried out by using the characterized RMs.

### Results

#### 1. Characterization of the RMs for in-situ Rb-Sr dating (Jegal et al. 2022, *Geostand. Geoanalytical Res.*)

Selected grains from CRPG RMs, including Mica-Mg phlogopite, Mica-Fe biotite, GL-O glauconite and FK-N potassium feldspar present variable degrees of heterogeneity by SEM and EPMA imaging and chemical mapping. The ID-TIMS and MC-ICP-MS analyses yield the mean  $^{87}\text{Rb}/^{86}\text{Sr}$  ratios of 155.6 for Mica-Mg ( $\pm 4.7\%$ , RSD), 1815 for Mica-Fe ( $\pm 14\%$ ), 36.17 for GL-O ( $\pm 11\%$ ) and 69.9 for FK-N ( $\pm 5.9\%$ ). The mean  $^{87}\text{Sr}/^{86}\text{Sr}$  ratios are  $1.8622 \pm 0.36\%$  (RSD, as for other RM) for Mica-Mg,  $7.99 \pm 13\%$  for Mica-Fe,  $0.75305 \pm 0.12\%$  for GL-O, and  $1.2114 \pm 0.17\%$  for FK-N. The four RMs show variable degree of dispersion in  $^{87}\text{Sr}/^{86}\text{Sr}$  and Rb-Sr concentrations, reflecting their initial heterogeneity. The most homogeneous RM is Mica-Mg and the most heterogeneous RMs are GL-O and Mica-Fe.

#### 2. Rb-Sr isotopic analysis of the RMs by SIMS

SIMS analyses of Mica-Mg, Mica-Fe and FK-N have been conducted to test its capability and feasibility for in-situ Rb-Sr isotopic analysis. The results show the interferences of  $\text{FeSi}^+$  (mass 84, 86, 87, 88) on Sr isotopes in mica RMs, which contain high Fe contents (FeO  $>9$  wt.%), that could not be solved by the MRP in this study. Better internal (2 SE) and external (2 SD) precisions of  $^{88}\text{Sr}/^{86}\text{Sr}$  ratios are obtained for NIST 610 (0.09-0.35%, 0.07%-0.53%) by SIMS compared to LA-ICP-MS/MS (0.62-0.93%, 0.52-2.1%). Therefore, Sr isotopic analysis by SIMS allows for accurate and precise in-situ analysis for mineral phases with high Sr and low Fe and Rb contents such as apatite<sup>[1]</sup> reported by previous studies.

Yujin JEGAL

LABORATORY: CRPG, GeoRessources

PROJET LEADER: Etienne Deloule, Julien Mercadier

### 3. In-Situ Rb-Sr isotope measurements by LA-ICP-MS/MS on different matrices

Potential factors that influence on the accuracy and precision of Rb-Sr isotopic data and ages by in-situ LA-ICP-MS/MS approach were investigated based on the measured Rb-Sr isotopic data of various matrix RMs and mineral samples. The measured  $^{87}\text{Rb}/^{86}\text{Sr}$  data offsets of the RMs calibrated using NIST 610 relative to published data show a relatively strong correlation with major compositions of the RMs by yielding linear regressions with negative (e.g.,  $\text{SiO}_2$ , Fig. 1a) or positive (e.g.,  $\text{Al}_2\text{O}_3$ ) slopes, while the relations of the offsets with Rb-Sr compositions and ablation properties (i.e., down-hole fractionation, ablation pit volume) display no correlations. The accuracy of Rb-Sr isotopic ratios and ages could be improved by using the matrix-matched mineral RMs such as Mica-Mg for mica samples (Fig. 1b). However, there was a limitation of the investigated mineral RMs due to its heterogeneity and high uncertainties of Rb/Sr ratios<sup>[2]</sup>. Alternative approaches using non-matrix matched RMs such as NIST 610 with similar major element compositions to unknown samples and correction factor (CF) using the linear regressions were proposed for enhancing the precision of in-situ Rb/Sr isotopic data and ages (Fig. 1b). This correction produced better precision of Rb/Sr data and ages than approaches using the mineral RMs.

### 4. In-situ Rb-Sr dating by LA-ICP-MS/MS: the Quiberon detachment zone

Representative rock samples of leucogranite and associated dykes were collected from the Vivier outcrops in the Quiberon peninsula that records geological processes active during the development of the detachment zone linked to the South Armorican Shear Zone during the Carboniferous and Permian. In-situ Rb-Sr dating on multiple phases of micas, feldspars, apatite and tourmaline by LA-ICP-MS/MS (Fig. 1b) was applied in combination with other isotopic systems (U-Pb,  $^{40}\text{Ar}$ - $^{39}\text{Ar}$ ) to constrain the ages and duration of magmatic and hydrothermal processes in the Quiberon detachment zone. The established in-situ Rb-Sr dating approach provides Rb-Sr globally younger ( $300.6 \pm 3.8$  Ma on pegmatite- $281.2 \pm 3.8$  Ma on granite) than the ages obtained with other isotopic systems (319-300 Ma of  $^{40}\text{Ar}$ - $^{39}\text{Ar}$  on muscovite<sup>[3]</sup>, 315-290 Ma of U-Pb on apatite<sup>[4]</sup>). The late reset of the Rb-Sr isotopic system is probably linked to late circulation of salt-rich and Ca-rich fluids. The circulations of such type of fluids are indeed known in the Quiberon detachment zone during the 300-270 Ma period, as main driver of formation of U mineralization<sup>[5,6]</sup>.

### Perspectives

In-situ Rb-Sr dating approaches by LA-ICP-MS/MS have been established at GeoRessources and could be applied in the future to numerous geological case studies. Proposed Rb-Sr isotopic values and uncertainties for the four tested RMs are used for in-situ Rb-Sr dating by LA-ICP-MS/MS of unknown samples. For future work, the development of mineral RMs for calibration of high Rb-minerals which display Rb/Sr isotopic homogeneity with low uncertainty is suggested in the form of nano-powders or fused glasses. SIMS analysis yields better precision of Sr isotopic ratios relative to LA-ICP-MS/MS analysis. Therefore, coupling the two in-situ methods 'LA-ICP-MS/MS' and 'SIMS' for Rb-Sr isotope measurements can lead to a wide range of Rb-Sr dating and Sr isotopic tracing applications, with improved precision and accuracy of Rb-Sr isotopic data and ages to investigate complex geological processes, duration and timing of deposition processes in mineral and ore deposits.

[1] Decrée et al. 2020, *Contrib. to Mineral. Petrol.* [2] Jegal et al. 2022, *Geostand. Geoanalytical Res.* [3] Dusséaux et al., 2022, *J. Struct. Geol.* [4] Branquet et al., in prep [5] Ballouard et al., 2017, *Ore Geol. Rev.*; 2018 *Miner Deposita*

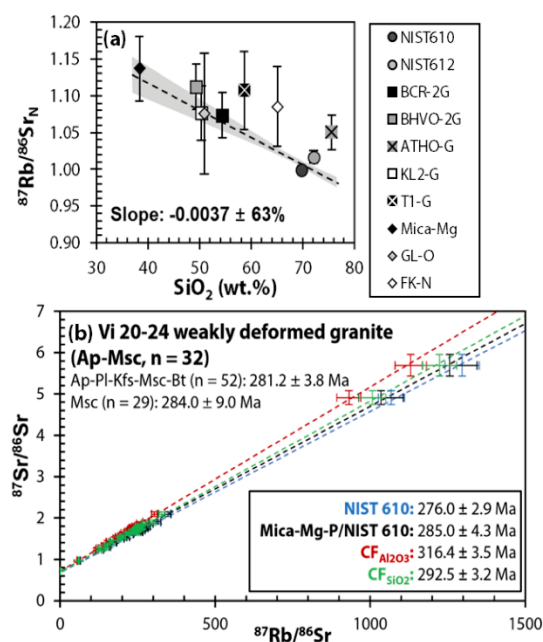


Figure 1. (a) Measured  $^{87}\text{Rb}/^{86}\text{Sr}_N$  (measured/published) ratios calibrated using NIST 610 for the RMs as a function of  $\text{SiO}_2$  of the RMs. The linear regressions and their associated uncertainties are computed in IsoplotR v5.0 (Vermeesch 2018), represented by dotted lines and shade area, respectively. (b) Rb-Sr isochrons for Vi 20-24 sample by using RMs (NIST610, Mica-Mg) and CF calculated from regression results of  $\text{Al}_2\text{O}_3$  ( $\text{CF}_{\text{Al}_2\text{O}_3}$ ) and  $\text{SiO}_2$  ( $\text{CF}_{\text{SiO}_2}$ ). Error bars are total uncertainties (2 SD).

## ACQUISITION & IMPLEMENTATION OF A NEW ELECTRON PROBE AT CRPG: A TOOL DEDICATED TO CHEMICAL MAPPING

Lydéric FRANCE; Laurent Tissandier; Julia Neukampf

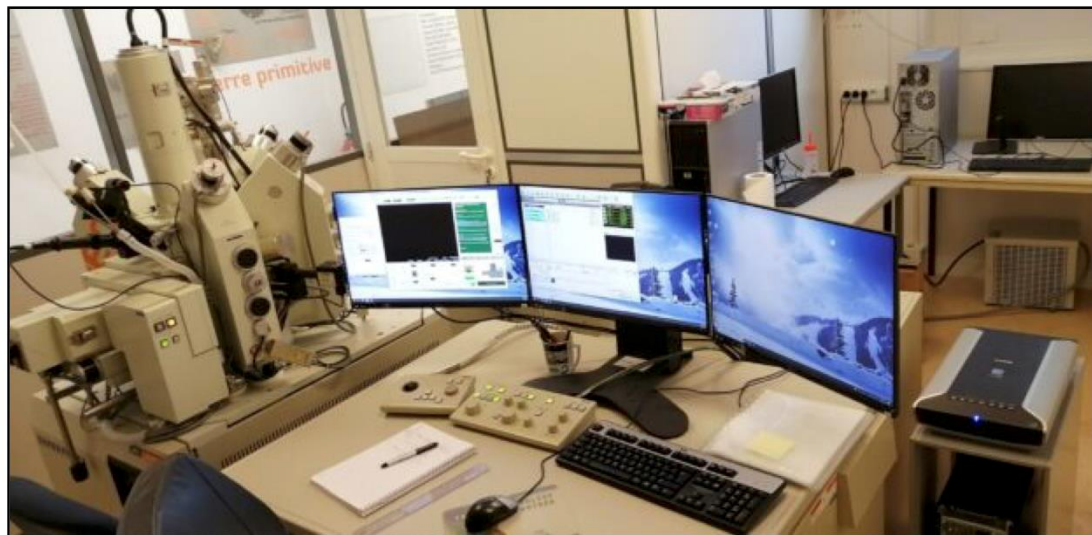
### General framework

The Microscopy and Electron Microprobe (MeMi) platform of the CRPG allows qualitative, semi-quantitative and quantitative imaging of terrestrial, extraterrestrial, and experimental geological materials. This platform is new at the CRPG (launch of the platform in 2022), it implements a scanning electron microscope (SEM; acquired in 2010), as well as an electron microprobe (EPMA; acquired in 2021; [Figure 1](#)). The new EPMA was funded by CRPG researchers, by CRPG laboratory, and its implementation was supported by LabEx Ressources21, and by OTELO. The main objective of this new platform for the next five years will be to continue semi-quantitative analysis and imaging on the SEM, and to develop numerous analytical approaches in semi-quantitative and quantitative mapping on the EPMA.

dispersive spectrometers (WDS), each with 2 or 4 monochromator crystals and a P-10 or Xenon X-ray counter. This configuration allows accurate quantitative in-situ analysis of chemical elements ranging from boron to uranium. In addition, an energy dispersive spectrometer (EDS) allows rapid elemental identification and can be combined with the other spectrometers for simultaneous analysis of elements in very different concentrations. Secondary electron (SE) and backscattered electron (BSE) detectors allow the acquisition of images with magnifications ranging from 40 to ~100,000. BSE images reveal compositional contrasts based on the molecular weight (Z average) of the sample at the analysis level. A panchromatic cathodoluminescence (CL) detector is also attached to this apparatus and reveals very efficiently defects and zonations in crystals (olivine, quartz, zircons, apatites for example...).

The spatial resolution will depend on the conditions used but can be estimated at about  $1 \mu\text{m}^3$  for classical silicate analyses, this volume being reduced at lower acceleration voltage, and for denser samples. However, if very mobile elements must be quantified (alkalis, ...), a defocused mode can be applied (up to  $20 \mu\text{m}$  diameter).

The detection limits will also depend on the



8230 installed at CRPG in 2021.

### Objectives

The CRPG acquired in 2021 an EPMA of the type JEOL JXA 8230. This machine is dedicated to quantitative chemical mapping ([Figure 2](#)). The electron gun works with a tungsten filament (W), and the acceleration voltage can be set between 0.2 and 30kV depending on the use. This probe is equipped with 5 wavelength

analytical conditions (higher for light elements from boron to fluorine) and are generally between 10 and 200 ppm. The wide range of elements that can be analyzed also implies a very large and well characterized catalog of standards.

The samples to be analyzed must be solid and preferably in the form of thin slides or sections (ideally 1 inch in diameter) perfectly polished. For non-conductive samples (natural rocks, experimental silicate samples, ...) a carbon

metallization of 20 - 30 nm is necessary to avoid that incident electrons accumulate on the surface and degrade the results.

collaborate closely, and where the more classical spot analyses are mainly performed.

### Possible measurements

-Simple quantitative point by point analysis: all the elements selected will be quantified in order to quantify the composition of the sample at the location of the analytic point (area of ~ 1 to 20  $\mu\text{m}$  in diameter);

-Qualitative and quantitative elemental maps: the spatial distribution (2D) of the selected elements will be obtained by scanning the surface of the sample and will be represented as maps for each element or in combination. Chemical maps of several centimeters can be obtained.

### Future developments

In the coming years our goal is to develop tools to provide constraints on redox conditions, and on crystallization conditions of different geological materials (magmatic, metamorphic, terrestrial or extraterrestrial rocks):

-redox conditions: Our objective is to develop approaches to quantify the  $\text{Fe}^{3+}/\text{Fe}^{2+}$  ratios in different materials (garnets, glasses of different compositions, clinopyroxenes, spinels,...). One of the approaches that will be particularly explored will be the "flank method". For these future developments we will work in close collaboration with the CoMaX platform since syntheses of standards will be necessary.

-Crystallization conditions: Crystal morphologies as well as their possible chemical zonations are essential tools for the study of mineral growth conditions. The acquisition of an electron probe at the CRPG was driven by a collective need to develop high resolution imaging of these figures. In particular, we will use cathodoluminescence imaging, BSE, or X-ray mapping of major, minor, and trace elements. Many parameters can influence the quality of the obtained maps (in particular for high current maps for trace elements analysis); these different measurements require each one, and for each type of mineral considered (diamond, olivine, feldspars, apatite, topaz, pyroxenes, spinels...) a development phase aiming at optimizing the measurement conditions, and the standards used.

The electron probe acquired by the CRPG is intended to be used for these various methodological developments (flank method, high current maps...) which require a lot of machine time. It is complementary to the other electron probes present in Nancy on the SCMEM platform with which we

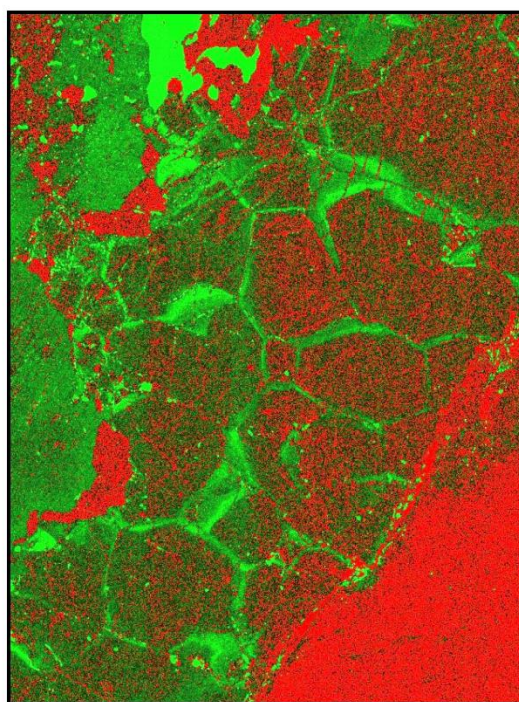
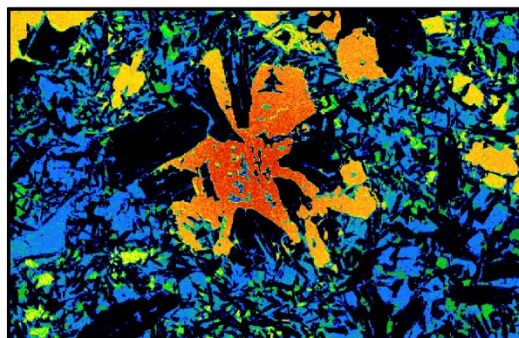


Figure 2. Exemples de cartographies chimiques pour des éléments majeurs, e.g., Mg dans l'olivine et le pyroxène (haut) et traces, e.g., P dans l'olivine (bas).

Guillaume SALZET

LABORATORY: UMR 1443 Bureau d'Economie Théorique et Appliquée (BETA)

PROJET LEADER: Sylvain CAURLA

**PHD PROJECT: SUSTAINABILITY OF FRENCH GUIANA FOREST SECTOR: A SPATIAL BIOECONOMICS MODELLING**

**SALZET Guillaume**

**CAURLA Sylvain – TRAISSAC Stéphane – MARCON Eric**

**General framework**

With its undisturbed tropical rain forest covering 96% of its territory (more than 8 million hectares), French Guiana represents one of the most important biodiversity ‘hot spots’ in France. However, these ecosystems and their associated services are threatened by the exploitation of forest resources in response to a marked and growing social demand (Piponiot et al. 2019).

Despite their good state of conservation (Brunaux and Binet 2014) and the application of low-impact logging methods, the forests of French Guiana are undergoing an increasing anthropogenic pressure driven by (1) the rising demand for construction timber claimed by the growing population and (2) the new demand for biomass energy as part of the energy sector’s diversification strategy. Furthermore there is the need to secure food and energy to the part of the population living of subsistence farming, which is the leading cause of local deforestation and conversion to agricultural land (Dezecache et al. 2017). Finally, the forest sector interacts in a complex way with the gold-mining industry, which

represents, with aerospace, one of the pillars of the territory’s development.

The forests are owned and managed by the French state through the National Forestry Office (ONF). These managed forests are grouped under the name of Permanent Forest Domain (PFD). Forests here undergo a conservative management strategy / policy characterised by reduced impact logging (RIL). Furthermore, the French state distributes funds for the development of downstream wood-based industries, which are currently in deficit and dependent on public investment.

**Objectives**

The study of French Guiana’s sustainable development trajectories requires to take into account the feedback between the different parts of the bio-economic system that compose French Guiana’s territory. Nonetheless a tool that simulates in an integrated manner the issues of ecosystem conservation and wood production for French Guiana is still lacking. To explore these trajectories and their consequences, this doctoral project aims to:

- simulate spatialised production of ecosystem services (carbon stock, functional diversity, commercial timber volume and game density) at the regional scale and their response to logging (Axis I).
- modelling the forest sector in French Guiana through a hybrid game-theoretic and partial

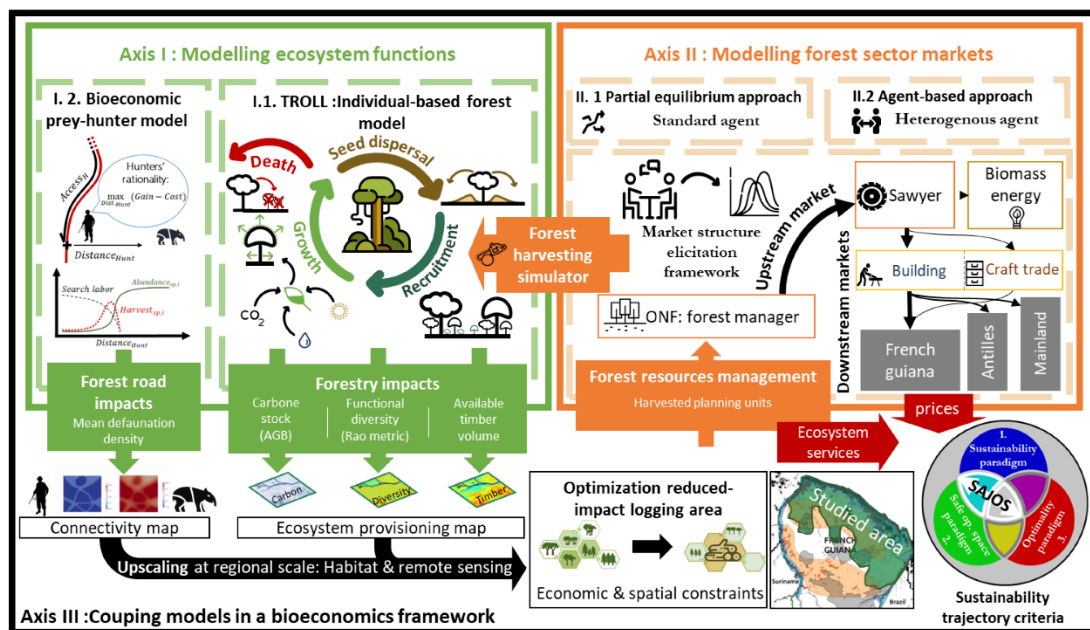


Figure 1. Graphical summary of research axis and data exchanges between modules



Guillaume SALZET

LABORATORY: UMR 1443 Bureau d'Economie Théorique et Appliquée (BETA)

PROJET LEADER: Sylvain CAURLA

---

equilibrium model of the regional sector markets (Axis II).

—coupling the spatial dynamics of ecosystems and the forest economic market model to estimate impacts and viability intervals of different development trajectories (axis III).

### Preliminary results

#### Axis I: Understanding and modelling the impact of timber harvesting on ecosystem services

To estimate the response of the mosaic of forest habitats to logging, we choose to use the model based on ecophysiological processes TROLL (Maréchaux 2016; Maréchaux and Chave 2017). This model proposes a mechanistic approach to diversity to better predict the responses of plant communities and ecosystem services (carbon storage and commercial volume) to different types of disturbance such as selective logging and climate change. For this purpose, we developed two R packages: the *rcontroll* and *LoggingLab*.

The *rcontroll* R package provides in a seamless integration of all the capacities of the TROLL model. Relying on up-to-date ecophysiology approaches, the TROLL model allows simulating realistic long-term evolution of tropical forest. We are currently working on a specific calibration process which gathers multiple sources of data from field inventories to large-scale remote-sensing data on forest structure (GEDI). The development is the result of a collaboration with the TROLL developers.

The *LoggingLab* R package is a spatially explicit forest harvesting simulator which mimics the forest manager rationality and the forest harvester impacts. All the parameters have been calibrated to scale the simulated impacts at observed level for the current forest management in French Guiana. The R package has been developed for the ManagFores project and my PhD.

Those packages can interact dynamically with each other and other R packages. The main advantage of interfacing with R package ecosystem is to rely on already available edge cutting methods like the surrogating method implemented in *hetGP* package. Using heteroscedastic Gaussian processes, a very flexible function to fit noisy nonlinear model's response, we could calibrate TROLL model for ecosystem metrics of one forest habitat of French Guiana.

With the French Biodiversity Office, we designed a spatially explicit model of hunter dispersal to evaluate the impact of an accessibility increase due

to the spreading forest road network. We found, consistent results with previous studies on small range impact along forest road network. But we also shredded in light long-range effects of hunter on animal populations through the behaviour adaptation of hunters.

#### Axis II: Modelling the dynamics of material and financial flows in the markets of the forest-wood sector in French Guiana.

Modelling the dynamics of the wood sector is a key issue for decision makers in order to choose the most resilient, safest and least costly in natural capital territorial development paths.

The specific features of the French Guiana forestry-forest sector lie in the structure of markets between agents, which are very different from neoclassical frameworks. In this context, we collected an economic monography of the socioeconomic system through 30 interviews of the economic agents implied in the forest sector (from the upstream agent like the forest manager to the downstream agent like the architects).

We summarised the goals, the resources and the strategies for each agent type and are developing an agent-based model with a hybrid approach of endogenous prices that falls, for the upstream part, within the field of game theory (Mohammadi Limaie and Lohmander 2008; Koskela and Ollikainen 2011) and for the downstream will be more traditional (Rivière and Caurla 2020).

The link between the ecological axis and the economic model is already designed. Relying on integer linear programming solvers, we designed the optimised regional harvesting program for the forest manager which ensures a pre-cautious non-decreasing flow of extracted wood subject to ecological constraints.

### Perspectives

We would like to expand the calibration approach to the regional scale to provide ecological asset maps. These maps could be a crucial to inform the stakeholders for conservation and industrial development policies.

This main task for 2023 will be to scale up models to give results at regional scale and couple ecological model with economic one.



# Education and Dissemination

# labEx R21 Education Committee

Led by Antonin Richard, Associate Professor and Lecturer, the Education Committee (EC) of the LabEx R21 is composed of 15 members, each involved in teaching and/or research activities in Labex R21 at the Université de Lorraine (UL). The role of the EC is to encourage, develop and implement the initiatives in higher education. To do so, LabEx R21 launches a call for educational project proposals every year. The actions covered within these proposals are listed below.

## **Master internships**

The second year Master internships are of high importance to the Labex R21 EC as they represent a stepping stone for PhD projects of R21. In 2022, the EC has granted nine MSc internships (representing 54 months of scholarships for students, 30 k€). The internships took place in laboratories of the LabEx R21 community (LSE – 1 project, CRPG – 1 projects, LIEC – 2 projects, GeoRessources – 5 projects).

## **Equipment for education**

Equipment for education is one of the priorities of the EC as it helps the students to learn in the best conditions and acquire up-to-date practical skills. In 2022, LabEx R21 has dedicated 14k€ to the project “Equipment for field trips” proposed by Cécile Fabre on behalf of the Département Géosciences (DG), the Ecole Nationale Supérieure de Géologie (ENSG) and Master Gestion de l’Environnement (GESTE) of the Université de Lorraine. This project allowed to provide the BSc and MSc students studying in geology, geophysics and hydrology with modern portable equipment for the field studies, enabling them to learn how to acquire and process the quantitative data from the field – a key skill for every student aiming to work in industry or academia.

## **Field trips and workshops**

The field trips and workshops are another key component in the successful student training. In 2022, the EC has co-funded several field trips and workshops organized by DG and ENSG. A recently organized co-financed field trip (5 k€ LabEx R21, 1 k€ CREGU, 0.5 k€ ANDRA) took place in France. It allowed 15 second year master students of DG to familiarize with the past and present rare metals and uranium mining activities in the French Massif Central. Another four-day trip was funded to the Congrès de la Société de l’Industrie Minérale in Lille (France) for 16 third year ENSG students (4.6 k€ Labex, 5.5 k€ SIM, 3.6k€ ENSG). A three-day trip was funded to the Ecole Thématique Ressources Minérales (CNRS, BRGM) in Orléans (France) for 15 second year master students (3.0 k€ Labex).

## **Invited professors**

LabEx R21 encourages the mobility of professors with unique competences through financially supporting the visits of the invited lecturers to the UL and the educational missions of the LabEx R21 members to partner universities. These activities allow to enrich and keep updated the educational programme of the students of the Université de Lorraine and to further contribute to the LabEx R21 international recognition. In 2022, the EC has funded the venue of Michel Jébrak (Emeritus Professor at UQAM, Canada) for a 20-hour course on Economics and Geopolitics of Mineral Raw Materials for Masters in ENSG and Ecole des Mines (2.5 k€). The EC has also funded travelling expenses for Emilie Thomassot (Lecturer at ENSG / CRPG) to the Université de Guyane where she gave a 36 hours course of Geochemistry at the BSc level (1.9 k€).

# Thematic doctoral school in Saxon-Sion, Lorraine, France

The 8th edition of doc-ECE on Green Hydrogen Production in the Circular Economy has taken place in Colline de Sion near Nancy (France) in November of 2022. This edition hosted by the University of Lorraine, LabEX RESSOURCES21 was open to any PhD candidates or recently graduated students with an affinity for developing new business models in a world of limited resources. The thematic school welcomed participants from various backgrounds, including: science and engineering (materials, chemical, electrical, and manufacturing), business and economics, law and product design.

The doctoral school was aimed to bring together highly motivated PhD candidates from a variety of disciplines to foster entrepreneurial thinking, increase their awareness regarding circular economy opportunities and provide them with skills and tools to translate technological ideas into relevant and viable business initiatives for a more sustainable future.

The core of the programme was the intense 5-day winter school during which the participants were working in multidisciplinary environment solving a challenge provided by an industrial partner (John Cockerill), while being coached by the doc-ECE experts and invited speakers. On the last day of the course, the outcome was presented to a jury in the form of a business pitch.

**KU LEUVEN** **RI SE** **LIÈGE université** **RWTH AACHEN UNIVERSITY**  **Mineral and Energy Economy Research Institute**  
Polish Academy of Sciences  **John Cockerill**

 **PhD school on Entrepreneurship in the Circular Economy** *Hosted by*   **UNIVERSITÉ DE LORRAINE**

*Where?* Saxon-Sion, Lorraine, France  
*When?* 28 November – 2 December 2022

Pre-register now on  
<https://circulareconomy.education>

 **RawMaterials**  
Connecting matters  
Co-funded by the European Union 

## Thematic doctoral school in Saxon-Sion, Lorraine, France

In the framework of European project Doc-SUM-ECE (Doctoral Summer School on Entrepreneurship in a Circular Economy) financed by EIT Raw Materials, University of KU Leuven (Belgium), Université de Lorraine (France), Research Institute RISE (Sweden), University of Liege (Belgium), University of Aachen (Germany), and Mineral and Energy Economy Research Institute of the Polish Academy of Sciences (Poland) have gathered twelve highly motivated PhD students from various disciplines and geographical origins (Spain, Poland, Germany, France and Estonia) to reflect on sustainable hydrogen production. This thematic school introduced the doctoral students to entrepreneurship and circular economy and provided them with skills and tools necessary to make products and processes more circular and sustainable, allowing to contribute to the implementation of the circular economy in the technological sector.

In this multidisciplinary environment the students were able to work on the sustainable production of hydrogen with the help of John Cockerill – the company recognized worldwide in the manufacturing of electrolyzers for hydrogen production – together with coaches and scientific experts from partner-universities of this European project.

**Alexandre Chagnes, main organizer and host of the thematic school in Colline de Sion**





**2022**  
90<sup>th</sup> Anniversary

# THE WORLD'S PREMIER MINERAL EXPLORATION & MINING CONVENTION

[pdac.ca/convention](http://pdac.ca/convention) | #PDAC2022

Participants: A.S. André-Mayer, Y. Foucaud, P. Ledru, A. Hauteville

Report by: Yann Foucaud, Alix Hauteville, Anne-Sylvie André-Mayer, Patrick Ledru  
Summary and translation: Olga Chernoburova, Alexandre Chagnes, Michel Cathelineau

Since the 1930s, PDAC (Prospectors & Developers Association of Canada) convention has been bringing together investors and exploration geologists in Toronto to find the financial means to exploit their discoveries. In more recent years, the convention welcomes all mining professionals: exploration companies, mining companies, geological services, investors, service companies and universities.

The members of the Université de Lorraine have attended the PDAC since 2012, bringing their contribution and strengthening the collaboration between the University and the mining industry at the international level.

The PDAC convention gives us the opportunity among others to:

- Promote international student recruitment (in 2022, UL was the only participating University);
- Get in contact with international mining companies to promote the Master's courses in the fields of exploration, ore processing, and mining;
- Establish cooperation and scientific research activities with North American academic actors;
- Establish relations with the industrial players in the minerals business to potentially gain access to the deposits they exploit with an aim of conducting academic research;
- Stay up to date with the current international mining projects and recent scientific works in the field of prospecting and economic geology;
- Preserve or enhance contacts with European colleagues active in Raw Materials projects and show the dynamics of the University of Lorraine to Europe (representatives attend PDAC since 2020);
- Contribute to the international reputation of the University of Lorraine.

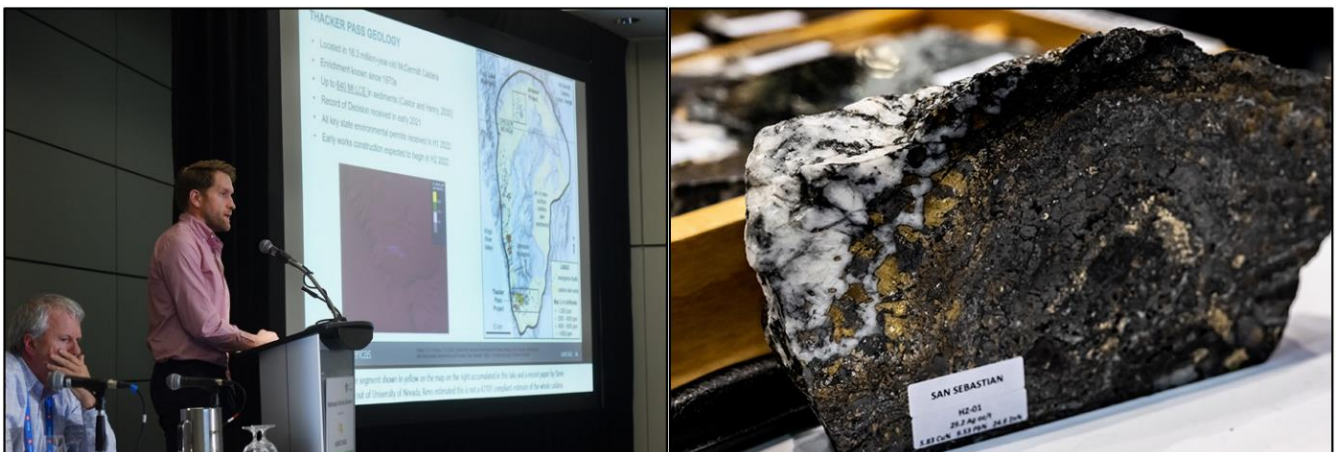


Figure : on the left – plenary presentation of a new lithium deposit discovered in McDermitt Caldera (Oregon, USA), on the right – presentation of a new gold deposit discovered in El Salvador; some drill core fragments exceed 25 g/t of Au

# Postdoctoral fellows and researchers in 2022

Laboratory	PRT/ PRA	Subject	Researcher
CRPG	PRT1, PRA4	Xp-PaREE : Premières contraintes sur les prémices du processus concentrateur en REE dans les magmas alcalins formant les principaux gisements sur Terre : contraintes expérimentales sur le partage des REE, et sur la série de différenciation	<i>Dr Sumith Abeykoon</i>
GeoRessources	PRT1	Facteur d'enrichissement de nickel dans les minerais saprolitiques de Nouvelle Calédonie	<i>Dr Yoram Teiter</i>
GeoRessources	PRT1	Minéralogie quantitative sur le granite de Beauvoir	<i>Dr Steven Kahou</i>
GeoRessources	PRT3, PRT5, PRA1	Reconfigurations de la géo-économie du lithium. Une approche par les réseaux globaux de production (GPN) et les dynamiques socio-spatiales en Australie et en Amérique latine	<i>Dr Vincent Bos</i>
GeoRessources	PRT4, PRA1	Développement de la datation K-Ar sur les micas lithinifères : chronologie magmato-hydrothermale des enrichissements en Li	<i>Dr Marie Gerardin</i>
University of Queensland	PRT2, PRA2	Novel methodologies for measuring the metallome in (hyperaccumulator) plants	Dr Anthony Van Der Ent

# PhD theses defended in 2022

**Bastien JALLY**

Defended on 22-02-2022

**Expanding Agromining to the rare-earth elements: Key elements of success from a chemical engineering perspective**

**Under the supervision of Marie-Odile Simonnot and Yetao Tang**

## **Abstract**

Agromine is a flagship theme of LabEx Resources 21. Widely studied for nickel recovery, it has been explored for other metals and elements. As part of the Joint International Laboratory Ecoland (University of Lorraine, INRA - Sun Yat-sen University of Canton), research conducted at the LRGP in collaboration with the LSE have shown that it is possible to recover rare earth extracted from the soil by phytoextraction, using the fern *Dicranopteris dichotoma*, from mine tailings from South China (thesis of Z. Chour, defense scheduled for late 2018). The objective of the work proposed here is to acquire more generic knowledge on the recovery of rare earths from the biomass of hyperaccumulator plants, using hydrometallurgical processes. In addition, these plants also accumulate aluminum, the recovery of which has never been studied. First of all, it will be necessary to complete the knowledge acquired with *Dicranopteris dichotoma*. New separation strategies will be considered to complement those already studied (precipitation, ion exchange). Optimization will be sought, with a view to achieving an efficient process in terms of yield, and with low impacts on the environment. Other plants have recently shown interest in the accumulation of rare earths and aluminum, especially *Phytolacca americana*, a perennial herb, also present in temperate climates (Yuang et al., 2017). This plant has very different characteristics of the fern, the latter being distinguished by a high silica content. Therefore, the strategy of recovery of rare earths will be very different. To sum up, the scientific objectives concern the hydrometallurgical separation processes that make it possible to valorize the rare earths and aluminum contained in the biomasses of the two types of accumulators, including the understanding of the solid phase and solution speciation, the mechanisms in play, the measurement of equilibrium and kinetics governing separations. Beyond scientific perspectives, this research will identify one or more innovative processes that could then be scaled up (from the laboratory to the pilot) for a possible industrial transfer (e.g. Econick). This PhD thesis will be conducted under structure of LIA Ecoland, under the direction of MO Simonnot, Pr, and B. Laubie, MC (LRGP) on the French side and Y. Tang, Pr, and RL Qiu, Pr (Professor @Lorraine) Chinese side. A committee will be set up to include experts in agromine, including JL Morel, Pr (LSE), hydrometallurgy, such as A. Chagnes, Pr (Géoressources) and mineral resources, particularly in rare earths elements. The thesis proposal responds to a strong need for research in a field in full development at the level of the various partners involved.



# PhD theses defended in 2022

**Yujin JEGAL**

Defended on 26-01-2022


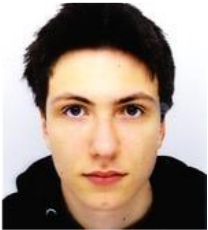
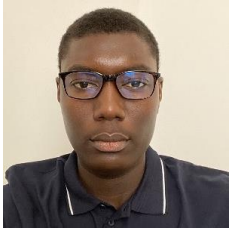


**In-Situ K-Ca and Rb-Sr datings and tracing by SIMS and LA-ICP-MS**

**Under the supervision of Cécile Fabre and Jean Cauzid**

## **Abstract**

Mineral exploration focused on deeply concealed targets at depth requires effective techniques applicable in the field in order to identify ore-forming systems on a large scale and pathfinders to locate ore on a smaller scale. According to the rapid development of portable equipment in recent years, the importance of near real-time analysis in the field has been increasing by helping fast decision-making support before laboratory requests. Spectroscopic analysis using individual equipment has been widely used in the exploration of mineral resources, but it is rare to apply integrated data from several techniques to characterize “vectors”, which provide variations in lithology, geochemistry, mineralogy, and mineral chemistry. In addition, it is even rarer if the combination of spectral data is obtained from various portable instruments. Therefore, this study aims at reconciling geochemical data acquired from portable spectroscopic devices in order to determine the best geochemical information from each technique applied by combining the mineralogical and elemental information. Elemental and mineralogical data are provided in this study by six portable techniques: (i) elemental analyses such as XRF and LIBS for major, trace, and light elements, and (ii) mineralogical analyses such as Raman, VNIR-SWIR, MIR, and XRD to constrain rock-forming, ore, and alteration minerals. The final objective of this study is to identify vectors to the ore by applying the reconciled multi-spectral data obtained from the “real” sample in the Elvira volcanogenic massive sulfide (VMS) deposit. To achieve this, step-by-step procedures were carried out: (i) methodological understanding of each technique, (ii) establishment of a spectral database consisting of naturally monomineralic minerals, (iii) design of a decision tree to classify by mineral or mineral classes based on diagnostic bands, and mineral identification and quantification of (iv) carbonate and (v) phyllosilicate minerals (i.e., trioctahedral chlorites and dioctahedral micas), which are indicators of the target deposit. Several limitations of portable spectroscopy were confirmed based on the device itself and the geological environment in the Elvira deposit. Nevertheless, portable spectroscopy is effective in identifying the presence and compositional changes of various minerals from heterogeneous rock samples. Therefore, spectroscopic analysis on-site can be one of the vectoring tools to determine the implication for ore mineralization in hidden ore explorations.



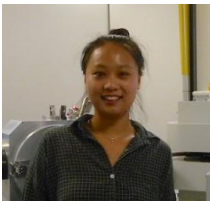

# Ongoing PhD theses in 2022

Laboratory	PRT/ PRA	Subject	Doctoral student
GeoRessources	PRT5, PRA 5.1	Multidisciplinary risk analysis of the mining sector for territorial planning. Development of a prototype decision support tool on the example of gold mining in Guyana	 <i>Nina Fermet Quinet</i>
LSE/LRGP	PRT3, PRA 3.2, PRA 2.2	Agromining and hyperaccumulation of gold by plants in French Guiana	 <i>Thomas Monnot</i>
LSE/LRGP	PRT 2, PRA2.2	Breeding the Ultimate European Nickel Phytomining Crop: A Biomolecular and Eco-physiological Study	 <i>Sérigne Ly</i>
GeoRessources	PRT3, PRA3.2	Development of boron extraction process within the framework of lithium recovery from brine: Case of the Hombre Muerto salar (Argentina)	 <i>Abdoul Fattah Kiemde</i>
LIEC	PRT2, PRA2.1	Multiscale analysis of the impact of lithium on microorganisms	 <i>Nicolas Fierling</i>

# Ongoing PhD theses in 2022

Laboratory	PRT/ PRA	Subject	Doctoral student
GeoRessources	PRT3, PRT1	Portable, quick and quantitative analysis of light elements (Li, Be, F) in rare metal bearing felsic rocks: the Beauvoir case study	 <i>Naila Mezoued</i>
CRPG/ GeoRessources	PRT1.1, PRA1.1, PRA2 PRT1.1, PRA 2	BeauLiY: Understanding protracted differentiation and its role in Li & rare metals concentration: Petrogenetic evolution & assembly duration of the Beauvoir granite.	 <i>Nicolas Esteves</i>
GeoRessources	PRT1.1, PRA 2	The hydrothermal system of the beauvoir granite and its impact on the distribution of critical metals	 <i>Océane Rocher</i>
GeoRessources	PRT31, PRT1.3	Geometallurgical evaluation of Li recovery by flotation from rare metal granites: mineralogical and textural variability study	 <i>Chloé Korbé</i>
CRPG	PRT1, PRT4	Reconstructing early orogenesis and sediment sources in the linking zone between the Alps and the Pyrenees (Late Cretaceous – Paleogene)	 <i>Julien Léger</i>

# Ongoing PhD theses in 2022

Laboratory	PRT/ PRA	Subject	Doctoral student
LIEC	PRT2	Faisabilité du traitement des eaux arséniées par la souche <i>Clostridium acidisolis</i> CK74	<i>Xiating Chen</i>
BETA	PRT 5, PRA 5.1, PRA 5.2	La durabilité de la forêt et de la filière bois en Guyane française : approche spécialisée par la modélisation bio-économique	 <i>Guillaume Salzet</i>
LIEC, CRPG	PRT2, PRA 2.1	Lithium et Santé-Environnement : Etude des effets in-vitro et in-vivo du lithium en milieu aquatique	 <i>Nicolas Dupuy</i>
GeoRessources	PRT1, PRA 1.1, PRA 1.2, PRT4, PRA 4.2	Analyse isotopique du lithium et du bore dans les inclusions fluides comme traceur des circulations de fluide	<i>Kristijan Rajic</i>
CRPG	PRT1, PRT4	In-Situ K-Ca and Rb-Sr datings and tracing by SIMS and LA-ICP-MS	 <i>Yujin Jegal</i>
GeoRessources	PRA4.4	Facteur d'enrichissement de nickel dans les minerais saprolitiques de Nouvelle Calédonie	 <i>Sylvain Favier</i>

# MSc theses funded in 2022

Supervisors	Laboratory	Title
Michel Cathelineau	GeoRessources	Formation des concentrations en métaux rares dans les aplites-pegmatites de Segura (Portugal)
Alexandre Tarantola, Jean Cauzid	GeoRessources	Détection des métaux critiques par outils portables dans les systèmes porphyres-épithermaux
Antonin Richard, Alexandre Chagnes	GeoRessources	Processus de concentration et voies de valorisation des métaux dans les systèmes hydrothermaux actifs
Inna Filippova, Lev Filippov	GeoRessources	Flottation des fines particules à partir des résidus miniers
Lev Filippov	GeoRessources	Récupération des métaux critiques (Ta, Nb, W) à partir des fractions fines des granites à métaux rares
Marie le Jean	LIEC	Etude des ligands des terres rares in planta
Damien Blaudez	LIEC	Etude des mécanismes gouvernant l'hypertolérance et l'accumulation de terres rares chez des espèces fongiques
Faure François, Combeau Hervé	ENSG	Quantification expérimentale du degré de surfusion de nucléation : implication sur la cristallisation des magmas komatiitiques
Lydéric France, Nathalie Gey	CRPG, LEM3	Collaboration LabEx R21 - DAMAS: Propagation de misorientations cristallines lors de la croissance en déséquilibre de silicates et de métaux
Thibault Sterckeman, Pierre Leglize, Catherine Lorgeoux	GeoRessources, LSE	Développement d'une méthodologie de dosage exhaustif des rhizodépôts par GC/MS et GC/MS-MS
Jean Cauzid, Andrei Lecomte, Lise Salsi, Saïd Sadeg	GeoRessources	Imagerie chimique : aide à la réalisation de masques

# MSc theses funded in 2022

Supervisors	Laboratory	Title
Alexandre Tarantola, Jean Cauzid, Cécile Fabre	GeoResources	Distribution de l'Ag dans les minéralisations des mines de Thorikos (Laurion, Grèce)
Damien Blaudez	LIEC	Identification par métatranscriptomique fonctionnelle de nouveaux gènes de tolérance aux métaux critiques
Aurélien Eglinger, Anne-Sylvie André-Mayer, Alix Hauteville	GeoResources	Apport de la géochimie des sulfures et de l'isotopie du bore des tourmalines sur la compréhension du système métallogénique aurifère du bouclier guyanais
SIRGUEY Catherine LAYET Clément	LSE	Couplage de la biolixiviation et de la phytoextraction des terres rares des sols (PHYTOLIXTER)
Christophe Ballouard Simon Couzinié	GeoResources	Evolution métamorphique et magmatique et protolithes métasédimentaires d'une province métallogénique à métaux rares (Li-Ta-Sn-W) de la chaîne varisque : géochronologie U-Pb de la région de la Sioule au nord du Massif central
Antonin Richard	GeoResources	Plomberie hydrothermal des zones de détachements
Julien Mercadier, Danièle Bartier, Gaétan Milesi, Marie Gerardin	GeoResources	Caractérisations des circulations de fluides et des altérations associées aux failles du bassin d'Athabasca (Canada)
Karine Devineau, Nathalie Gey	CRPG	Collaboration LabEx R21-DAMAS : Etude de la formation de la texture graphique à travers des échantillons naturels de pegmatites
Davide A.L. Vignati, Carole Leguille	LIEC	Spéciation et écotoxicité des mélanges Cr/Ni dans un milieu ultramafique non soumis à des pressions anthropiques
Laure Giamberini	LIEC	Assessment of the impact of sediment resuspension on the transfer of La and Gd from sediment to the water body and the impact on different trophic levels within a restricted biological community : biological approaches



# Publications

# Articles published in 2022

## LabEx RESSOURCES21 sponsored 39 articles in 2022

- Aharchaou, I., Maul, A., Pons, M.-N., Pauly, D., Poirot, H., Flayac, J., Rodius, F., Rousselle, P., Beuret, M., Battaglia, E., Vignati, D.A.L., 2022. Effects and bioaccumulation of Cr(III), Cr(VI) and their mixture in the freshwater mussel *Corbicula fluminea*. *Chemosphere* 297, 134090. <https://doi.org/10.1016/j.chemosphere.2022.134090>
- Bertauts, M., Janots, E., Rossi, M., Duhamel-Achin, I., Boiron, M.-C., Airaghi, L., Lanari, P., Lach, P., Peiffert, C., Magnin, V., 2022. A New Alpine Metallogenic Model for the Pb-Ag Orogenic Deposits of Macô-la Plagne and Peisey-Nancroix (Western Alps, France). *Geosciences* 12, 331. <https://doi.org/10.3390/geosciences12090331>
- Carocci, E., Truche, L., Cathelineau, M., Caumon, M.-C., Bazarkina, E.F., 2022. Tungsten (VI) speciation in hydrothermal solutions up to 400°C as revealed by in-situ Raman spectroscopy. *Geochimica et Cosmochimica Acta* 317, 306–324. <https://doi.org/10.1016/j.gca.2021.11.004>
- Carr, P.A., Moreira, E., Neymark, L., Norman, M.D., Mercadier, J., 2023. A LA-ICP-MS Comparison of Reference Materials Used in Cassiterite U-Pb Geochronology. *Geostandards and Geoanalytical Research* 47, 67–87. <https://doi.org/10.1111/ggr.12469>
- Combes, V., Eglinger, A., André-Mayer, A.-S., Teitler, Y., Jessell, M., Zeh, A., Reisberg, L., Heuret, A., Gibert, P., 2022. Integrated geological-geophysical investigation of gold-hosting Rhyacian intrusions (Yaou, French Guiana), from deposit-to district-scale. *Journal of South American Earth Sciences* 114, 103708. <https://doi.org/10.1016/j.jsames.2021.103708>
- Corzo Remigio, A., Nkrumah, P.N., Pošćić, F., Edraki, M., Baker, A.J.M., van der Ent, A., 2022. Thallium accumulation and distribution in *Silene latifolia* (Caryophyllaceae) grown in hydroponics. *Plant Soil* 480, 213–226. <https://doi.org/10.1007/s11104-022-05575-2>
- Decrée, S., Pašava, J., Baele, J.-M., Mercadier, J., Rösel, D., Frimmel, H., 2022. In-situ trace element and Sr isotope signature of apatite: A new key to unravelling the genesis of polymetallic mineralisation in black shales of the Early Cambrian Niutitang Formation, Southern China. *Ore Geology Reviews* 150, 105130. <https://doi.org/10.1016/j.oregeorev.2022.105130>
- Fabre, C., Ourti, N.E., Ballouard, C., Mercadier, J., Cauzid, J., 2022. Handheld LIBS analysis for in situ quantification of Li and detection of the trace elements (Be, Rb and Cs). *Journal of Geochemical Exploration* 236, 106979. <https://doi.org/10.1016/j.gexplo.2022.106979>
- Favier, S., Teitler, Y., Golfier, F., Cathelineau, M., 2022. Multiscale physical-chemical analysis of the impact of fracture networks on weathering: Application to nickel redistribution in the formation of Ni-laterite ores, New Caledonia. *Ore Geology Reviews* 147, 104971. <https://doi.org/10.1016/j.oregeorev.2022.104971>
- Filippov, L.O., Filippova, I.V., Crumiere, G., Sousa, R., Machado Leite, M., Botelho de Sousa, A., Korbel, C., Tripathy, S.K., 2022. Separation of lepidolite from hard-rock pegmatite ore via dry processing and flotation. *Minerals Engineering* 187, 107768. <https://doi.org/10.1016/j.mineng.2022.107768>
- Fosu, A.Y., Kanari, N., Bartier, D., Vaughan, J., Chagnes, A., 2022. Novel extraction route of lithium from  $\alpha$ -spodumene by dry chlorination. *RSC Adv.* 12, 21468–21481. <https://doi.org/10.1039/D2RA03233C>
- Foucaud, Y., Collet, A., Filippova, I.V., Badawi, M., Filippov, L.O., 2022. Synergistic effects between fatty acids and non-ionic reagents for the selective flotation of scheelite from a complex tungsten skarn ore. *Minerals Engineering* 182, 107566. <https://doi.org/10.1016/j.mineng.2022.107566>
- Gmar, S., Chagnes, A., Lutin, F., Muhr, L., 2022a. Application of Electrodialysis for the Selective Lithium Extraction Towards Cobalt, Nickel and Manganese from Leach Solutions Containing High Divalent Cations/Li Ratio. *Recycling* 7, 14. <https://doi.org/10.3390/recycling7020014>
- Gmar, S., Muhr, L., Lutin, F., Chagnes, A., 2022b. Lithium-Ion Battery Recycling: Metal Recovery from Electrolyte and Cathode Materials by Electrodialysis. *Metals* 12, 1859. <https://doi.org/10.3390/met12111859>



# Articles published in 2022

- Grosjean, N., Le Jean, M., Armengaud, J., Schikora, A., Chalot, M., Gross, E.M., Blaudez, D., 2022. Combined omics approaches reveal distinct responses between light and heavy rare earth elements in *Saccharomyces cerevisiae*. *Journal of Hazardous Materials* 425, 127830. <https://doi.org/10.1016/j.jhazmat.2021.127830>
- Guo, M.-N., Zhong, X., Liu, W.-S., Wang, G.-B., Chao, Y.-Q., Huot, H., Qiu, R.-L., Morel, J.L., Watteau, F., Séré, G., Tang, Y.-T., 2022. Biogeochemical dynamics of nutrients and rare earth elements (REEs) during natural succession from biocrusts to pioneer plants in REE mine tailings in southern China. *Science of The Total Environment* 828, 154361. <https://doi.org/10.1016/j.scitotenv.2022.154361>
- Hu, R., Beguiristain, T., De Junet, A., Leyval, C., 2022. Transfer of La, Ce, Sm and Yb to alfalfa and ryegrass from spiked soil and the role of *Funneliformis mosseae*. *Mycorrhiza* 32, 165–175. <https://doi.org/10.1007/s00572-022-01073-6>
- Jegal, Y., Zimmermann, C., Reisberg, L., Yeghicheyan, D., Cloquet, C., Peiffert, C., Gerardin, M., Deloule, E., Mercadier, J., 2022. Characterisation of Reference Materials for In Situ Rb-Sr Dating by LA-ICP-MS/MS. *Geostandards and Geoanalytical Research* 46, 645–671. <https://doi.org/10.1111/ggr.12456>
- Kumar, P., Sahu, N., Roshan, A., Rout, B.N., Tripathy, S.K., 2022. Influence of process parameters on impurity level in ferrochrome production—An industrial-scale analysis. *Mineral Processing and Extractive Metallurgy Review* 43, 622–632. <https://doi.org/10.1080/08827508.2021.1913154>
- Lachaux, N., Catrouillet, C., Marsac, R., Poirier, L., Pain-Devin, S., Gross, E.M., Giamberini, L., 2022a. Implications of speciation on rare earth element toxicity: A focus on organic matter influence in *Daphnia magna* standard test. *Environmental Pollution* 307, 119554. <https://doi.org/10.1016/j.envpol.2022.119554>
- Lachaux, N., Cossu-Leguille, C., Poirier, L., Gross, E.M., Giamberini, L., 2022b. Integrated environmental risk assessment of rare earth elements mixture on aquatic ecosystems. *Frontiers in Environmental Science* 10.
- Lacroix, E., Cauzid, J., Teitler, Y., Cathelineau, M., 2021. Near real-time management of spectral interferences with portable X-ray fluorescence spectrometers: application to Sc quantification in nickeliferous laterite ores. *Geochemistry: Exploration, Environment, Analysis* 21, geochem2021-015. <https://doi.org/10.1144/geochem2021-015>
- Liu, C., Liu, W., Huot, H., Yang, Y., Guo, M., Morel, J.L., Tang, Y., Qiu, R., 2022a. Responses of ramie (*Boehmeria nivea* L.) to increasing rare earth element (REE) concentrations in a hydroponic system. *Journal of Rare Earths* 40, 840–846. <https://doi.org/10.1016/j.jre.2021.04.002>
- Liu, C., Liu, W.-S., Huot, H., Guo, M.-N., Zhu, S.-C., Zheng, H.-X., Morel, J.L., Tang, Y.-T., Qiu, R.-L., 2022b. Biogeochemical cycles of nutrients, rare earth elements (REEs) and Al in soil-plant system in ion-adsorption REE mine tailings remediated with amendment and ramie (*Boehmeria nivea* L.). *Science of The Total Environment* 809, 152075. <https://doi.org/10.1016/j.scitotenv.2021.152075>
- Lopez, S., Morel, J.L., Benizri, E., 2022. The parameters determining hyperaccumulator rhizobacteria diversity depend on the study scale. *Science of The Total Environment* 834, 155274. <https://doi.org/10.1016/j.scitotenv.2022.155274>
- Mamane Mamadou, M., Cathelineau, M., Deloule, E., Reisberg, L., Cardon, O., Vallance, J., Brouand, M., 2022. The Tim Mersoï Basin uranium deposits (Northern Niger): Geochronology and genetic model. *Ore Geology Reviews* 145, 104905. <https://doi.org/10.1016/j.oregeorev.2022.104905>
- Martins, I., Mateus, A., Cathelineau, M., Boiron, M.C., Ribeiro da Costa, I., Dias da Silva, Í., Gaspar, M., 2022. The Lanthanide “Tetrad Effect” as an Exploration Tool for Granite-Related Rare Metal Ore Systems: Examples from the Iberian Variscan Belt. *Minerals* 12, 1067. <https://doi.org/10.3390/min12091067>

# Articles published in 2022

- Neukampf, J., Laurent, O., Tollan, P., Bouvier, A.-S., Magna, T., Ulmer, P., France, L., Ellis, B.S., Bachmann, O., 2022. Degassing from magma reservoir to eruption in silicic systems: The Li elemental and isotopic record from rhyolitic melt inclusions and host quartz in a Yellowstone rhyolite. *Geochimica et Cosmochimica Acta* 326, 56–76. <https://doi.org/10.1016/j.gca.2022.03.037>
- Nkrumah, P.N., Corzo Remigio, A., van der Ent, A., 2022. Proof-of-concept of polymetallic phyto-extraction of base metal mine tailings from Queensland, Australia. *Plant Soil* 480, 349–367. <https://doi.org/10.1007/s11104-022-05586-z>
- Purwadi, I., Casey, L.W., Ryan, C.G., Erskine, P.D., van der Ent, A., 2022. X-ray fluorescence spectroscopy (XRF) for metallome analysis of herbarium specimens. *Plant Methods* 18, 139. <https://doi.org/10.1186/s13007-022-00958-z>
- Rotureau, E., Pinheiro, J.P., Duval, J.F.L., 2022. On the evaluation of the intrinsic stability of indium-nanoparticulate organic matter complexes. *Colloids and Surfaces A: Physicochemical and Engineering Aspects* 645, 128859. <https://doi.org/10.1016/j.colsurfa.2022.128859>
- Scammacca, O., Mehdizadeh, R., Gunzburger, Y., 2022. Territorial Mining Scenarios for Sustainable Land-Planning: A Risk-Based Comparison on the Example of Gold Mining in French Guiana. *Sustainability* 14, 10476. <https://doi.org/10.3390/su141710476>
- Spiers, K.M., Brueckner, D., Garrovoet, J., Falkenberg, G., van der Ent, A., 2022. Synchrotron XFM tomography for elucidating metals and metalloids in hyperaccumulator plants. *Metallomics* 14, mfac069. <https://doi.org/10.1093/mtomcs/mfac069>
- Teitler, Y., Favier, S., Ambrosi, J.-P., Sevin, B., Golfier, F., Cathelineau, M., 2022. Evaluation of Sc Concentrations in Ni-Co Laterites Using Al as a Geochemical Proxy. *Minerals* 12, 615. <https://doi.org/10.3390/min12050615>
- Tisserand, R., Nkrumah, P.N., van der Ent, A., Sumail, S., Zeller, B., Echevarria, G., 2022. Biogeochemical cycling of nickel and nutrients in a natural high-density stand of the hyperaccumulator *Phyllanthus rufuschaneyi* in Sabah, Malaysia. *Chemoecology* 32, 15–29. <https://doi.org/10.1007/s00049-021-00363-3>
- Trépo, E., Caruso, S., Yang, J., Imbeaud, S., Couchy, G., Bayard, Q., Letouzé, E., Ganne-Carrié, N., Moreno, C., Oussalah, A., Féray, C., Blanc, J.F., Clément, B., Hillon, P., Boursier, J., Paradis, V., Calderaro, J., Gnemmi, V., Nault, J.-C., Guéant, J.-L., Devière, J., Archambeaud, I., Vitellius, C., Turlin, B., Bronowicki, J.-P., Gustot, T., Sutton, A., Meiller, C., Cao, Q., Hirsch, T.Z., Rebouissou, S., Degré, D., Sanchez, L.O., Rosewick, N., Quertinmont, E., Desille-Dugast, M., François-Vié, M., Moins, C., Leteurtre, E., Lassailly, G., Ningarhari, M., Boleslawski, E., Cottet, V., Zioli, M., Nahon, P., Zucman-Rossi, J., 2022. Common genetic variation in alcohol-related hepatocellular carcinoma: a case-control genome-wide association study. *The Lancet Oncology* 23, 161–171. [https://doi.org/10.1016/S1470-2045\(21\)00603-3](https://doi.org/10.1016/S1470-2045(21)00603-3)
- van der Ent, A., Nkrumah, P.N., Purwadi, I., Erskine, P.D., 2022. Rare earth element (hyper)accumulation in some Proteaceae from Queensland, Australia. *Plant Soil*. <https://doi.org/10.1007/s11104-022-05805-7>
- Xuan, W., Chagnes, A., Xiao, X., Olsson, R.T., Forsberg, K., 2022a. Antisolvent Precipitation for Metal Recovery from Citric Acid Solution in Recycling of NMC Cathode Materials. *Metals* 12, 607. <https://doi.org/10.3390/met12040607>
- Xuan, W., de Souza Braga, A., Chagnes, A., 2022b. Development of a Novel Solvent Extraction Process to Recover Cobalt, Nickel, Manganese, and Lithium from Cathodic Materials of Spent Lithium-Ion Batteries. *ACS Sustainable Chem. Eng.* 10, 582–593. <https://doi.org/10.1021/acssuschemeng.1c07109>

## Articles published in 2021, not included in annual report 2020/2021

- Cardoso-Fernandes, J., Silva, J., Dias, F., Lima, A., Teodoro, A., Barres, O., Cauzid, J., Perrotta, M., Roda-Robles, E., Ribeiro, M., 2021. Tools for Remote Exploration: A Lithium (Li) Dedicated Spectral Library of the Fregeneda-Almendra Aplite-Pegmatite Field. *Data* 6. <https://doi.org/10.3390/data6030033>
- Combes, V., Eglinger, A., André-Mayer, A.-S., Teitler, Y., Heuret, A., Gibert, P., Béziat, D., 2021. Polyphase Gold Mineralization at the Yaou Deposit, French Guiana. Geological Society, London, Special Publications 516, SP516-2020. <https://doi.org/10.1144/SP516-2020-29>
- Dehaine, Q., Filippov, L.O., Filippova, I.V., Tijsseling, L.T., Glass, H.J., 2021. Novel approach for processing complex carbonate-rich copper-cobalt mixed ores via reverse flotation. *Minerals Engineering* 161, 106710. <https://doi.org/10.1016/j.mineng.2020.106710>
- Farrokhpay, S., Filippov, L., Fornasiero, D., 2021. Flotation of Fine Particles: A Review. *Mineral Processing and Extractive Metallurgy Review* 42, 473–483. <https://doi.org/10.1080/08827508.2020.1793140>
- Kaba, O.B., Filippov, L.O., Filippova, I.V., Badawi, M., 2021. Interaction between fine particles of fluorapatite and phosphoric acid unraveled by surface spectroscopies. *Powder Technology* 382, 368–377. <https://doi.org/10.1016/j.powtec.2020.12.058>
- Menad, N.-E., Kana, N., Seron, A., Kanari, N., 2021. New EAF Slag Characterization Methodology for Strategic Metal Recovery. *Materials* 14, 1513. <https://doi.org/10.3390/ma14061513>
- Tripathy, S.K., Murthy, Y.R., Farrokhpay, S., Filippov, L.O., 2021. Design and Analysis of Dewatering Circuits for a Chromite Processing Plant Tailing Slurry. *Mineral Processing and Extractive Metallurgy Review* 42, 102–114. <https://doi.org/10.1080/08827508.2019.1700983>